Biology Dissertations

Department of Biology

4-23-2007

Analysis of the Cellular Proteins, TIA-1 and TIAR, and their Interaction with the West Nile Virus (WNV) 3' SL Minus-Strand RNA

Mohamed Maged Emara
Georgia State University

Follow this and additional works at: https://scholarworks.gsu.edu/biology_diss

Part of the Biology Commons

Analysis of the cellular proteins, TIA-1 and TIAR, and their interaction with the

West Nile virus (WNV) 3′ SL minus-strand RNA

by

Mohamed Emara

Under the Direction of Margo A. Brinton

ABSTRACT

The 3′ terminal stem loop of the WNV minus-strand [WNV3′(-) SL] RNA was previously shown to bind the cell protein, T-cell intracellular antigen-1 (TIA-1), and the related protein, TIAR. These two proteins are known to bind AU-rich sequences in the 3′UTRs of some cellular mRNAs. AU stretches are located in three single-stranded loops (L1, L2, and L3) of the WNV3′(-) SL RNA. The RNA binding activity of both proteins was reduced when L1 or L2, but not L3, AU sequences were deleted or substituted with Cs. Deletion or substitution with Cs of the entire AU-rich sequence in either L1 or L2 in a WNV infectious clone was lethal for the virus while mutation of some of these nt decreased the efficiency of virus replication. Mutant viral RNAs with small plaque or lethal phenotypes had similar translational efficiencies to wildtype RNA, but showed decreased levels of plus-strand RNA synthesis. These results correlated well with the efficiency of TIA-1 and/or TIAR binding in *in vitro* assays.

In normal cells, TIA-1 and TIAR are evenly distributed in the cytoplasm and nucleus. Between 6 and 24 hr after WNV infection, TIAR concentrated in the perinuclear region and TIA-1 localization to this region began by 24 hr. Similar observations were made in DV2 infected cells but at later times after infection. In infected cells, both

proteins colocalized with dsRNA, a marker for viral replication complexes, and with viral non-structural proteins. Anti-TIAR or anti-TIA-1 antibody coimmunoprecipitated viral NS3 and possibly other viral nonstructural proteins. In response to different types stress, TIA-1 and TIAR recruit cell mRNA poly(A)$^+$ into cytoplasmic stress granules (SG) leading to general translational arrest in these cells. SG were not induced by flavivirus infection and cells became increasingly resistant to arsenite induction of SG with time after infection. Processing Body (PB) assembly was also decreased beginning at 24 hr. These data suggest that the sequestration of first TIAR and then TIA-1 via their interaction with viral components in flavivirus infected cells inhibits SG formation and prevents the shutoff of host translation.

Analysis of the cellular proteins, TIA-1 and TIAR, and their interaction with the

West Nile virus (WNV) 3′ SL minus-strand RNA

by

Mohamed Emara

A Dissertation Submitted in Partial Fulfillment of the Requirements for the Degree

of Doctor of Philosophy

in the College of Arts and Sciences

Georgia State University

2007

Analysis of the cellular proteins, TIA-1 and TIAR, and their interaction with the

West Nile virus (WNV) 3′ SL minus-strand RNA

by

Mohamed Emara

Major Professor:	Margo A.Brinton
Committee Members:	Teryl K. Frey
	Irene T. Weber

Electronic Version Approved by:

Office of Graduate Studies
College of Arts and Sciences
Georgia State University
April 2007

DEDICATION AND ACKNOWLEDGEMENTS

TABLE OF CONTENTS

LIST OF FIGUERS

CHAPTER I

INTRODUCTION

Classification and Medical Importance of Flaviviruses.

Flaviviruses and alphaviruses were previously classified as members of the family *Togaviridae*. However, due to differences in the replication and assembly strategies (Westaway et al., 1980), as well as the genome structures (Rice et al., 1985) of flaviviruses and alphaviruses, flaviviruses were reclassified as members of the genus flavivirus within the family *Flaviviridae*. The family *Flaviviridae* currently includes two other genera, the pestiviruses and the hepaciviruses (Lindenbach and Rice, 2007). The genus flavivirus contains more than 68 members that are separated into twelve antigenic serogroups (Heinz et al., 2000). Some flaviviruses such as dengue virus (DV), Japanese encephalitis virus (JEV), yellow fever virus (YFV), West Nile virus (WNV), St. Louis encephalitis virus (SLEV), Murray Valley encephalitis virus (MVEV), and tick-borne encephalitis virus (TBEV), are important human pathogens.

Most of the flaviviruses are transmitted to vertebrates via infected blood-sucking arthropods, and are therefore called arthropod-borne viruses or "arboviruses" (Lindenbach and Rice, 2007). Approximately 65% of the flaviviruses are transmitted by mosquitoes, 22% by ticks, and the remaining 13% have no known arthropod vector (Porterfield, 1996). All of the members of the YFV, DV, and JE serogroups are mosquito-borne. Neuroinvasiveness is a common feature of those flaviviruses that cause substantial human and animal disease. Symptoms include fever, meningitis, and

encephalitis. Although YFV can be prevented by vaccine, outbreaks and epidemics caused by YFV have risen dramatically in the recent years in South America and sub-Saharan countries in Africa, because of the difficulties of vaccinating many at-risk populations (Monath, 1994). YFV infections have a mortality rate that can be as high as 20%. DV infects 50-100 million humans annually in tropical and subtropical regions (Gubler, 2002). Symptoms range from a self-limiting febrile illness to the life threatening dengue hemorrhagic fever and dengue shock syndrome (DHF-DSS), with a mortality rate of ~10%. Members of the JEV serogroup such as JEV, WNV, SLEV, and MVEV, are responsible for periodic epidemics and scattered cases of human central nervous system (CNS) disease (Lindenbach and Rice, 2007). WNV is endemic in Africa, the Middle East, Europe, central Asia, and most recently, North America. WNV infections in the USA first occurred in the summer of 1999 (Asnis et al., 2000). In 2006, the Centers for Disease Control and Prevention (CDC) reported 4261 positive human WNV cases in the US. Also, the tick-borne flaviviruses, such as Powassan, louping ill, Kyasanur Forest Disease, Russian Spring-Summer encephalitis viruses, and TBEV cause human meningitis and/or encephalitis with a case fatality ranging from 1-30% (Shope, 1980).

Virion Morphology and Composition.

The flavivirus virion is spherical, enveloped and has a diameter of 40-60 nm (Murphy, 1980). The virion is composed of three structural proteins, the envelope (E) protein, the membrane (M) protein, and the capsid (C) protein; the E and M proteins are located in the lipid envelope of the virion, while the C protein forms the viral capsid

(Lindenbach and Rice, 2007). Cryo-electron microscopy data suggested that the virions have icosahedral symmetry (Heinz and Allison, 2000). Recent studies indicated that this symmetry is imposed by interactions between E surface proteins, rather than by interactions between capsid monomers (Kuhn et al., 2002).

Flavivirus replication cycle.

Flavivirus surface protein binds to unknown receptor(s) on the host cell surface followed by virus entry via receptor-mediated endocytosis (Fig. 1.1A). The viral nucleocapsid is subsequently released into the cytoplasm of the infected cells by acidic-pH fusion of the virion envelop with the endosomal membrane (Gollins and Porterfield, 1985; Gollins and Porterfield, 1986; Nawa, 1998). After uncoating of the nucleocapsid by an unknown process, the viral genome is released into the cell cytoplasm and is then translated into a single polyprotein (Fig. 1.1B). The poly protein is processed by viral and cellular proteases into the mature viral structural and nonstructural proteins (Fig. 1.1C) (Heinz et al., 1994). The genome RNA also serves as the template for transcription of the complementary minus strand RNA. The minus-strand RNA in turn serves as a template for the synthesis of genomic RNA. The minus-strand RNA is always present in infected cells in association with the plus-strand RNA in a replicative form (RF) (Fig. 1.1D) or a replicative intermediate (RI) (Fig. 1.1E) complex (Lindenbach and Rice, 2007). Flavivirus RNA synthesis is postulated to occur via asymmetric and semiconservative mode of replication (Chu and Westaway, 1985; Cleaves, Ryan, and Schlesinger, 1981). Each plus-strand RNA template is thought to synthesize only one minus-strand RNA at a

time forming the RF, while the minus-strand template is efficiently reinitiated and simultaneously synthesizes multiple copies of the plus strand RNA forming the RI. The synthesis of plus and minus-strand viral RNA is disproportionate; about 10 times more plus strand RNA than the minus-strand RNA is produced (Chu and Westaway, 1985). Flavivirus replication takes place in viral replication complexes located on membranes in the perinuclear region of the cytoplasm of infected cells.

Flavivirus infection causes extensive rearrangement and proliferation of the cytoplasmic membranes present in the perinuclear region to provide an environment that enhances virus replication (Brinton, 2002; Lindenbach and Rice, 2007). Later in the infection cycle, these rearrangements induce the formation of smooth membrane vesicle clusters known as vesicle packets (VP), that are found associated with smooth endoplasmic reticulum (SER) or Golgi-like membranes (Mackenzie, Jones, and Westaway, 1999). VP appear to be associated with another randomly folded membrane structure, called convoluted membranes (CM) or paracrystalline arrays (PC) (Mackenzie et al., 1998). Previous studies showed that the viral RNA as well as the viral replication proteins are localized within the VP, suggesting that these structures might be sites of RNA replication (Mackenzie et al., 1998; Westaway, Khromykh, and Mackenzie, 1999). The viral serine protease NS3 and cofactor NS2B colocalize in the CM/PC structures indicating that these are sites of proteolytic processing (Westaway et al., 1997b). It is noteworthy that VP have only been observed at later times after infection, thus the site(s) of early viral RNA synthesis is still not known.

Although flavivirus packaging and release mechanisms are not well understood, electron microscopy studies demonstrated that progeny virion assemblies formed in the lumen of the ER (Lindenbach and Rice, 2007) (Fig. 1.1 G). Immature virions containing prM-E heterodimers are found in cytoplasmic vesicles (Fig. 1.1 G and H). Mature virions are generated in the *trans*-Golgi network via cleavage of the N-terminal portion of prM to M (Stadler et al., 1997; Wengler and Wengler, 1989) and mature virions are released from the infected cell by exocytosis after fusion of virion-containing cytoplasmic vesicles with the plasma membrane (Stollar, Stevens, and Schlesinger, 1966) (Fig. 1.1I). The release of the flavivirus particles from the infected cells starts at about 12 hr after infection. For WNV and JEV, maximal virus titers are produced by 24 hr after infection (Trent, Swensen, and Qureshi, 1969).

Flavivirus genome organization.

The WNV genome is a single-stranded RNA with positive polarity that is approximately 11 Kb in length (Rice et al., 1985). It contains a type I cap at the 5′ end, but lacks a poly (A) tract at the 3′ end. The genome contains a single, long open reading frame and serves as the only viral mRNA in WNV infected cells. The viral mRNA encodes a single polyprotein, which is translated and co- and posttranslationally processed by viral and cellular proteases into three structural (C, M, and E) proteins and
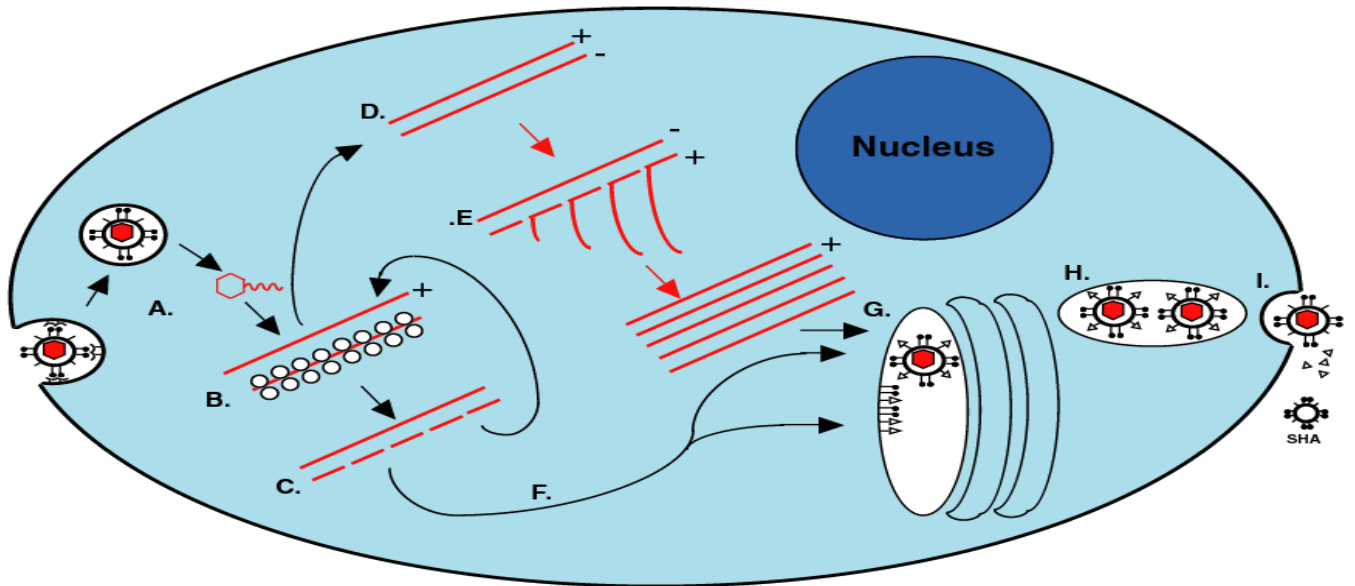
Figure 1.1:   Flavivirus replication cycle. A. Attachment, entry, and uncoating. B. Polyprotein translation. C. Polyprotein processing. D. (-) RNA synthesis. E. Nascent (+) RNA synthesis. F. Transport of the structural proteins to membranes.   G. Virion assembly. H. Virion movement to the cell surface. I. Release of nascent virions. See text for details. Figure was taken from Brinton (2002).

seven nonstructural (NS1, NS2a, NS2b, NS3, NS4a, NS4b and NS5) proteins (Fig. 1.2) (Chambers et al., 1990).

The terminal 5′ and 3′ noncoding regions (NCRs) of the WNV genome RNA are 96 and 631 nucleotides (nts) long, respectively (Chambers et al., 1990). Previous studies have indicated that both the 3′ and 5′ terminal nucleotides of the flavivirus genome can form conserved stem-loop (SL) structures (Fig. 1.2) (Brinton and Dispoto, 1988; Brinton, Fernandez, and Dispoto, 1986; Chambers et al., 1990). The SL structure formed by the 3′-terminal nts is more stable than the structure formed by the 5′-terminal nts. The conservation of the terminal structures as well as of short sequence elements within these structures among divergent flaviviruses suggest that they may function as *cis*-acting elements (Brinton, 2002). Evidence supporting the formation of a SL structure by the 3′ terminal nt of the complementary minus-strand (Shi, Li, and Brinton, 1996) was previously obtained by RNase structure probing. Deletion of either the 3′ or 5′ terminal SL in flavivirus infectious clones was lethal strongly suggesting that these regions contain essential *cis*-acting elements for virus replication (Bredenbeek et al., 2003; Cahour et al., 1995; Men et al., 1996). Particular host cell proteins have previously been reported to bind specifically to regions within the 3′ and 5′ NCRs of a number of animal RNA virus genomes (Lai, 1998). The 3′-terminal structure of the WNV complementary minus strand RNA was previously reported to bind specifically to cell proteins. UV-induced cross-linking studies indicated that the molecular masses of these RNA binding proteins were about 42, 50, 60, and 108 kDa. One of these proteins, p42, was identified as TIAR (Li et al., 2002). TIAR is closely related to TIA-1.

Protein	Position (nts)
C	(97-465)
prM	(466-741)
M	(742-966)
E	(967-2469)
NS1	(2470-3525)
NS2A	(3526-4218)
NS2B	(4219-4611)
NS3	(4612-6468)
NS4A	(6469-6915)
NS4B	(6916-7680)
NS5	(7681-10395)
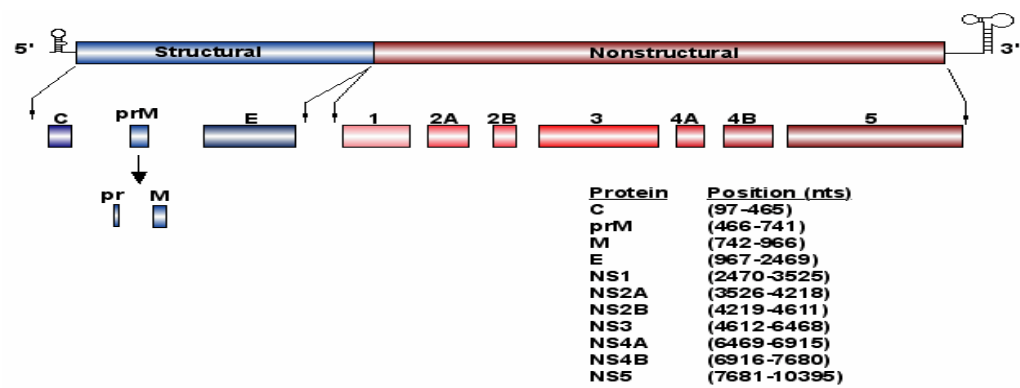
Figure 1.2: The WNV genome. Noncoding regions (terminal black lines), structural proteins (blue bars), and nonstructural proteins (red bars). See text for details. Figure from Brinton (2002).

Structural proteins.

The C protein.

Mature C protein is produced by the cleavage of a hydrophobic region from the C protein precursor, designated anchored C (anch C), by the viral serine protease NS3 (Amberg et al., 1994; Yamshchikov and Compans, 1994). Peptides in the hydrophobic region of anch C were reported to serve as signals for the translocation of prM into the endoplasmic reticulum (ER) lumen (Nowak et al., 1989). The mature C protein is small (~11 kDa) and contains highly basic residues in its N- and C-termini (Rice et al., 1985), that may facilitate its interaction with the genomic RNA during the formation of the ribonucleoprotein complex. The middle portion of mature C contains a hydrophobic region that facilies membrane association and this may play a role in virus assembly (Markoff, Falgout, and Chang, 1997). At late times after infection, the C protein was found in the cytoplasm as well as the nucleus of infected cells (Westaway et al., 1997a).

The M protein.

The M protein is the smallest protein (~8 kDa) in the virus particle. It is initially expressed as the precursor protein M (prM). prM is incorporated into immature virions. During egress of virions, prM is cleaved by the Golgi-network enzyme furin to generate the mature structural protein M (Stadler et al., 1997). The mature M protein consists of an ectodomain (~40 aa long) followed by two transmembrane domains (Chambers et al., 1990; Lindenbach and Rice, 2007). Although M protein is not defined as the viral protein that binds to cell receptors, previous studies demonstrated that the M ectodomain can

induce neutralizing antibody response (Bray and Lai, 1991; Vazquez et al., 2002), suggesting that it can maintain protective immunity.

The E protein.

E is a type I integral membrane protein of ~ 53 kDa that is located on the outer surface of the virion. The E protein is thought to facilitate the binding and entrance of the virus particle into the cell by mediating fusion of the viral envelope with cellular membrane. In immature virions, the E protein forms a heterodimer with the prM protein to maintain the correct folding and stabilization of E until prM is cleaved by cellular protease to yield the mature virion (Heinz and Allison, 2000). The E protein contains six intramolecular disulfide bonds that are conserved among all flaviviruses (Rey et al., 1995). A high-resolution crystal structure of a soluble fragment of TBE E protein showed that the mature E protein forms elongated head-to-tail homodimers that were prepared to lie fairly parallel with the virus envelope with the distal end of each monomer anchored in the membrane (Heinz and Allison, 2000). Each subunit of the E protein is divided into three domains (I, II, and III) that corresponded to previously defined antigenic domains (Mandl et al., 2000; Mandl et al., 1989). Several studies have demonstrated that the E protein contains the major determinants that elect neutralizing antibodies and generate a protective immune response (Lindenbach and Rice, 2007).

Nonstructural proteins.

The flavivirus nonstructural proteins are multifunctional proteins (Mackenzie et al., 1998). All seven of the nonstructural proteins were previously shown to be components of viral RNA replication complexes (Kapoor et al., 1995; Uchil and Satchidanandam, 2003; Vasudevan et al., 2001). However, exactly how each of these viral nonstructural proteins is involved in the formation and functioning of the flavivirus replication complexes is not well understood.

NS1.

NS1 is a ~ 46 kDa glycoprotein, which is found both in the cytoplasm as well as on the surface of infected cells and is slowly secreted by mammalian cells (Smith and Wright, 1985). The NS1-E junction is cleaved by host signal peptidase after NS1 has been translocated into the lumen of the ER (Chambers et al., 1990). NS2A is cleaved from the C-terminal end of NS1 by an unknown host protease associated with the ER (Falgout and Markoff, 1995). Although, NS1 forms homodimers that are hydrophobic and membrane-associated (Smith and Wright, 1985; Winkler et al., 1989; Winkler et al., 1988), it is not clear how NS1 associates with cell membranes. A Kunjin NS1 mutation that completely inhibited NS1 dimer formation (Hall et al., 1999), was shown to reduce the level of virus growth by 100-fold compared to wild-type virus, but had no effect on NS1 secretion (Hall et al., 1999). These observations indicate that NS1 dimerization enhances, but is not essential for its function in virus replication.

A role for NS1 in viral RNA replication (Lindenbach and Rice, 1997; Muylaert, Galler, and Rice, 1997) has also been reported. Studies with dual labeled cryosections showed that DV NS1 colocalized with viral dsRNA in VP, the most likely sites of RNA replication, in infected Vero cells (Mackenzie, Jones, and Young, 1996; Westaway et al., 1997b). Moreover, the accumulation of both the positive- and the negative-strand RNA during the first phase of viral RNA synthesis was significantly reduced in cells infected with a mutant YFV that contained a large in frame deletion in the NS1 gene (Lindenbach and Rice, 1997). Providing wildtype NS1 in *trans* successfully complemented this mutant virus RNA and restored viral RNA replication to wildtype levels, suggesting that NS1 plays functions prior to or early in minus-strand synthesis. However, the YFV NS1 deletion mutant RNA could not be *trans*-complemented by a DV NS1 suggesting that the function of NS1 may be mediated by an interaction with another viral protein. Mutation in NS4A suppressed this defect, indicating that an interaction between NS1 and NS4A is required for viral RNA synthesis (Lindenbach and Rice, 1999).

NS2A, NS2B, NS4A, and NS4B.

The four small hydrophobic, nonstructural proteins (NS2A, NS2B, NS4A, and NS4B) are tightly associated with cytoplasmic membranes and together with NS3, NS5, and NS1 were previously shown to be components of membrane bound viral RNA replication complexes located in the perinuclear region of infected cells. Little is known about the specific functions of these four proteins.

NS2A.

NS2A is found in infected cells in two forms, the full-length protein of ~ 22 kDa and a smaller 20 kDa C-terminally truncated form (Chambers et al., 1990; Nestorowicz, Chambers, and Rice, 1994). It was previously shown that mutagenesis of the C-terminus of either full length or truncated NS2A was lethal for YFV replication (Nestorowicz, Chambers, and Rice, 1994). Cryo-immunogold staining studies showed that NS2A localized in VP, which is thought to be the site for virus RNA replication (Mackenzie et al., 1998). Also, a recombinant NS2A protein was previously reported to bind *in vitro* to NS3 and NS5 as well as to regions within the 3′ NCR of Kunjin virus genomic RNA (Mackenzie et al., 1998). Mutational analysis of NS2A in a Kunjin virus infectious clone indicated an essential role for this protein in virus assembly (Liu, Chen, and Khromykh, 2003). A recent study using Kunjin virus subgenomic replicons, demonstrated that a single amino acid substitution in NS2A significantly reduced the viral inhibitory effect of interferon beta (Liu et al., 2004). Together these data suggest that NS2A may be involved in RNA packaging, RNA replication, and interference with the host cell immune response.

NS2B.

NS2B is ~ 14 kDa protein that has a conserved central hydrophilic domain flanked by two hydrophobic domains. It forms a stable complex with the viral serine protease (NS3), and functions as a cofactor for the serine protease activity (Chambers et al., 1993; Falgout, Miller, and Lai, 1993). The interaction between NS2B and NS3 is mediated by

the central hydrophilic region of NS2B and the N-terminal region of NS3 (Chambers et al., 1993; Droll, Krishna Murthy, and Chambers, 2000; Falgout, Miller, and Lai, 1993). This viral protein complex mediates cleavage at the junctions between anch C/virion C, NS2A-NS2B, NS2B-NS3, NS3-NS4A, and NS4B-NS5 (Amberg et al., 1994; Cahour, Falgout, and Lai, 1992; Chambers, Grakoui, and Rice, 1991; Falgout et al., 1991; Zhang, Mohan, and Padmanabhan, 1992). Deletion analysis indicates that the 40 aa hydrophilic domain of NS2B is required for NS3 serine protease activity. Mutations within the hydrophilic region that disrupt the NS2B-NS3 interaction also abolish serine protease activity (Chambers et al., 1993; Clum, Ebner, and Padmanabhan, 1997; Droll, Krishna Murthy, and Chambers, 2000; Falgout, Miller, and Lai, 1993). The hydrophobic regions of NS2B are involved in anchoring NS2B to ER membranes (Clum, Ebner, and Padmanabhan, 1997).

NS3.

NS3 is a large (~70 kDa) multifunctional protein that has several enzymatic activities, which are required for polyprotein processing, viral RNA replication, and RNA capping (Westaway, Mackenzie, and Khromykh, 2003). The N-terminus of NS3 has serine protease activity (Lindenbach and Rice, 2007), which is activated only after interacting with NS2B. It was previously reported that the NS3-NS2B complex is associated with membranes and is required for efficient polyprotein processing. The C-terminal portion of NS3 contains helicase and NTPase activities (Borowski et al., 2001). The precise functions of these enzymes are not known yet, however, the helicase is thought to unwind

the 3′ terminal secondary structures, which are involved in template recognition. NS3 not only has these two activities, but the C-terminal region also encodes RNA triphosphatase (RTPase) (Wengler and Wengler, 1993), which is postulated to dephosphorylate the 5′ end of the viral RNA before its cap methylation by the polymerase NS5. In a previous study using coimmunoprecipitation and immunoblotting experiments a protein-protein interaction between NS3 and NS5 was demonstrated (Kapoor et al., 1995) and the NTPase (Cui et al., 1998; Yon et al., 2005) as well as RTPase (Yon et al., 2005) activities of a recombinant dengue NS3 were enhanced by the presence of NS5. These observations indicate that the interaction of NS3 and NS5 might regulate the activity of NS3 during virus replication.

NS5.

NS5 is the largest (103 kDa) and most highly conserved flavivirus protein. The C-terminal portion of NS5 contains the eight RNA dependent RNA polymerase (RdRp) motifs, that are highly homologues to the sequences of the RdRps of other positive-strand RNA viruses (Koonin, 1993). Previous *in vitro* studies using purified recombinant NS5 protein (Ackermann and Padmanabhan, 2001; Nomaguchi et al., 2004; Tan et al., 1996) confirmed the polymerase activity of NS5. Previous studies indicated that flavirus NS5 performs *de novo* RNA synthesis (Ackermann and Padmanabhan, 2001; Selisko et al., 2006). As concluded from comparison of the kinetics of the *de novo* RNA synthesis by different *Flavivirdae* members RdRps, DV RdRP showed a higher degree of conformational flexibility than that of the WNV RdRp in the transition process from

initiation to elongation (Selisko et al., 2006). In a recent study, the crystal structure of the WNV RdRp was determined and it was shown that this structure is similar to that of two other members of the family *Flaviviridae*, hepatitis C virus (HCV) and bovine virus diarrhea virus (BVDV) (Malet et al., 2007). The overall structure has the classic fold of an RdRP, which consists of palm, thumb, and finger domains as well as specific flavivirus features such as the priming loop that provides a platform which stabilizes the viral RNA initiation complexes during the *de novo* initiation of flavivirus RNA syntheisis (Malet et al., 2007). The N-terminal part of this protein contains a methyltransferase that is predicted to function as an RNA capping enzyme (Koonin, 1993). NS5 was shown to have both guanine-N-7 and ribose 2′-O methylation activities (Ray et al., 2006). A recent mutational analysis of the terminal 74 nt WNV5′(+)SL structure of WNV showed that the second and third nt of the viral genome as well as the bottom two helices of the WNV5′(+)SL RNA structure are required for N-7 methylation. Also, a minimum sequence of 20 nt in the 5′(+)SL that includes the first and the second nt was essential for 2′-OH ribose methylation (Dong et al., 2007). Although the presence of the MTase domain did not influence RdRp activity (Selisko et al., 2006), mutagenesis studies confirmed that both RdRp (Khromykh, Sedlak, and Westaway, 1999) and MTase (Zhou et al., 2007) are required for WNV life cycle.

TIA-1 and TIAR cellular proteins.

T-cell intracellular antigen-1 (TIA-1) and T-cell intracellular antigen related protein (TIAR) are two evolutionary, conserved, multifunctional proteins that have been reported

to regulate alternative splicing of particular pre-mRNAs, translationally silence some mRNAs, and sequester cytoplasmic mRNAs in stress granules (SG) (Kedersha and Anderson, 2002). Although first discovered in T cells, TIA-1 and TIAR are expressed in most types of cells, including brain, spleen, and macrophages, which are sites of flavivirus replication *in vivo*. Both proteins are found in the cytoplasm and the nucleus and shuttle between the two compartments (Beck et al., 1996). Both proteins were also shown to be essential for embryonic development (Beck et al., 1998; Piecyk et al., 2000). For homozygous TIAR knock outs, embryo lethality was 100% in BALB/c mice and 90% in C57BL/6 mice. For TIA-1 knock outs in both strains, the rate of embryonic lethality was 50% (Piecyk et al., 2000). Attempts to knock out both proteins in mice were unsuccessful (Piecyk et al., 2000) and suppression of both TIA-1 and TIAR in DT40 chicken cells resulted in cell death (Le Guiner, Gesnel, and Breathnach, 2003).

Two isoforms of both TIA-1 and TIAR have been reported and are translated from alternatively spliced mRNAs (Fig. 1.3). The two isoforms of TIA-1 differ from each other by the presence (TIA-1a) or absence (TIA-1b) of a mini exon encoding an 11–amino acid peptide within the RRM1. TIARa includes a mini exon that encodes a 17–amino acid peptide within RRM1, whereas TIARb lacks this exon. The long isoforms of both proteins have molecular weights of ~ 42 kDa, whereas the short isoforms have molecular weights of ~ 40 kDa. It was previously shown that the two TIA-1 isoforms are equally abundant in cells, whereas the short isoform of TIAR is 6 times more abundant in cells than is the long isoform (Beck et al., 1996).

TIA-1 and TIAR are members of the RNA recognition motif (RRM) family of RNA binding proteins (Anderson, 1995). Both proteins contain three RRM domains near their amino termini and a glutamine rich domain at their carboxyl termini (Fig. 1.3). The glutamine rich domain is also called prion related domain (PRD), which shares structural and functional characteristics with the aggregation domains of mammalian and yeast prion proteins (Gilks et al., 2004). Each RNA-binding domain contains two-ribonucleoprotein sequences (RNP 1 and RNP2) that are conserved among all RNA binding proteins. TIA-1 and TIAR proteins share 80% overall amino acid identity with the highest degree of similarity (91% identity) in the RRM domain 3 and the lowest degree of similarity (51% identity) in the carboxyl terminal domain (Kawakami et al., 1992). Although RRM2 is sufficient for the specific binding of either protein to uridylate-rich RNA, RRM1 and RRM3 enhance RRM2 RNA binding (Dember et al., 1996). In somatic cells, RRM2 and the first half of the C-terminal domain mediate TIA-1 and TIAR nuclear accumulation, whereas RRM3 facilitates nuclear export (Zhang et al., 2005).

TIA-1 and TIAR protein binding sites were previously mapped to AU-rich regions within the 3′UTRs of a subset of cellular mRNAs, that included TNF-α (Gueydan et al., 1999; Piecyk et al., 2000), cyclooxgenase-2 (COX-2) (Cok et al., 2004; Dixon et al., 2003), and β_2-adrenegic receptor (β_2-AR) (Kandasamy et al., 2005) mRNAs. For the TNF-α mRNA, TIAR binding was mapped to a 39 nt region within the 3′UTR that contained a 35 nt AU tract (Gueydan et al., 1999; Lewis et al., 1998). However, the minimal sequences required for protein binding were not fine mapped in any of these

3′UTRs. The 3′terminal region of the WNV complementary minus strand RNA differs from RNAs previously reported to bind to TIA-1 and TIAR in having AU rich sequences within loops of a secondary structure. This binding is mediated through the RRM2 domain of TIA-1 and TIAR proteins. Kinetic studies showed that the binding activity of TIA-1 RRM2 for the WNV3′(-)SL RNA was 10 times lower than that of the TIAR RRM2 for this RNA (Li et al., 2002) .

Stress granules.

Mammalian stress granules (SG) are ribonucleoprotein aggregates or discrete cytoplasmic foci, which are formed in response to environmental stresses such as oxidative phosphorylation ER stress, and some viral infections (Fig. 1.4) (Anderson and Kedersha, 2006). Several cell proteins, including TIA-1, TIAR, and Ras-Gap-SH3 domain-binding protein (G3BP) are involved in SG assembly (Anderson and Kedersha, 2006). SG are sites at which transient storage of untranslated mRNAs takes place in stressed cells. The sequestration of these mRNAs in SG is initiated by the phosphorylation of eukaryotic translation initiation factor 2 α (eIF2α), a key regulatory factor in translation initiation, and this inhibits translation by preventing the assembly of active preinitiation complexes. After eIF2α phosphorylation occurs, TIA-1 and TIAR bind to the translationally inactive initiation complexes as well as to the mRNA poly(A)$^{+}$ and self-aggregate forming SG (Kedersha and Anderson, 2002). Both the RRM domains and the PRD of TIA-1 were previously shown to be essential for SG formation (Gilks et
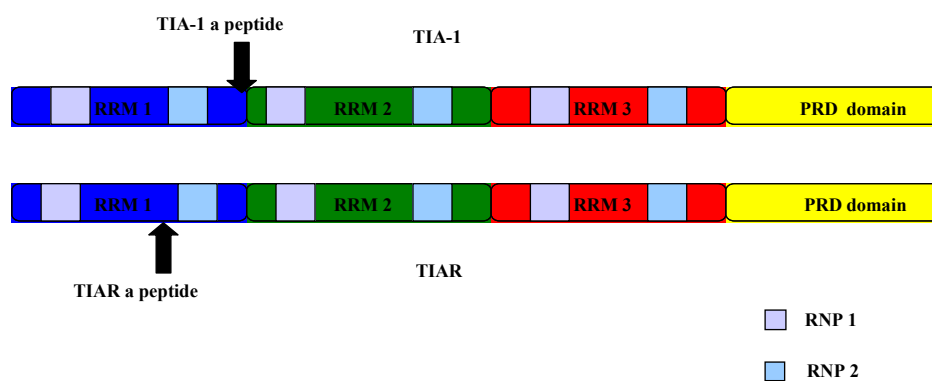
Figure 1.3: Schematic structure of TIA-1 and TIAR. RRM1 (blue), RRM2 (green), RRM3 (red), and the C-terminal glutamine rich prion related domain (yellow). Each RRM domain contains two ribonucleoprotein sequences (RNP 1 and RNP2). The positions of the additional mini peptides in the long isoforms of TIA-1 and TIAR are indicated by arrows.

al., 2004; Kedersha et al., 1999). A recombinant TIA-1 protein lacking the three RNA binding domains was unable to bind poly(A)$^+$ RNA and recruit it to SG (Kedersha et al., 1999). Deletion of the TIA-1 PRD inhibited protein aggregation and SG assembly (Gilks et al., 2004). In mammalian cells SG were found to be physically associated with another type of foci, known as processing bodies (PB) (Kedersha et al., 2005). PB are spheroid particles (Cougot, Babajko, and Seraphin, 2004; Kedersha et al., 2005; Wilczynska et al., 2005) that were identified in the cytoplasm of eukaryotic cells (Bashkirov et al., 1997; Eystathioy et al., 2002; Eystathioy et al., 2003; Sheth and Parker, 2003) and were reported to contain components of the 5′-3′ mRNA degradation pathway such as decapping enzymes DCP1/2, 5′-3′ exonuclease XRN1 (van Dijk et al., 2002).
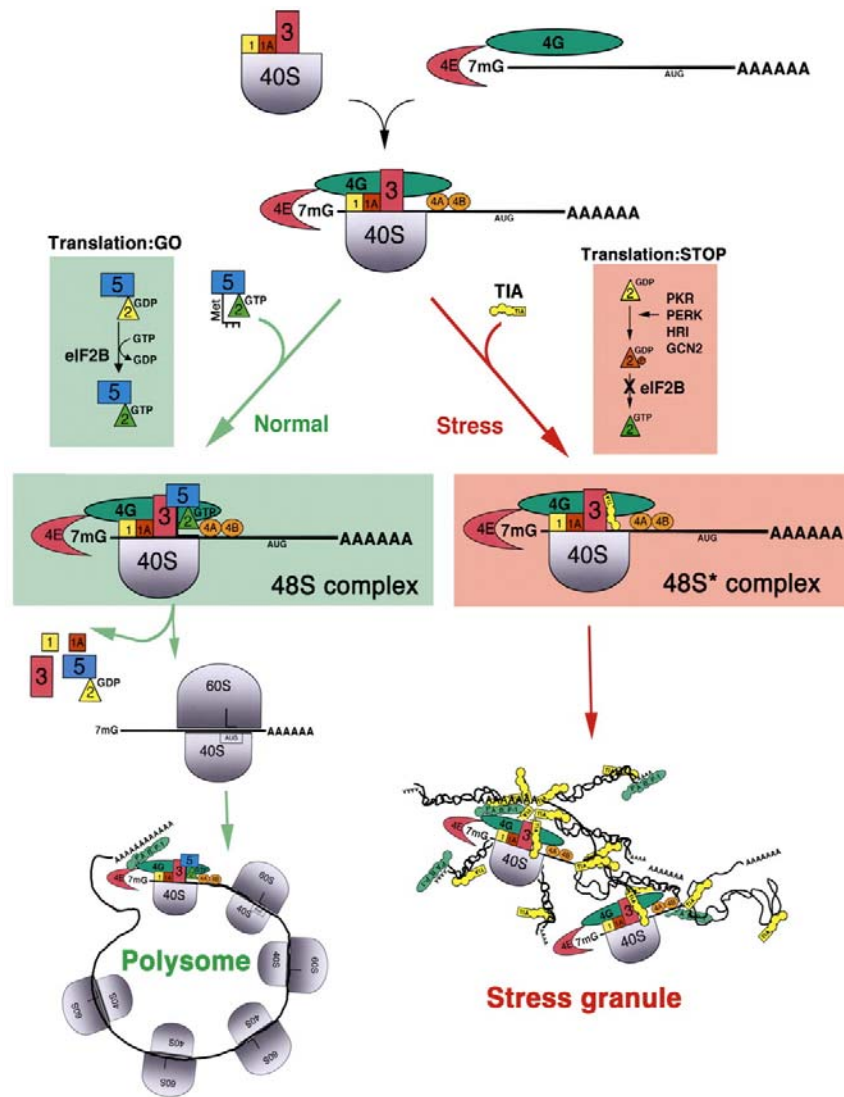
Figure 1.4: Translation initiation in the absence or presence of stress factors. (Green panels) in the absence of stress. (Red panels) in the presence of stress. The assembly of translationally inactive initiation complexes lacking eIF2 allows the RNA-binding protein TIA-1 to redirect untranslated mRNAs from polyribosomes to SGs. Figure from Kedersha and Anderson (2002).

GOALS OF THIS DISSERTATION

1. Mapping the binding site(s) of the TIA-1 and TIAR proteins on the WNV3′(-)SL RNA.

Data from previous *in vitro* selection/amplification (SELEX) experiments showed that the two cellular proteins, TIA-1 and TIAR, bind to AU stretches in RNAs. However, the optimal RNA sequences recognized by TIA-1 in SELEX assays were not the same as those recognized by TIAR (Dember et al., 1996). In another previous study, the binding sites for both TIA-1 and TIAR in the 3′NCR of the tumor necrosis factor alpha (TNF-α) mRNA were mapped to a large fragment of AU-rich sequence containing clustered AUUUA pentamers (Gueydan et al., 1999). These cell mRNA binding sites for TIA-1 and TIAR were considered to be linear. In the WNV3′(-)SL RNA, the AU rich sequences are located in single stranded loops (L1, L2, and L3) within a secondary structure. Because TIA- and TIAR are ARE-binding proteins, the AU sequences will be the initial mutation targets in experiments designed to identify nucleotides in the WNV3′(-)SL RNA required for TIA-1 and TIAR protein binding.

Recombinant TIA-1 and TIAR proteins will be overexpressed in bacteria, purified, and used for the analysis of RNA-protein interactions in gel mobility shift assay experiments. The binding sites of both proteins will be mapped by measuring the relative binding activities of each purified protein for different WNV 3′(-)SL RNA mutant probes containing mutations and/or deletions in the three predicted single stranded loops. First, global mapping of the three loops will be done to determine which loop(s) is

essential for binding by deleting or replacing each loop separately or in combination with a track of C residues. Subsequently, fine mapping of the binding sites will be done by mutating A and U nt in the loops.

2. Determine whether the mapped binding site nt are *cis*-acting in the context of a virus infection.

Deletion of either the 3′ or 5′ terminal SL in various flavivirus infectious clones was lethal, which strongly suggested that these regions contain essential *cis*-acting elements for virus replication (Bredenbeek et al., 2003; Cahour et al., 1995; Men et al., 1996). In a previous study, the growth of WNV in cells lacking TIAR was six to eight fold lower than in wild type cells. In TIA-1 knock out cells, WNV grew to peak virus titers 6 hours later than in the wild type cells (Li et al., 2002). These results suggested that both proteins may play a role in the WNV replication cycle. To test this hypothesis more directly, mutations and/or deletions in the mapped TIA-1 and TIAR binding sites within the WNV3′(-)SL will be introduced into the a WNV infectious clone to test the effect of these mutations on virus production. Those mutations and/or deletions found to have a negative effect on virus production will be also tested for their effect on the translational efficiency of the viral RNA in transfected BHK cells by detecting viral antigen production by immunoflourescence. The effect of mutations and/or deletions found to have a negative effect on virus production on the efficiency of viral plus-strand and minus-strand RNA synthesis will be quantified by real-time RT-PCR.

3. Determine whether the TIA-1/TIAR-viral RNA interactions occur *in vivo* and test the effect of WNV infection on cellular SG formation.

In previous *in vitro* RNA-protein interaction assays, the TIA-1/TIAR proteins were shown to bind specifically to the WNV3′(-)SL RNA (Li et al., 2002). The minus-strand RNA of flaviviruses is present in infected cells only in RNA replication complexes (Lindenbach and Rice, 2007). An antibody to dsRNA that does not detect either cellular ribosomal RNA or tRNA was previously utilized to detect flavivirus replication complexes in infected cells (Miller, Sparacio, and Bartenschlager, 2006). To test whether TIA-1/TIAR colocalize with viral dsRNA and/or viral protein(s) in infected cells, BHK cells will be infected with WNV and incubated with anti-WNV hyperimmune serum or anti-dsRNA and anti-TIA-1 or anti-TIAR antibody and colocalization of cell and viral proteins will be analyzed by confocal microscopy.

A number of detailed studies have shown that TIA-1 and TIAR are core components of SG and that they recruit cell mRNAs into cytoplasmic foci formed in response to stress factors (Kedersha et al., 2002). Sequestration of cell mRNAs in SG leads to repression of their translation until the cells recover from stress or die (Kedersha et al., 2002). To determine the effect of WNV infection on cellular SG formation, BHK infected with WNV will be treated with sodium arsenite to induce SG at different times after infection and SG will be detected by confocal microscopy.

REFERENCES

Ackermann, M., and Padmanabhan, R. (2001). De novo synthesis of RNA by the dengue virus RNA-dependent RNA polymerase exhibits temperature dependence at the initiation but not elongation phase. *J Biol Chem* **276**(43)**,** 39926-37.

Amberg, S. M., Nestorowicz, A., McCourt, D. W., and Rice, C. M. (1994). NS2B-3 proteinase-mediated processing in the yellow fever virus structural region: in vitro and in vivo studies. *J Virol* **68**(6)**,** 3794-802.

Anderson, P. (1995). TIA-1: structural and functional studies on a new class of cytolytic effector molecule. *Curr Top Microbiol Immunol* **198,** 131-43.

Anderson, P., and Kedersha, N. (2006). RNA granules. *J Cell Biol* **172**(6)**,** 803-8.

Asnis, D. S., Conetta, R., Teixeira, A. A., Waldman, G., and Sampson, B. A. (2000). The West Nile Virus outbreak of 1999 in New York: the Flushing Hospital experience. *Clin Infect Dis* **30**(3)**,** 413-8.

Bashkirov, V. I., Scherthan, H., Solinger, J. A., Buerstedde, J. M., and Heyer, W. D. (1997). A mouse cytoplasmic exoribonuclease (mXRN1p) with preference for G4 tetraplex substrates. *J Cell Biol* **136**(4)**,** 761-73.

Beck, A. R., Medley, Q. G., O'Brien, S., Anderson, P., and Streuli, M. (1996). Structure, tissue distribution and genomic organization of the murine RRM-type RNA binding proteins TIA-1 and TIAR. *Nucleic Acids Res* **24**(19)**,** 3829-35.

Beck, A. R., Miller, I. J., Anderson, P., and Streuli, M. (1998). RNA-binding protein TIAR is essential for primordial germ cell development. *Proc Natl Acad Sci U S A* **95**(5)**,** 2331-6.

Borowski, P., Niebuhr, A., Mueller, O., Bretner, M., Felczak, K., Kulikowski, T., and Schmitz, H. (2001). Purification and characterization of West Nile virus

nucleoside triphosphatase (NTPase)/helicase: evidence for dissociation of the NTPase and helicase activities of the enzyme. *J Virol* **75**(7)**,** 3220-9.

Bray, M., and Lai, C. J. (1991). Dengue virus premembrane and membrane proteins elicit a protective immune response. *Virology* **185**(1)**,** 505-8.

Bredenbeek, P. J., Kooi, E. A., Lindenbach, B., Huijkman, N., Rice, C. M., and Spaan, W. J. (2003). A stable full-length yellow fever virus cDNA clone and the role of conserved RNA elements in flavivirus replication. *J Gen Virol* **84**(Pt 5)**,** 1261-8.

Brinton, M. A. (2002). The molecular biology of West Nile Virus: a new invader of the western hemisphere. *Annu Rev Microbiol* **56,** 371-402.

Brinton, M. A., and Dispoto, J. H. (1988). Sequence and secondary structure analysis of the 5'-terminal region of flavivirus genome RNA. *Virology* **162**(2)**,** 290-9.

Brinton, M. A., Fernandez, A. V., and Dispoto, J. H. (1986). The 3'-nucleotides of flavivirus genomic RNA form a conserved secondary structure. *Virology* **153**(1)**,** 113-21.

Cahour, A., Falgout, B., and Lai, C. J. (1992). Cleavage of the dengue virus polyprotein at the NS3/NS4A and NS4B/NS5 junctions is mediated by viral protease NS2B-NS3, whereas NS4A/NS4B may be processed by a cellular protease. *J Virol* **66**(3)**,** 1535-42.

Cahour, A., Pletnev, A., Vazielle-Falcoz, M., Rosen, L., and Lai, C. J. (1995). Growth-restricted dengue virus mutants containing deletions in the 5' noncoding region of the RNA genome. *Virology* **207**(1)**,** 68-76.

Chambers, T. J., Grakoui, A., and Rice, C. M. (1991). Processing of the yellow fever virus nonstructural polyprotein: a catalytically active NS3 proteinase domain and NS2B are required for cleavages at dibasic sites. *J Virol* **65**(11)**,** 6042-50.

Chambers, T. J., Hahn, C. S., Galler, R., and Rice, C. M. (1990). Flavivirus genome organization, expression, and replication. *Annu Rev Microbiol* **44,** 649-88.

Chambers, T. J., Nestorowicz, A., Amberg, S. M., and Rice, C. M. (1993). Mutagenesis of the yellow fever virus NS2B protein: effects on proteolytic processing, NS2B-NS3 complex formation, and viral replication. *J Virol* **67**(11)**,** 6797-807.

Chu, P. W., and Westaway, E. G. (1985). Replication strategy of Kunjin virus: evidence for recycling role of replicative form RNA as template in semiconservative and asymmetric replication. *Virology* **140**(1)**,** 68-79.

Cleaves, G. R., Ryan, T. E., and Schlesinger, R. W. (1981). Identification and characterization of type 2 dengue virus replicative intermediate and replicative form RNAs. *Virology* **111**(1)**,** 73-83.

Clum, S., Ebner, K. E., and Padmanabhan, R. (1997). Cotranslational membrane insertion of the serine proteinase precursor NS2B-NS3(Pro) of dengue virus type 2 is required for efficient in vitro processing and is mediated through the hydrophobic regions of NS2B. *J Biol Chem* **272**(49)**,** 30715-23.

Cok, S. J., Acton, S. J., Sexton, A. E., and Morrison, A. R. (2004). Identification of RNA-binding proteins in RAW 264.7 cells that recognize a lipopolysaccharide-responsive element in the 3-untranslated region of the murine cyclooxygenase-2 mRNA. *J Biol Chem* **279**(9)**,** 8196-205.

Cougot, N., Babajko, S., and Seraphin, B. (2004). Cytoplasmic foci are sites of mRNA decay in human cells. *J Cell Biol* **165**(1)**,** 31-40.

Cui, T., Sugrue, R. J., Xu, Q., Lee, A. K., Chan, Y. C., and Fu, J. (1998). Recombinant dengue virus type 1 NS3 protein exhibits specific viral RNA binding and NTPase activity regulated by the NS5 protein. *Virology* **246**(2)**,** 409-17.

Dember, L. M., Kim, N. D., Liu, K. Q., and Anderson, P. (1996). Individual RNA recognition motifs of TIA-1 and TIAR have different RNA binding specificities. *J Biol Chem* **271**(5)**,** 2783-8.

Dixon, D. A., Balch, G. C., Kedersha, N., Anderson, P., Zimmerman, G. A., Beauchamp, R. D., and Prescott, S. M. (2003). Regulation of cyclooxygenase-2 expression by the translational silencer TIA-1. *J Exp Med* **198**(3)**,** 475-81.

Dong, H., Ray, D., Ren, S., Zhang, B., Puig-Basagoiti, F., Takagi, Y., Ho, C. K., Li, H., and Shi, P. Y. (2007). Distinct RNA elements confer specificity to flavivirus RNA cap methylation events. *J Virol*.

Droll, D. A., Krishna Murthy, H. M., and Chambers, T. J. (2000). Yellow fever virus NS2B-NS3 protease: charged-to-alanine mutagenesis and deletion analysis define regions important for protease complex formation and function. *Virology* **275**(2)**,** 335-47.

Eystathioy, T., Chan, E. K., Tenenbaum, S. A., Keene, J. D., Griffith, K., and Fritzler, M. J. (2002). A phosphorylated cytoplasmic autoantigen, GW182, associates with a unique population of human mRNAs within novel cytoplasmic speckles. *Mol Biol Cell* **13**(4)**,** 1338-51.

Eystathioy, T., Jakymiw, A., Chan, E. K., Seraphin, B., Cougot, N., and Fritzler, M. J. (2003). The GW182 protein colocalizes with mRNA degradation associated proteins hDcp1 and hLSm4 in cytoplasmic GW bodies. *Rna* **9**(10)**,** 1171-3.

Falgout, B., and Markoff, L. (1995). Evidence that flavivirus NS1-NS2A cleavage is mediated by a membrane-bound host protease in the endoplasmic reticulum. *J Virol* **69**(11)**,** 7232-43.

Falgout, B., Miller, R. H., and Lai, C. J. (1993). Deletion analysis of dengue virus type 4 nonstructural protein NS2B: identification of a domain required for NS2B-NS3 protease activity. *J Virol* **67**(4)**,** 2034-42.

Falgout, B., Pethel, M., Zhang, Y. M., and Lai, C. J. (1991). Both nonstructural proteins NS2B and NS3 are required for the proteolytic processing of dengue virus nonstructural proteins. *J Virol* **65**(5)**,** 2467-75.

Gilks, N., Kedersha, N., Ayodele, M., Shen, L., Stoecklin, G., Dember, L. M., and Anderson, P. (2004). Stress granule assembly is mediated by prion-like aggregation of TIA-1. *Mol Biol Cell* **15**(12)**,** 5383-98.

Gollins, S. W., and Porterfield, J. S. (1985). Flavivirus infection enhancement in macrophages: an electron microscopic study of viral cellular entry. *J Gen Virol* **66 (Pt 9),** 1969-82.

Gollins, S. W., and Porterfield, J. S. (1986). pH-dependent fusion between the flavivirus West Nile and liposomal model membranes. *J Gen Virol* **67 (Pt 1),** 157-66.

Gubler, D. J. (2002). Epidemic dengue/dengue hemorrhagic fever as a public health, social and economic problem in the 21st century. *Trends Microbiol* **10**(2)**,** 100-3.

Gueydan, C., Droogmans, L., Chalon, P., Huez, G., Caput, D., and Kruys, V. (1999). Identification of TIAR as a protein binding to the translational regulatory AU-rich element of tumor necrosis factor alpha mRNA. *J Biol Chem* **274**(4)**,** 2322-6.

Hall, R. A., Khromykh, A. A., Mackenzie, J. M., Scherret, J. H., Khromykh, T. I., and Mackenzie, J. S. (1999). Loss of dimerisation of the nonstructural protein NS1 of Kunjin virus delays viral replication and reduces virulence in mice, but still allows secretion of NS1. *Virology* **264**(1)**,** 66-75.

Heinz, F. X., and Allison, S. L. (2000). Structures and mechanisms in flavivirus fusion. *Adv Virus Res* **55,** 231-69.

Heinz, F. X., Auer, G., Stiasny, K., Holzmann, H., Mandl, C., Guirakhoo, F., and Kunz, C. (1994). The interactions of the flavivirus envelope proteins: implications for virus entry and release. *Arch Virol Suppl* **9,** 339-48.

Heinz, F. X., Purcell, M. S., Gould, E. A., Howard, C. R., Houghton, M., et al. (2000). Family Flaviviridae. In: van Regenmorteel, M. H. V., Fauquet, C. M., Bishop, D.H.L., Carstens, E. B., Estes, M. K., Lemon, S. M., et al., (Eds.), Virus Taxonomy: classification and nomenclature of viruses, San Diego: Academic press, 860-78.

Kandasamy, K., Joseph, K., Subramaniam, K., Raymond, J. R., and Tholanikunnel, B. G. (2005). Translational control of beta2-adrenergic receptor mRNA by T-cell-restricted intracellular antigen-related protein. *J Biol Chem* **280**(3)**,** 1931-43.

Kapoor, M., Zhang, L., Ramachandra, M., Kusukawa, J., Ebner, K. E., and Padmanabhan, R. (1995). Association between NS3 and NS5 proteins of dengue virus type 2 in the putative RNA replicase is linked to differential phosphorylation of NS5. *J Biol Chem* **270**(32)**,** 19100-6.

Kawakami, A., Tian, Q., Duan, X., Streuli, M., Schlossman, S. F., and Anderson, P. (1992). Identification and functional characterization of a TIA-1-related nucleolysin. *Proc Natl Acad Sci U S A* **89**(18)**,** 8681-5.

Kedersha, N., and Anderson, P. (2002). Stress granules: sites of mRNA triage that regulate mRNA stability and translatability. *Biochem Soc Trans* **30**(Pt 6)**,** 963-9.

Kedersha, N., Chen, S., Gilks, N., Li, W., Miller, I. J., Stahl, J., and Anderson, P. (2002). Evidence that ternary complex (eIF2-GTP-tRNA(i)(Met))-deficient preinitiation complexes are core constituents of mammalian stress granules. *Mol Biol Cell* **13**(1)**,** 195-210.

Kedersha, N., Stoecklin, G., Ayodele, M., Yacono, P., Lykke-Andersen, J., Fritzler, M. J., Scheuner, D., Kaufman, R. J., Golan, D. E., and Anderson, P. (2005). Stress granules and processing bodies are dynamically linked sites of mRNP remodeling. *J Cell Biol* **169**(6)**,** 871-84.

Kedersha, N. L., Gupta, M., Li, W., Miller, I., and Anderson, P. (1999). RNA-binding proteins TIA-1 and TIAR link the phosphorylation of eIF-2 alpha to the assembly of mammalian stress granules. *J Cell Biol* **147**(7)**,** 1431-42.

Khromykh, A. A., Sedlak, P. L., and Westaway, E. G. (1999). trans-Complementation analysis of the flavivirus Kunjin ns5 gene reveals an essential role for translation of its N-terminal half in RNA replication. *J Virol* **73**(11)**,** 9247-55.

Koonin, E. V. (1993). Computer-assisted identification of a putative methyltransferase domain in NS5 protein of flaviviruses and lambda 2 protein of reovirus. *J Gen Virol* **74 (Pt 4),** 733-40.

Kuhn, R. J., Zhang, W., Rossmann, M. G., Pletnev, S. V., Corver, J., Lenches, E., Jones, C. T., Mukhopadhyay, S., Chipman, P. R., Strauss, E. G., Baker, T. S., and Strauss, J. H. (2002). Structure of dengue virus: implications for flavivirus organization, maturation, and fusion. *Cell* **108**(5)**,** 717-25.

Lai, M. M. (1998). Cellular factors in the transcription and replication of viral RNA genomes: a parallel to DNA-dependent RNA transcription. *Virology* **244**(1)**,** 1-12.

Le Guiner, C., Gesnel, M. C., and Breathnach, R. (2003). TIA-1 or TIAR is required for DT40 cell viability. *J Biol Chem* **278**(12)**,** 10465-76.

Lewis, T., Gueydan, C., Huez, G., Toulme, J. J., and Kruys, V. (1998). Mapping of a minimal AU-rich sequence required for lipopolysaccharide-induced binding of a 55-kDa protein on tumor necrosis factor-alpha mRNA. *J Biol Chem* **273**(22)**,** 13781-6.

Li, W., Li, Y., Kedersha, N., Anderson, P., Emara, M., Swiderek, K. M., Moreno, G. T., and Brinton, M. A. (2002). Cell proteins TIA-1 and TIAR interact with the 3' stem-loop of the West Nile virus complementary minus-strand RNA and facilitate virus replication. *J Virol* **76**(23)**,** 11989-2000.

Lindenbach, B. D., and Rice, C. M. (1997). trans-Complementation of yellow fever virus NS1 reveals a role in early RNA replication. *J Virol* **71**(12)**,** 9608-17.

Lindenbach, B. D., and Rice, C. M. (1999). Genetic interaction of flavivirus nonstructural proteins NS1 and NS4A as a determinant of replicase function. *J Virol* **73**(6)**,** 4611-21.

Lindenbach, B. D., and Rice, C. M. (2007). Flaviviridae: The viruses and their replication. In: Fields, B. N., Knipe, D. N., Howley, P. M., Griffin, D. E., Martin,

M. A., Lamb, R. A., Roizman, B., Straus, S. E., (Eds.), Fields Virology, 5th ed., Lippincott William and Wilkins, Philadelphia, Pennsylvania, pp. 1101-52.

Liu, W. J., Chen, H. B., and Khromykh, A. A. (2003). Molecular and functional analyses of Kunjin virus infectious cDNA clones demonstrate the essential roles for NS2A in virus assembly and for a nonconservative residue in NS3 in RNA replication. *J Virol* **77**(14)**,** 7804-13.

Liu, W. J., Chen, H. B., Wang, X. J., Huang, H., and Khromykh, A. A. (2004). Analysis of adaptive mutations in Kunjin virus replicon RNA reveals a novel role for the flavivirus nonstructural protein NS2A in inhibition of beta interferon promoter-driven transcription. *J Virol* **78**(22)**,** 12225-35.

Mackenzie, J. M., Jones, M. K., and Westaway, E. G. (1999). Markers for trans-Golgi membranes and the intermediate compartment localize to induced membranes with distinct replication functions in flavivirus-infected cells. *J Virol* **73**(11)**,** 9555-67.

Mackenzie, J. M., Jones, M. K., and Young, P. R. (1996). Immunolocalization of the dengue virus nonstructural glycoprotein NS1 suggests a role in viral RNA replication. *Virology* **220**(1)**,** 232-40.

Mackenzie, J. M., Khromykh, A. A., Jones, M. K., and Westaway, E. G. (1998). Subcellular localization and some biochemical properties of the flavivirus Kunjin nonstructural proteins NS2A and NS4A. *Virology* **245**(2)**,** 203-15.

Malet, H., Egloff, M. P., Selisko, B., Butcher, R. E., Wright, P. J., Roberts, M., Gruez, A., Sulzenbacher, G., Vonrhein, C., Bricogne, G., Mackenzie, J. M., Khromykh, A. A., Davidson, A. D., and Canard, B. (2007). Crystal Structure of the RNA Polymerase Domain of the West Nile Virus Non-structural Protein 5. *J Biol Chem* **282**(14)**,** 10678-89.

Mandl, C. W., Allison, S. L., Holzmann, H., Meixner, T., and Heinz, F. X. (2000). Attenuation of tick-borne encephalitis virus by structure-based site-specific mutagenesis of a putative flavivirus receptor binding site. *J Virol* **74**(20)**,** 9601-9.

Mandl, C. W., Guirakhoo, F., Holzmann, H., Heinz, F. X., and Kunz, C. (1989). Antigenic structure of the flavivirus envelope protein E at the molecular level, using tick-borne encephalitis virus as a model. *J Virol* **63**(2)**,** 564-71.

Markoff, L., Falgout, B., and Chang, A. (1997). A conserved internal hydrophobic domain mediates the stable membrane integration of the dengue virus capsid protein. *Virology* **233**(1)**,** 105-17.

Men, R., Bray, M., Clark, D., Chanock, R. M., and Lai, C. J. (1996). Dengue type 4 virus mutants containing deletions in the 3' noncoding region of the RNA genome: analysis of growth restriction in cell culture and altered viremia pattern and immunogenicity in rhesus monkeys. *J Virol* **70**(6)**,** 3930-7.

Miller, S., Sparacio, S., and Bartenschlager, R. (2006). Subcellular localization and membrane topology of the Dengue virus type 2 Non-structural protein 4B. *J Biol Chem* **281**(13)**,** 8854-63.

Monath, T. P. (1994). Dengue: the risk to developed and developing countries. *Proc Natl Acad Sci U S A* **91**(7)**,** 2395-400.

Murphy, F. A. (1980). Togavirus morphology and morphogenesis. In: Schlesinger RW, (Ed.), The *Togaviruses*: Biology, Structure, Replication, New York: Academic press, pp. 241-316.

Muylaert, I. R., Galler, R., and Rice, C. M. (1997). Genetic analysis of the yellow fever virus NS1 protein: identification of a temperature-sensitive mutation which blocks RNA accumulation. *J Virol* **71**(1)**,** 291-8.

Nawa, M. (1998). Effects of bafilomycin A1 on Japanese encephalitis virus in C6/36 mosquito cells. *Arch Virol* **143**(8)**,** 1555-68.

Nestorowicz, A., Chambers, T. J., and Rice, C. M. (1994). Mutagenesis of the yellow fever virus NS2A/2B cleavage site: effects on proteolytic processing, viral replication, and evidence for alternative processing of the NS2A protein. *Virology* **199**(1)**,** 114-23.

Nomaguchi, M., Teramoto, T., Yu, L., Markoff, L., and Padmanabhan, R. (2004). Requirements for West Nile virus (-)- and (+)-strand subgenomic RNA synthesis in vitro by the viral RNA-dependent RNA polymerase expressed in Escherichia coli. *J Biol Chem* **279**(13)**,** 12141-51.

Nowak, T., Farber, P. M., Wengler, G., and Wengler, G. (1989). Analyses of the terminal sequences of West Nile virus structural proteins and of the in vitro translation of these proteins allow the proposal of a complete scheme of the proteolytic cleavages involved in their synthesis. *Virology* **169**(2)**,** 365-76.

Piecyk, M., Wax, S., Beck, A. R., Kedersha, N., Gupta, M., Maritim, B., Chen, S., Gueydan, C., Kruys, V., Streuli, M., and Anderson, P. (2000). TIA-1 is a translational silencer that selectively regulates the expression of TNF-alpha. *Embo J* **19**(15)**,** 4154-63.

Porterfield, J. S. (1996). "Encephalitis viruses and related viruses causing hemorrhagic disease." Encephalitis viruses Academic press, San Diego, CA.

Ray, D., Shah, A., Tilgner, M., Guo, Y., Zhao, Y., Dong, H., Deas, T. S., Zhou, Y., Li, H., and Shi, P. Y. (2006). West Nile virus 5'-cap structure is formed by sequential guanine N-7 and ribose 2'-O methylations by nonstructural protein 5. *J Virol* **80**(17)**,** 8362-70.

Rey, F. A., Heinz, F. X., Mandl, C., Kunz, C., and Harrison, S. C. (1995). The envelope glycoprotein from tick-borne encephalitis virus at 2 A resolution. *Nature* **375**(6529)**,** 291-8.

Rice, C. M., Lenches, E. M., Eddy, S. R., Shin, S. J., Sheets, R. L., and Strauss, J. H. (1985). Nucleotide sequence of yellow fever virus: implications for flavivirus gene expression and evolution. *Science* **229**(4715)**,** 726-33.

Selisko, B., Dutartre, H., Guillemot, J. C., Debarnot, C., Benarroch, D., Khromykh, A., Despres, P., Egloff, M. P., and Canard, B. (2006). Comparative mechanistic studies of de novo RNA synthesis by flavivirus RNA-dependent RNA polymerases. *Virology* **351**(1)**,** 145-58.

Sheth, U., and Parker, R. (2003). Decapping and decay of messenger RNA occur in cytoplasmic processing bodies. *Science* **300**(5620)**,** 805-8.

Shi, P. Y., Li, W., and Brinton, M. A. (1996). Cell proteins bind specifically to West Nile virus minus-strand 3' stem-loop RNA. *J Virol* **70**(9)**,** 6278-87.

Shope, R. E. (1980). Medical significance of togaviruses: an overview of diseases caused by togaviruses in man and in domestic and wild vertebrate animals. In: Schlesinger RW, (Ed.), The togaviruses, New York: Academic press, pp. 47-83.

Smith, G. W., and Wright, P. J. (1985). Synthesis of proteins and glycoproteins in dengue type 2 virus-infected vero and Aedes albopictus cells. *J Gen Virol* **66 (Pt 3),** 559-71.

Stadler, K., Allison, S. L., Schalich, J., and Heinz, F. X. (1997). Proteolytic activation of tick-borne encephalitis virus by furin. *J Virol* **71**(11)**,** 8475-81.

Stollar, V., Stevens, T. M., and Schlesinger, R. W. (1966). Studies on the nature of dengue viruses. II. Characterization of viral RNA and effects of inhibitors of RNA synthesis. *Virology* **30**(2)**,** 303-12.

Tan, B. H., Fu, J., Sugrue, R. J., Yap, E. H., Chan, Y. C., and Tan, Y. H. (1996). Recombinant dengue type 1 virus NS5 protein expressed in Escherichia coli exhibits RNA-dependent RNA polymerase activity. *Virology* **216**(2)**,** 317-25.

Trent, D. W., Swensen, C. C., and Qureshi, A. A. (1969). Synthesis of Saint Louis encephalitis virus ribonucleic acid in BHK-21-13 cells. *J Virol* **3**(4)**,** 385-94.

Uchil, P. D., and Satchidanandam, V. (2003). Architecture of the flaviviral replication complex. Protease, nuclease, and detergents reveal encasement within double-layered membrane compartments. *J Biol Chem* **278**(27)**,** 24388-98.

van Dijk, E., Cougot, N., Meyer, S., Babajko, S., Wahle, E., and Seraphin, B. (2002). Human Dcp2: a catalytically active mRNA decapping enzyme located in specific cytoplasmic structures. *Embo J* **21**(24)**,** 6915-24.

Vasudevan, S. G., Johansson, M., Brooks, A. J., Llewellyn, L. E., and Jans, D. A. (2001). Characterisation of inter- and intra-molecular interactions of the dengue virus RNA dependent RNA polymerase as potential drug targets. *Farmaco* **56**(1-2)**,** 33-6.

Vazquez, S., Guzman, M. G., Guillen, G., Chinea, G., Perez, A. B., Pupo, M., Rodriguez, R., Reyes, O., Garay, H. E., Delgado, I., Garcia, G., and Alvarez, M. (2002). Immune response to synthetic peptides of dengue prM protein. *Vaccine* **20**(13-14)**,** 1823-30.

Wengler, G., and Wengler, G. (1989). Cell-associated West Nile flavivirus is covered with E+pre-M protein heterodimers which are destroyed and reorganized by proteolytic cleavage during virus release. *J Virol* **63**(6)**,** 2521-6.

Wengler, G., and Wengler, G. (1993). The NS 3 nonstructural protein of flaviviruses contains an RNA triphosphatase activity. *Virology* **197**(1)**,** 265-73.

Westaway, E. G., Khromykh, A. A., Kenney, M. T., Mackenzie, J. M., and Jones, M. K. (1997a). Proteins C and NS4B of the flavivirus Kunjin translocate independently into the nucleus. *Virology* **234**(1)**,** 31-41.

Westaway, E. G., Khromykh, A. A., and Mackenzie, J. M. (1999). Nascent flavivirus RNA colocalized in situ with double-stranded RNA in stable replication complexes. *Virology* **258**(1)**,** 108-17.

Westaway, E. G., Mackenzie, J. M., Kenney, M. T., Jones, M. K., and Khromykh, A. A. (1997b). Ultrastructure of Kunjin virus-infected cells: colocalization of NS1 and NS3 with double-stranded RNA, and of NS2B with NS3, in virus-induced membrane structures. *J Virol* **71**(9)**,** 6650-61.

Westaway, E. G., Mackenzie, J. M., and Khromykh, A. A. (2003). Kunjin RNA replication and applications of Kunjin replicons. *Adv Virus Res* **59,** 99-140.

Westaway, E. G., Schlesinger, R. W., Dalrymple, J. M., and Trent, D. W. (1980). Nomenclature of flavivirus-specified proteins. *Intervirology* **14**(2)**,** 114-7.

Wilczynska, A., Aigueperse, C., Kress, M., Dautry, F., and Weil, D. (2005). The translational regulator CPEB1 provides a link between dcp1 bodies and stress granules. *J Cell Sci* **118**(Pt 5)**,** 981-92.

Winkler, G., Maxwell, S. E., Ruemmler, C., and Stollar, V. (1989). Newly synthesized dengue-2 virus nonstructural protein NS1 is a soluble protein but becomes partially hydrophobic and membrane-associated after dimerization. *Virology* **171**(1)**,** 302-5.

Winkler, G., Randolph, V. B., Cleaves, G. R., Ryan, T. E., and Stollar, V. (1988). Evidence that the mature form of the flavivirus nonstructural protein NS1 is a dimer. *Virology* **162**(1)**,** 187-96.

Yamshchikov, V. F., and Compans, R. W. (1994). Processing of the intracellular form of the west Nile virus capsid protein by the viral NS2B-NS3 protease: an in vitro study. *J Virol* **68**(9)**,** 5765-71.

Yon, C., Teramoto, T., Mueller, N., Phelan, J., Ganesh, V. K., Murthy, K. H., and Padmanabhan, R. (2005). Modulation of the nucleoside triphosphatase/RNA helicase and 5'-RNA triphosphatase activities of Dengue virus type 2 nonstructural protein 3 (NS3) by interaction with NS5, the RNA-dependent RNA polymerase. *J Biol Chem* **280**(29)**,** 27412-9.

Zhang, L., Mohan, P. M., and Padmanabhan, R. (1992). Processing and localization of Dengue virus type 2 polyprotein precursor NS3-NS4A-NS4B-NS5. *J Virol* **66**(12)**,** 7549-54.

Zhang, T., Delestienne, N., Huez, G., Kruys, V., and Gueydan, C. (2005). Identification of the sequence determinants mediating the nucleo-cytoplasmic shuttling of TIAR and TIA-1 RNA-binding proteins. *J Cell Sci* **118**(Pt 23)**,** 5453-63.

Zhou, Y., Ray, D., Zhao, Y., Dong, H., Ren, S., Li, Z., Guo, Y., Bernard, K. A., Shi, P. Y., and Li, H. (2007). Structure and Function of Flavivirus NS5 Methyltransferase. *J Virol* **81**(8)**,** 3891-903.

CHAPTER II

Mutation of mapped TIA-1/TIAR binding sites within the West Nile virus 3′ terminal minus-strand RNA sequence in an infectious clone negatively affects viral plus-strand synthesis.

ABSTRACT

The 75 nt 3′ terminal stem loop (SL) of the West Nile virus minus-strand (WNV3′(-)SL) RNA was previously shown to bind specifically to T-cell intracellular antigen-1 (TIA-1) and the related protein TIAR. TIA-1 and TIAR were also reported to bind specifically to relatively long AU-rich sequences in the 3′UTRs of some cellular mRNAs. Three single-stranded loops (L1, L2, and L3) in the predicted WNV3′(-)SL RNA secondary structure each contain a single short AU stretch. Both TIA-1 and TIAR recombinant proteins bound less efficiently in *in vitro* gel mobility shift assays to WNV3′(-)SL RNA with the L1 or L2 UAAUU sequences deleted or substituted with Cs. The minimal binding site for both proteins in either L1 or L2 was UAA. In contrast, neither deletion of UAA in L3 nor substitution of L3 with Cs affected the binding of either protein. Deletion or C substitution of the entire AU-rich sequence in either L1 or L2 within the 3′(-) SL RNA in a WNV infectious clone was lethal. Analysis of mutants with partial deletions or substitutions in these sequences showed that AU sequences were needed in both L1 and L2. Immunofluorescence imaging of viral RNA transfected cells 3 hr post transfection showed that mutant viral RNAs with either small plaque or lethal phenotypes expressed similar amounts of viral proteins as wildtype RNA. In contrast, the

efficiency of plus-strand RNA synthesis correlated well with the efficiency of *in vitro* protein binding efficiency. Also, for each of the primary and secondary site revertants obtained, increased virus viability correlated with restoration of a protein binding site. These data support the hypothesis that the interaction between TIA-1/TIAR and the WNV3′(-)SL RNA facilitates the initiation of genome RNA synthesis from the minus-strand template.

INTRODUCTION

West Nile virus (WNV) is a spherical, enveloped virion that belongs to the family F*laviviridae,* genus *flavivirus* (Lindenbach and Rice, 2007). The WNV genome is a single-stranded positive sense RNA of approximately 11 kb in length. The viral genome has a 5′ type I cap, but no 3′ poly(A) tail. It contains a single, long open reading frame (ORF) and serves as the only viral mRNA during WNV replication. Viral replication takes place in the cytoplasm of the infected cells. The viral polyprotein is co- and posttranslationally processed by viral and cellular proteases into three structural (capsid, membrane and envelope) proteins and seven nonstructural [NS1, NS2a, NS2b, NS3, NS4a, NS4b, and NS5] proteins. The 5′end of the genome encodes the structural proteins, while the 3′ end of the genome encodes the nonstructural proteins (Lindenbach and Rice, 2007). The RNA genome also serves as the template for transcription of the complementary minus-strand RNA, which in turn serves as a template for the synthesis of nascent plus-strand genomic RNA. In infected cells, the minus-strand RNA is present only in association with the plus-strand RNA as a replicative form (RF) or a replicative

intermediate (RI) (Lindenbach and Rice, 2007). Previous evidence suggests that plus-strand RNA templates synthesize only a single minus-strand RNA at a time (RF), while minus-strand templates are efficiently reinitiated simultaneously synthesizing multiple copies of plus-strand RNA (RI) (Chu and Westaway, 1985). Plus and minus-strand RNA synthesis is disproportionate. About 10 to 100 times more plus-strand RNA than the minus-strand RNA is produced (Brinton, 2002).

The 5′noncoding region (NCR) of the WNV genome RNA is 96 nucleotides (nt) long while the 3′NCR is 631 nt in length (Chambers et al., 1990). Evidence supporting the formation of conserved stem-loop (SL) structures by the 3′terminal nt of the flavivirus genome (Brinton and Dispoto, 1988; Brinton, Fernandez, and Dispoto, 1986; Chambers et al., 1990) and the 3′ terminal nt of the complementary minus-strand (Shi, Li, and Brinton, 1996) was previously obtained by RNase structure probing. Deletion of either the 3′or 5′ terminal SL in flavivirus infectious clones was lethal strongly suggesting that these regions contain essential *cis*-acting elements for virus replication (Bredenbeek et al., 2003; Cahour et al., 1995; Men et al., 1996). Previous studies using purified *in vitro* expressed WNV NS5 in RdRP *in vitro* assay indicated that the terminal 230 nt of the 3′minus-strand RNA alone is sufficient for plus-strand RNA synthesis (Nomaguchi et al., 2004).

The WNV3′(-)SL RNA was previously reported to bind specifically to four hamster cell proteins of about 42, 50, 60, and 108 kDa (Shi, Li, and Brinton, 1996). p42 was identified as T-cell intracellular antigen related protein (TIAR) (Li et al., 2002). The closely related T-cell intracellular antigen-1 (TIA-1) protein (p42), was subsequently also

shown to bind to the WNV3′(-)SL RNA in gel mobility shift assays, but with a 10 fold lower efficiency (Li et al., 2002).

Although first discovered in T cells, TIA-1 (Anderson et al., 1990) and TIAR (Kawakami et al., 1992) have subsequently been shown to be expressed in most types of cells and tissues (Beck et al., 1996; Jin et al., 2000). Both proteins are found in the cytoplasm and the nucleus and shuttle between these two compartments. These evolutionarily conserved cellular proteins are multifunctional and have been reported to regulate alternative splicing (Dirksen, Mohamed, and Fisher, 2003; Shukla et al., 2005; Shukla et al., 2004; Yu et al., 2003; Zhu et al., 2003), to silence translation (Dixon et al., 2003; Kandasamy et al., 2005; Piecyk et al., 2000), to regulate Fas-mediated apoptosis (Li et al., 2004; Taupin et al., 1995; Tian et al., 1995), to sequester cytoplasmic mRNAs into stress granules (Kedersha et al., 2000; Kedersha et al., 1999) and to be functionally important during embryonic development (Beck et al., 1998; Piecyk et al., 2000). For homozygous TIAR knockouts, embryo lethality was 100% in BALB/c mice and 90% in C57BL/6 mice. In both mouse strains, the rate of embryonic lethality for homozygous TIA-1 knockouts was 50% (Piecyk et al., 2000). Attempts to knockout both proteins in mice were unsuccessful (Piecyk et al., 2000) and suppression of both TIA-1 and TIAR expression in DT40 chicken cells resulted in cell death (Le Guiner, Gesnel, and Breathnach, 2003).

TIA-1 and TIAR are members of the RNA recognition motif (RRM) family of RNA binding proteins (Anderson, 1995). Both proteins contain three N-terminal RRMs and a C-terminal glutamine-rich auxiliary domain (Kawakami et al., 1992; Tian et al., 1991).

The C-terminal domain was reported to be structurally similar to the prion domain (Gilks et al., 2004; Kawakami et al., 1992; Tian et al., 1991). TIA-1 and TIAR share 80% overall amino acid (aa) identity with the highest degree of similarity (91% identity) in the third RRM and the lowest (51% identity) in the C-terminal domain (Anderson, 1995; Beck et al., 1996; Kawakami et al., 1992). Although RRM2 is sufficient for the specific binding of either protein to linear uridylate-rich RNA *in vitro*, RRM1 and RRM3 enhance RRM2 RNA binding (Dember et al., 1996). In somatic cells, RRM2 and the first half of the C-terminal domain mediate TIA-1 and TIAR nuclear accumulation, whereas RRM3 facilitates nuclear export (Zhang et al., 2005).

Two isoforms of both TIA-1 and TIAR are translated from alternatively spliced mRNAs (Beck et al., 1996). The two TIA-1 isoforms differ by the presence (TIA-1a) or absence (TIA-1b) of a mini exon encoding 11 aa within RRM1. TIARa includes a mini exon that encodes 17 aa within RRM1, whereas TIARb lacks this exon. The molecular masses of the long isoforms of both proteins are ~ 42 kDa, whereas those of the short isoforms are ~ 40 kDa (Beck et al., 1996). The two TIA-1 isoforms are equally abundant in cells, while the short isoform of TIAR is 6 times more abundant than the long isoform (Beck et al., 1996).

In this study, the binding sites for TIA-1 and TIAR within the WNV3′(-)SL RNA secondary structure were mapped to two short single-stranded AU sequences. Mutation of these sequences within a WNV infectious clone showed a correlation between *in vitro* binding and the efficiency of genomic RNA synthesis and virus production. Similar translation efficiencies were observed for wildtype and all of the mutant RNAs.

RESULTS

Expression, purification, and RNA binding activities of recombinant TIA-1 and TIAR.

A previous study reported a specific interaction between the WNV3′(-)SL RNA and both TIA-1 and TIAR but the protein binding sites within the viral RNA were not mapped (Li et al., 2002). TIA-1 and TIAR are ARE binding proteins and have been reported to regulate the translation of a subset of cell mRNAs by binding to 3′UTR AU-rich sequences (Cok et al., 2004; Dixon et al., 2003). The WNV3′(-)SL RNA was predicted to contain three short (3 to 5 nt) AU stretches. The relative importance of each of these AU stretches for TIA-1/TIAR binding was investigated. For these studies, recombinant (r) TIA-1 and TIAR proteins were expressed from a pCRT7/CT-TOPO expression vector in *E. coli* Rosetta cells and partially purified on a cobalt affinity column as described in Materials and Methods (Fig. 2.1A). It was estimated that both recombinant proteins were purified to ~ 85% homogeneity. The presence of purified rTIA-1 or rTIAR protein was confirmed by Western blot analysis using protein specific polyclonal antibodies directed against the C-terminus of each protein (data not shown).

The binding activities of the partially purified proteins were tested in gel mobility shift assays with a WNV3′(-) SL RNA probe as described in Materials and Methods. For TIAR, binding activity was detected at concentrations as low as 5 nM (Fig. 2.1B), whereas for TIA-1 concentrations of ~50 nM were required to detect binding (Fig. 2.1C). This 10-fold difference in binding activity was consistent with data previously reported for recombinant GST fusion proteins (Li et al., 2002). Aggregation of RNA-protein

complexes was observed with both proteins at concentrations of 40-50 nM or higher (Fig. 2.1B and C). Competition gel-shift assays done as described in Materials and Methods were used to confirm the specificity of the interactions between the WNV3′(-)SL RNA and each of the recombinant proteins. For rTIA-1, a small amount of competition was observed only with the highest concentration of the non-specific competitors used [200 fold excess of poly I/C (1.0 ng) (Fig. 2.1D, lane 2, left panel) or 100 fold excess of tRNA (20 nM) (Fig. 2.1D, lane 3, left panel)]. In contrast, competition was observed with concentrations of unlabeled WNV3′(-)SL RNA as low as 0.2 nM (Fig. 2.1D, right panel). The binding efficiencies of two additional viral RNA probes, WNV3′(+)SL and WNV5′(+)SL, were also tested in gel mobility shift assays. rTIA-1 showed no binding to WNV3′(+)SL RNA probe and very low binding to WNV5′(+)SL with the highest concentration of TIA-1 (Fig. 2.1E). Similar results were observed with rTIAR (data not shown). These results demonstrate that among the WNV terminal SL RNAs, only the WNV3′(-)SL RNA binds to TIA-1 and TIAR.

Analysis of the WNV3′(-)SL RNA structure.

Two alternative secondary structures, 3′(-)S1 and 3′(-)S2 (Fig. 2.1F), with similar minimum free energy values were predicted for the 3′ terminal 75 nts of the WNV minus-strand RNA by M-fold version 3.1 (Zuker, 2003). The 3′(-)S1 structure, which contained three single-stranded loops, L1, L2, and L3 was similar to the one previously obtained from structure probing data by Shi et al. (1996). The 3′(-)S2 structure was similar to, but a mirror image of, the optimal structure predicted by M-fold for the first 75

nts of the complementary WNV5′(+)SL RNA (Fig. 2.1F). This structure was the optimal one predicted by M-fold when sequence lengths ranging from 75 to 3000 nt were folded and was also predicted by a whole WNV RNA genome (11,029 nts) fold (Personal communication, Drs. A. Palmenberg and J.-Y. Sgro, University of Wisconsin Madison).

To test which of the two WNV3′(-)SL RNA predicted structures was the optimal one for binding to TIA-1 and TIAR, mutations were introduced to lock the structure into one or the other of the predicted conformations (L2→As and MS2 RNA; Fig. 2.1F). A single optimal M-fold secondary structure was predicted for each of these mutant RNAs. The four RNAs migrated to the same position on a denaturing gel (Fig. 2.1G, left panel), but on the non-denaturing gel (Fig. 2.1G, right panel), the wildtype WNV3′(-)SL RNA and the L2→As RNA migrated to similar positions, while both the WNV5′(+)SL and MS2 RNAs migrated faster. When the binding efficiencies of TIA-1 and TIAR to the MS2 and L2→As RNAs were compared in gel mobility shift assays, minimal binding to the MS2 probe was detected with the highest concentrations of either protein, but both proteins bound efficiently to the L2→As probe (data not shown). Both TIA-1 and TIAR were previously reported to bind to poly(A) (Taupin et al., 1995; Tian et al., 1991). However, TIA-1 binds to poly(A) more efficiently than does TIAR (Kawakami et al., 1992; Taupin et al., 1995). Consistent with these results substituting L2 with As did not alter TIAR binding activity but enhanced TIA-1 binding activity by 8% at a protein concentration of 60 nM (data not shown). Since these results as well as those of Shi et al. (1996) indicated that 3′(-)S1 is the primary secondary structure of the WNV3′(-)SL RNA, this structure was used as the basis for designing mutant RNAs to map the protein binding sites.

Figure 2.1. Purification and RNA binding activities of recombinant TIA-1 and TIAR proteins. (A) Purification of rTIA-1 and rTIAR proteins on a cobalt affinity column followed by separation of the proteins by 10% SDS PAGE. Fractions of rTIAR (lanes 1 and 2) and rTIA-1 (lanes 3 and 4) eluted with 150 mM imidazole. Gel mobility shift assays done with increasing concentrations of (B) rTIAR and (C) rTIA-1 and a ^{32}P-WNV3′(-)SL RNA probe and analyzed on 5% non-denaturing polyacrylamide gels. Lane 1, Free probe (FP); Lanes 2-8, Probe plus the indicated concentration of purified protein. The positions of the RNA-protein complexes (RPC) are indicated by brackets. (D) Representative competition gelshift analyses using 600 nM rTIA-1 protein, ^{32}P-WNV3′(-)SL RNA and an excess of unlabeled non-specific competitor (left panel; Lane 1, FP; Lane 2, poly I/C; Lane 3, tRNA) or increasing concentrations of unlabelled WNV3′(-)SL RNA (right panel; Lane 1, FP; Lane 2, Probe without competitor; Lanes 3–5, Probe plus increasing concentrations of unlabelled specific competitor). (E) Representative gel mobility shift assays done with increasing concentrations of rTIA-1 and a ^{32}P-WNV5′(+)SL RNA probe (upper panel) or a ^{32}P-WNV3′(+)SL RNA probe (lower panel). (F) Secondary structures predicted for the WNV3′(-)SL RNA sequence [3′(-)S1 and 3′(-)S2], the complementary WNV5′(+)SL RNA [5′(+)S], and two mutated WNV3′(-)SL RNAs (L2→As and MS2). ΔG, minimum free energy values calculated for each structure. The three AU-rich loops (L1, L2, and L3) in the 3′(-)S1 RNA are indicated by arrows. AU-rich sequences within these loops are in bold. Substituted nt within these RNAs are indicated by asterisks. G. Migration of four of the ^{32}P RNA probes on denaturing (left panel) and non-denaturing (right panel) polyacrylamide gels. Lanes 1 and 5, MS2; Lanes 2 and 6, L2→As; Lanes 3 and 7, WNV5′(+)SL; and Lanes 4 and 8, wildtypeWNV3′(-)SL.
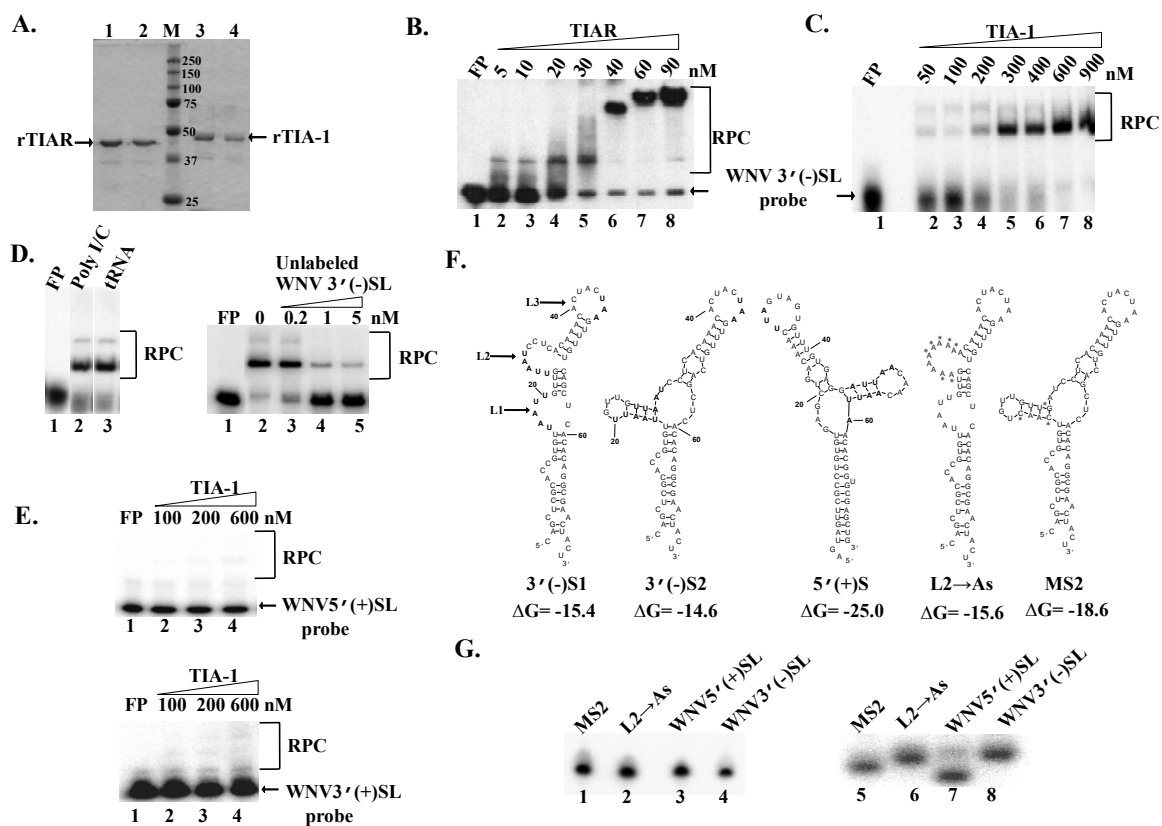
Mapping the binding sites for the TIA-1 and TIAR proteins within the WNV3′(-)SL

RNA.

Both TIA-1 and TIAR were previously reported to bind specifically to AU-rich

regions in the 3′UTRs of a subset of cell mRNAs and the binding region in the TNF-α

mRNA was mapped to a 39 nt AU-rich sequence. The 7 AUUUA repeats within this

sequence were hypothesized to be the protein binding sites (Gueydan et al., 1999; Lewis

et al., 1998). Inspection of the predicted structures of the MS2 and WNV5′(+)SL RNA

(Fig. 2.1F) indicated that the sequence of L3 was identical in the two structures and

contained one AU stretch, 5′UAA3′. In addition to the AU sequence in L3, both the

3′(-)S1 and L2→As structures contained AU or A stretches of 5 to 8 nt in L1 and L2.

These observations suggested that TIA-1 and TIAR can recognize the single-stranded AU

sequences in L1 and/or L2 of the WNV3′(-)SL RNA, but not those in L3.

The A and U nt in each loop were first replaced with Cs. These substitutions were

introduced at positions 16 to 20 (5′UAAUU3′, L1→Cs), at positions 26 to 29

(5′UAAU3′, L2→Cs), at positions 40 to 47 (5′ACUACUAA3′, L3→Cs), and at

positions 16 to 20 plus 26 to 29 (L1+L2→Cs) (Fig. 2.2A). M fold analysis indicated that

the predicted RNA secondary structure of the wildtype RNA was preserved in each of

these mutants. These mutant RNAs were used as probes in gel mobility shift assays with

the recombinant proteins. The gel mobility shift assays shown in this figure and in all

subsequent figures are representative of three replicate experiments. The binding

activities of both of the recombinant proteins for mutant RNAs L1→Cs and L2→Cs were

significantly reduced (Fig. 2B, Lanes 7-10 and 12-15; Fig. 2.2C and D) as compared to

those for the wildtype RNA (Fig. 2B, Lanes 2-5; Fig. 2.2C and D). Even less efficient binding to the L1+L2→Cs RNA was detected with both proteins (Fig. 2.2B, Lanes 17-20; Fig. 2.2C and D). In contrast, the mutant L3→ Cs RNA formed complexes with both proteins (Fig. 2.2B, lanes 22-25) as efficiently as the wildtype RNA (Fig. 2.2C and D).

As an alternative strategy, deletions in each loop were made separately or in combination. Only 3 nt could be deleted in L1 (U_{16}, U_{19}, and U_{20}, pΔL1) or in L3 (U_{45}, A_{46}, and A_{47}, ΔUAAL3) without affecting the predicted RNA secondary structure, while all of L2 (ΔL2) could be deleted (Fig. 2.3A). The reduction in binding observed for the pΔL1 and ΔL2 RNAs (Fig. 3B, lanes 7-10 and 12-15; Fig. 2.3C and D) was similar to that observed with the L1→Cs and L2→Cs RNAs (Fig. 2.2). No rTIA-1 RNA-protein complexes were detected with the pΔL1,ΔL2 RNA (Fig. 2.3B, upper panel, lanes 17-20; Fig. 2.3C) and minimal rTIAR binding was detected with this RNA (Fig. 2.3B, lower panel, lane 20; Fig. 2.3D). As observed with the L3→ Cs RNA, the binding activities of both proteins for the ΔUAAL3 RNA were similar to those for the wildtype RNA (Fig. 2.3B, lanes 22-25; Fig. 2.3C and D). These results indicate that AU sequences need to be present in both L1 and L2 for either TIA-1 and TIAR to bind efficiently to the WNV3′(-)SL RNA *in vitro*.

To determine the minimum sequence in each loop required for TIA-1 and TIAR binding, the nt deleted in the pΔL1 plus ΔL2 RNA were next sequentially restored. RNA with U_{20} restored was designated pΔL1+U,ΔL2 and RNA with both U_{19} and U_{20} restored
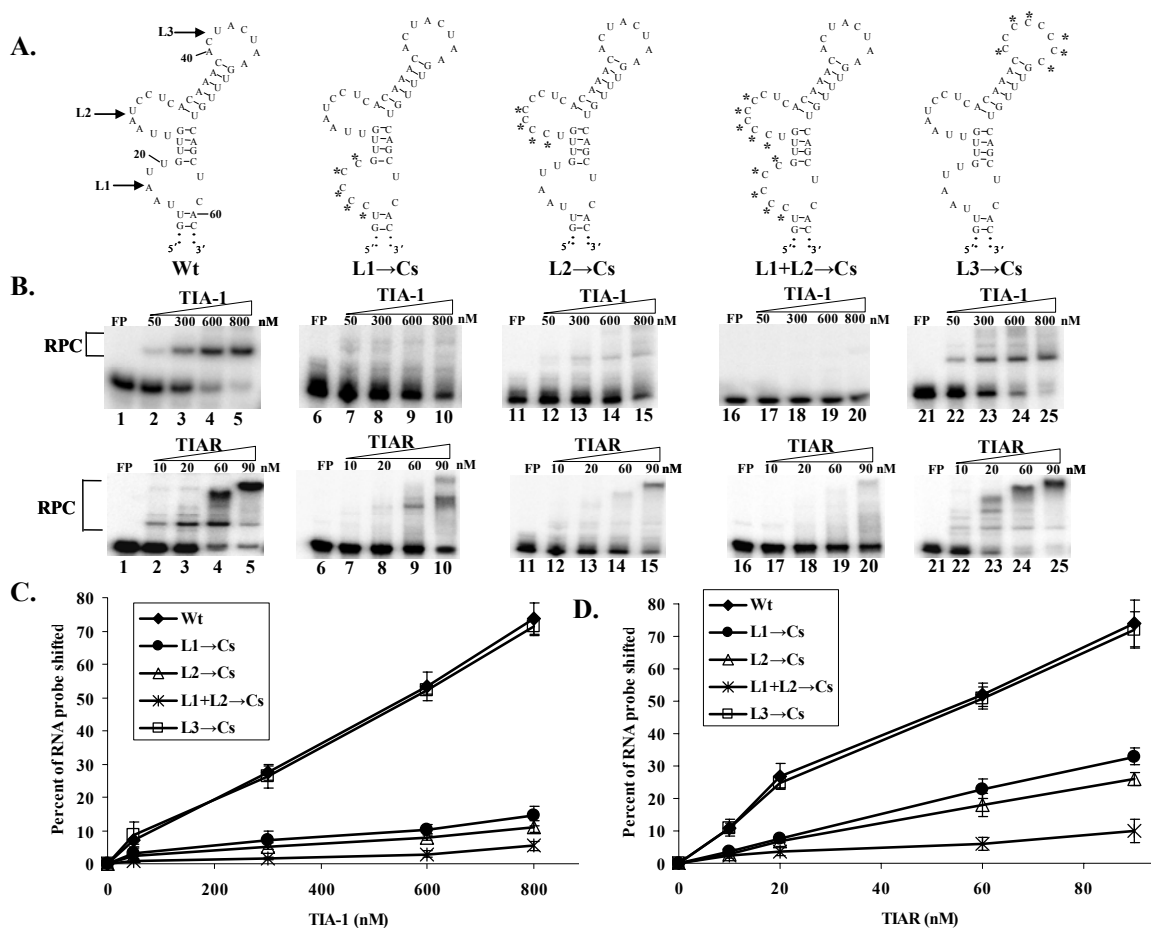
Figure 2.2. Effect of C substitutions in L1, L2, and L3 of the WNV3′(-)SL RNA on *in vitro* rTIA-1 and rTIAR binding activity. (A) Predicted secondary structures of the mutant RNAs. Substituted nt are indicated by asterisks. (B) Representative gel mobility shift assays with rTIA-1(upper panel) or rTIAR (lower panel) and each mutant RNA probe. Lanes 1-5, wildtype RNA; Lanes 6-10, L1→Cs RNA; Lanes 11-15, L2→Cs RNA; Lanes 16-20, L1+L2→Cs RNA; and Lanes 21-25, L3→Cs RNA. Gel mobility shift assays were done with increasing concentrations of each purified protein. In this and the subsequent figures the average percent RNA probe shifted was calculated from triplicate experiments and plotted against the concentration of (C) rTIA-1 or (D) rTIAR. Error bars indicate standard deviation of the mean.
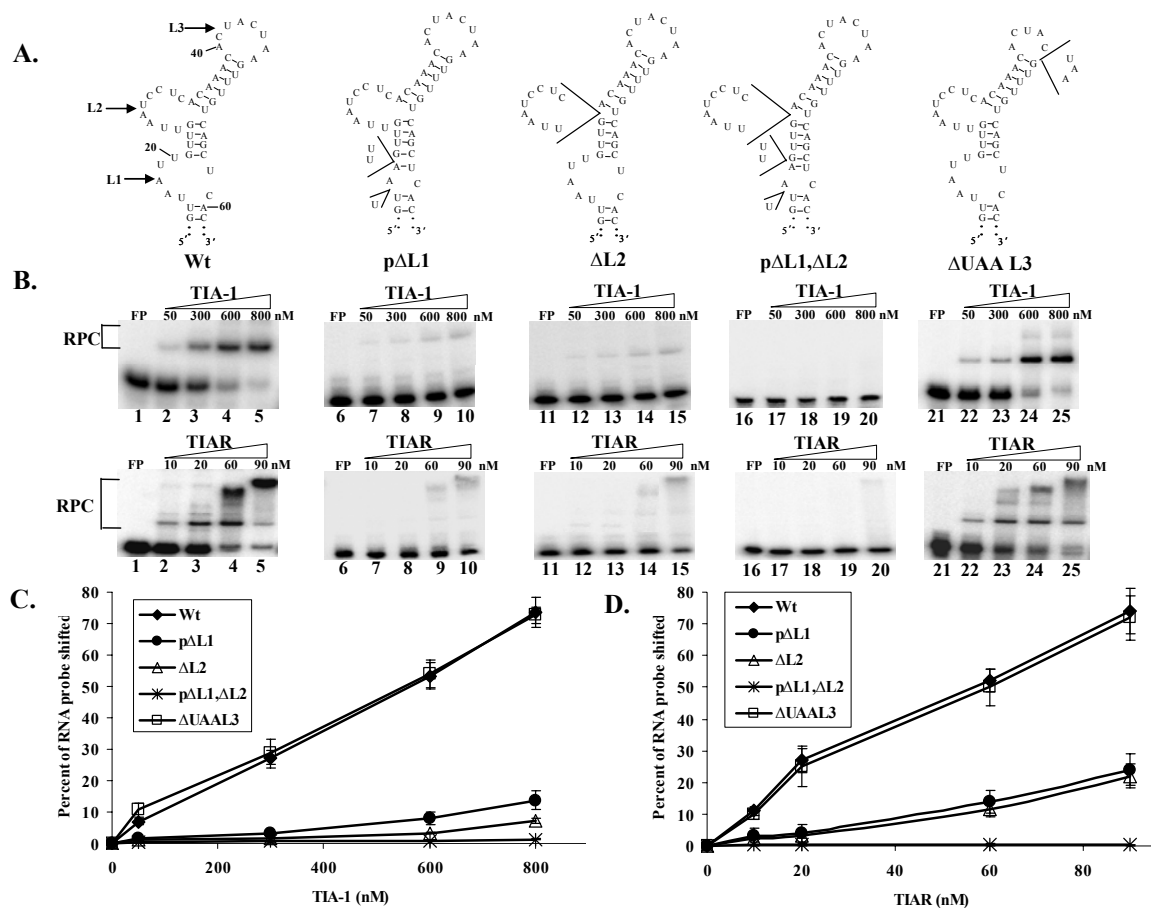
Figure 2.3. Effect of deletions in L1, L2, or L3 of the WNV3′(-)SL RNA on *in vitro* rTIA-1 and rTIAR binding activity. (A) Predicted secondary structures of the mutant RNAs. Only U nucleotides in L1 and UAA in L3 could be deleted without altering the predicted RNA secondary structure. Deleted nt are indicated by wedges. (B) Representative gel mobility shift assays with rTIA-1 (upper panel) or rTIAR (lower panel) and each mutant RNA probe. Lanes 1-5, wildtype RNA; Lanes 6-10, RNA with Us deleted in L1; Lanes 11-15, RNA with L2 deleted; Lanes 16-20, RNA with Us in L1 and L2 deleted; and Lanes 21-25, RNA with UAA in L3 deleted. (C) and (D) Percent RNA probe shifted.

was designated pΔL1+UU,ΔL2 (Fig. 2.4A). A slight increase in the percent of RNA probe shifted was observed with the restoration of U$_{19}$ and the restoration of both U$_{19}$ and U$_{20}$ further increased the binding efficiency of both proteins (Fig. 2.4C and D). Sequential restoration of U$_{25}$, U$_{26}$, A$_{27}$, and A$_{28}$ in the pΔL1,ΔL2 RNA was done in RNA probes designated pΔL1,ΔL2+U, pΔL1,ΔL2+UU, pΔL1,ΔL2+UUA, and pΔL1,ΔL2+UUAA, respectively (Fig. 2.4B). No increase in the binding activity of either protein was observed until three nt (5$'$UUA3$'$) had been restored to either L1 or L2 of the pΔL1,ΔL2 RNA (Fig. 2.4E and F). Further increases in the binding activities of both proteins were observed with the pΔL1,ΔL2+UUAA, ΔL2, and pΔL1 RNAs (Fig. 2.4E and F). As expected the binding activity observed with all of these RNAs was less efficient than when two functional binding sites were present.

Effect of substitution of L1 and L2 with Cs on virus production.

The mapping experiments described above indicated that the AU sequences in both L1 and L2 are required for efficient TIA-1 or TIAR binding to the WNV3$'$(-)SL RNA. The previous observation that the replication of WNV was reduced by 6- to 8-fold in TIAR knockout cells compared to control cells (Li et al., 2002) suggested that this viral RNA-cell protein interaction played a role in virus replication. To test this hypothesis more directly, mutations and/or deletions were introduced into L1 and/or L2 in a WNV infectious clone. Cs were substituted for Us or As in L1 or L2. First, individual substitutions were introduced at positions U$_{16}$, A$_{18}$, and U$_{20}$ in L1 to generate L1U16$\rightarrow$C,
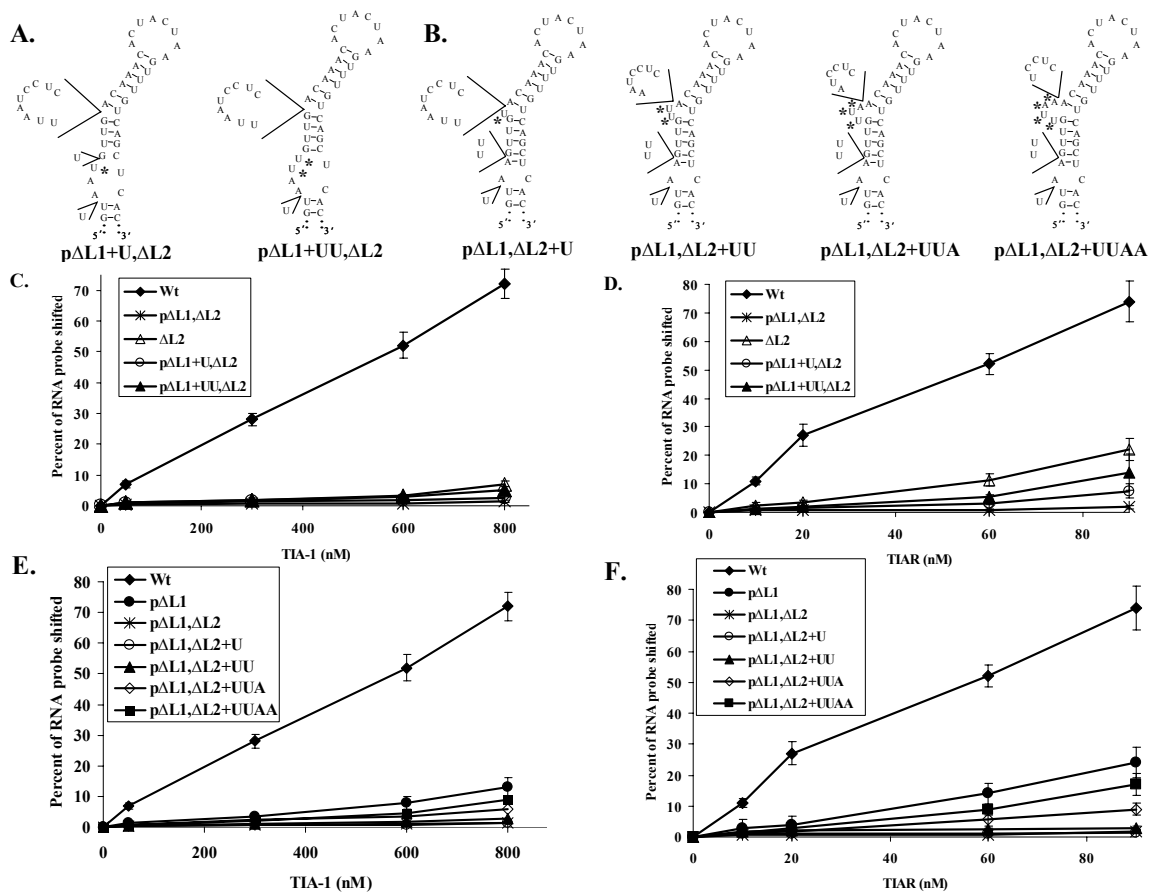
Figure 2.4. Effect of sequential restoration of deleted nt in L1 and L2 on *in vitro* rTIA-1 and rTIAR binding activity. Predicted secondary structures of (A) U_{19} and U_{20} or (B) U_{25}, U_{26}, A_{27}, and A_{28} sequentially restored in pΔL1,ΔL2 RNA. Restored nt are indicated by asterisks. (C), (D), (E), and (F) Percent RNA probe shifted.

L1A18→C, and L1U20→C RNAs (Fig. 2.5A), respectively, and at positions U_{25}, U_{26}, A_{27}, and U_{29} in L2 to create L2U25→C, L2U26→C, L2A27→C, and L2U29→C RNAs (Fig. 2.5C), respectively. None of these mutations were predicted to alter the secondary structure of the WNV3′(-)SL RNA. The L1U16→C viral RNA produced virus with a small plaque phenotype, whereas pinpoint plaques were observed with L2A27→C and L1A18→C RNAs (Fig. 2.5B and D). After one passage, sequence of these mutants and for L2A27→C also on the transfection plate, large plaques similar in size to those of the wildtype virus were observed and sequence analysis of the viral RNA extracted from these plaques showed that the introduced mutation had reverted to the wildtype sequence. An altered 3′(-)SL structure was predicted for (L1U19→C) (Fig. 2.5A), which was similar to that of MS2 (Fig. 2.1F). Only a few pinpoint plaques were observed by 72 hr after transfection of this RNA (Fig. 5B). After the first passage, large size plaques were observed and analysis of the sequence of viral RNA extracted from these plaques showed that C_{19} had reverted to the wildtype U. In contrast, L1U20→C, L2U26→C, and L2U29→C had no effect on plaque size or virus growth (Fig. 2.5B and D).

No plaques were detected at 72 hr after transfection of a viral RNA that had both U_{16} and A_{18} substituted with Cs (L1U16+A18→C) (Fig. 2.5B), but after one passage, both small plaques and pinpoint plaques were observed (data not shown). In RNA extracted from the small plaques, C_{16} had reverted to the wildtype U. In RNA extracted from the pinpoint plaques, C_{18} had reverted to the wildtype A. These two revertants were found in about equal abundance. Viral RNA containing both A_{27} and U_{29} substituted with C (L2U27+U29→C) produced virus with a pinpoint plaque phenotype. After one passage,

large plaques were observed (Fig. 2.5D) and in RNA extracted from these plaques only C_{27} had reverted to the wildtype A_{27} (equivalent to L2U29→C). Finally, substitutions were introduced at positions 16 through 20 (L1→Cs) (Fig. 2.5A), at positions 25 through 29 (L2→Cs), and at positions 40 through 47 (L3→Cs) (Fig. 5C). As observed with the pΔL1, ΔL2, or ΔL3 RNAs, the L1→Cs, L2→Cs and L3→Cs mutants were lethal (Fig. 2.5B and D). The observation that the mutations L1A18→C, L2U27→C, and L2U27+U29→C had a pinpoint plaque phenotype even though they had only two consecutive As or Us in either L1 or L2 suggested that when the AU sequence of one of these loops is intact, 2 nt of AU sequence in the other loop or either side of a C provided a sufficient amount of TIA-1 and TIAR binding to give a low level of virus production (pinpoint plaques). To test this hypothesis, L1A18→C, L2U27→C, and L2U27+U29→C 3′(-)SL RNAs were transcribed and used as probes in gel mobility shift assays with rTIA-1 or rTIAR. Both proteins bound less efficiently to these mutant RNAs than to the wild type RNA. Decreases of 7, 8, and 13% in the binding activity of rTIAR (60 nM) were observed with L2U27→C, L1A18→C, and L2U27+U29→C mutant RNAs, respectively, as compared to the wild type RNA (data not shown). The binding activity of rTIA-1 (600 nM) for the L2U27→C, L1A18→C, and L2U27+U29→C mutant RNAs was 9, 11, and 15% lower than that for the wild type RNA, respectively (data not shown). These results confirm that TIA-1 and/or TIAR binding could also occur when a single C interrupted the AU stretches in either L1 or L2.
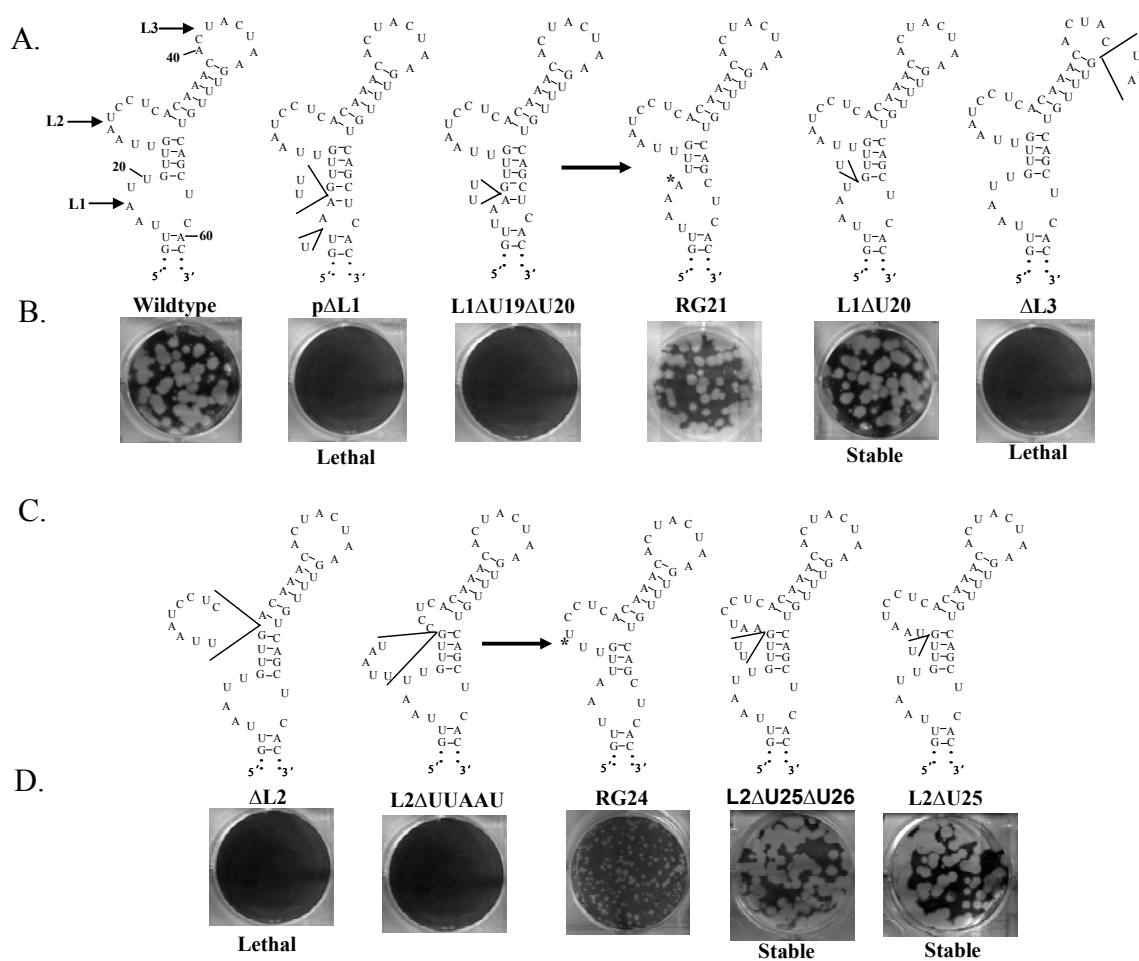
Figure 2.5. Effect of C substitutions in L1, L2, or L3 of the WNV3′(-)SL RNA on virus production. (A) and (C) Predicted secondary structures of the mutant RNAs. Substituted nt are indicated by asterisks. (B) and (D) Plaques produced by either the wildtype infectious clone RNA or the mutant RNAs by 72 hr on an RNA transfection well.

Effect of deletion of A and U nt in the mapped WNV3′(−)SL RNA TIA-1 and TIAR binding sites in a WNV infectious clone.

As an alternative mutational strategy, deletion of each loop was done separately or in combination (Fig. 2.6A and C). Only 3 nt could be deleted in L1 (U_{16}, U_{19}, and U_{20}, pΔL1), while all of L2 could be deleted (ΔL2), without affecting the predicted RNA secondary structure (Fig. 2.6C). Deletion of both U_{19} and U_{20} in L1 or 5′UAAUU3′ in L2 created the L1$\Delta U_{19}U_{20}$ and L2ΔUAAUU RNAs, respectively (Fig. 2.6A and C). BHK monolayers were transfected with wildtype or mutant infectious clone RNA as described in Materials and Methods and virus plaques produced by 72 hr after transfection in the overlayed transfection plates were assayed. No plaques were observed in plates transfected with pΔL1, ΔL2, L1$\Delta U_{19}U_{20}$, or L2ΔUAAUU RNA (Fig. 2.6B and D).

To test whether any of the mutant RNAs that produced no plaques by 72 hr after transfection still grew to a low level and could revert, culture media harvested from a non-overlayed duplicate well was serially passaged three times in BHK cells and the infectivity of the 72 hr harvest from each passage was assessed by plaque assay. Also, the viral RNA in each passage supernatant was extracted, amplified by RT-PCR, and the cDNA was sequenced. For pΔL1 and ΔL2, neither viral plaques nor viral RNA was detected after any of the passages. In contrast, after the first passage, large plaques were observed with L1$\Delta U_{19}U_{20}$, while pinpoint plaques were observed with L2ΔUAAUU (Fig. 2.6B and D). RNA extracted from the L1$\Delta U_{19}U_{20}$ large plaque virus contained a second site mutation G_{21} to A (RG$_{21}$) (Fig. 2.6A), whereas RNA extracted from the ΔUAAUUL2 pinpoint plaque virus contained a second site mutation G_{24} to a U (RG24) (Fig. 2.6C).

Both of these mutations altered the secondary structure so that either three adjacent As or Us were present in the loop that was mutated (Fig. 2.6A and C). In RG21, the G21A mutation created a new L1 sequence of 4 nt (5′UAAA3′) and reduced the number of base pairs between L1 and L2 from 4 to 3. In contrast, in RG24, L1 was reduced from 5 to 3 nt (5′UAA3′) and the other 2 nt (5′UU3′) in L1 became part of the stem between L1 and L2 (5′UUU3′), L2 increased from 4 to 7 nt, and the number of base pairs between L1 and L2 decreased by 1. Deletion of a single U from either L1 or L2 (U_{20} in L1, L1ΔU20 or U_{25} in L2, L2ΔU25) or 2 Us from L2 (U_{25} and U_{26}, L2ΔU25Δ26) had no effect on virus growth (Fig. 2.6B and D). In each of these mutants, a minimum sequence of UAA was still present in both L1 and L2. AU sequences in L1 and L2 that were 3 nt in length gave detectable TIA-1 and TIAR binding *in vitro*, but viral RNA with an AU sequence in only L1 or L2 was not viable. These results suggested that the minimal levels of TIA-1/TIAR *in vitro* binding detected when 2 or 3 AU nt were present in L1 or L2, was not sufficient to support virus production. Although deletion of 5′UAA3′ in L3 (ΔL3) had no effect on TIA-1 and TIAR binding *in vitro* (see Fig. 2.3), this deletion was lethal in the infectious clone (Fig. 2.6D), suggesting that the L3 sequence or its complement may be involved in other essential interactions.

Effect of mutations in the WNV3′(-)SL RNA on the viral RNA translation.

Although the sequence of the terminal SL at the 5′end of the genome is complementary to that of the WNV3′(-)SL RNA the optimal predicted structures formed by these sequences are not mirror images due to G-U base pairing. Mutations introduced
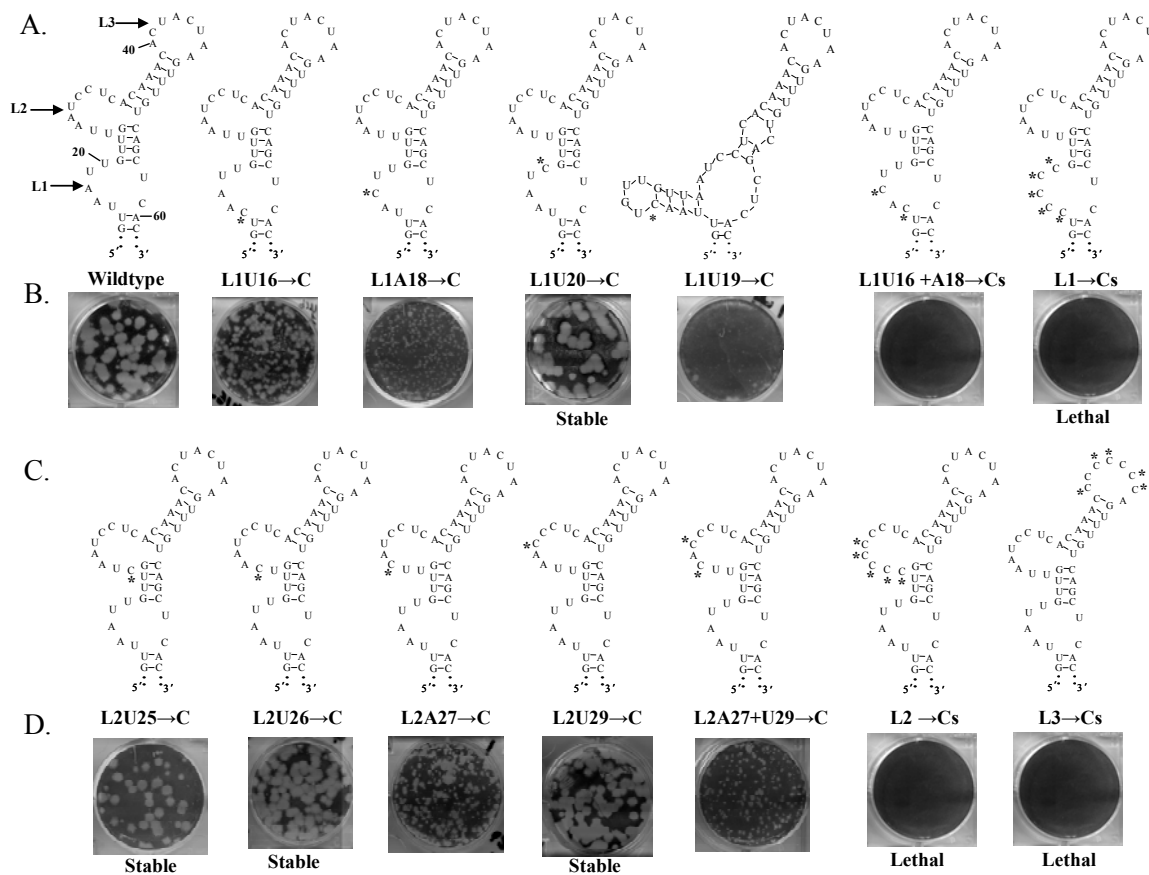
Figure 2.6. Effect of deletion of A and U nucleotides in L1, L2, or L3 of the WNV3′(-)SL RNA on virus production. (A) and (C) Predicted secondary structures of the mutant and the second site mutant RNAs. Only the U nucleotides in L1 and UAA in L3 could be deleted without altering the predicted RNA secondary structure. Deleted nts are shown in wedges. Second site mutations are indicated by asterisks. (B) and (D) Plaques produced by either the wildtype infectious clone RNA, the mutant RNAs, or second site mutant RNAs by 72 hr on an RNA transfection well.

in the WNV3′(-)SL RNA therefore might alter the complementary 5′(+)SL RNA, which in turn could affect the efficiency of translation initiation from the 5′ sequence of the genomic RNA. To determine the effect of the L1 or L2 mutations on viral RNA translation, BHK cells were transfected with either wildtype RNA or selected mutant viral RNAs. At 3 hr posttransfection, cells were fixed, permeabilized, incubated with anti-WNV hyperimmune serum, and then visualized by immunofluorescence microscopy as described in Materials and Methods. After transfection with wildtype RNA, bright WNV protein staining was observed throughout the cytoplasm in about 90% of the cells (Fig. 2.7A). No fluorescence was observed in the mock-infected cells. A similar distribution of viral antigen as well as a similar intensity of fluorescence (Fig. 2.7A) was detected after transfection of either L1U16→C RNA, which produced small plaques, L1A18→C RNA, which produced pin point plaques, L2ΔU25 RNA, which produced wildtype plaques, pΔL1, ΔL2, and L1→Cs RNAs, all of which had a lethal phenotype, indicating that none of these mutations introduced affected translation efficiency.

Relative quantification of viral RNA replication by real-time RT-PCR.

The WNV3′(-)SL RNA is thought to contain *cis*-acting elements for the initiation of plus-strand RNA synthesis and if this is the case, mutations in this region would be expected to affect the efficiency of plus-strand RNA synthesis. To determine the effect of mutations in the WNV3′(-)SL L1 and L2 regions on plus-strand RNA synthesis, total cell RNA was extracted from BHK cells at 6, 48, and 72 hr after transfection with wildtype or selected mutant viral RNAs and the amount of viral plus-strand RNA was

quantified by real-time RT-PCR using primers targeting the NS1 region. GADPH mRNA was used to normalize variation between samples and the viral RNA levels were normalized to the amount of input viral RNA detected at 6 hr post transfection. After transfection of the wildtype RNA, an increase in intracellular plus-strand RNA over input RNA was observed by 48 hr and further increased by 72 hr post transfection (Fig. 2.7B). Similar plus-strand RNA levels were observed with the L2ΔU25 mutant RNA, which produced wildtype plaques. With the L1U16→ C mutant RNA, which produced small plaques, about 10-fold less plus-strand RNA was detected by 72 hr after transfection (Fig. 2.7B). Even ~30-fold less plus-strand RNA levels were detected by 72 hr with L1A18→ C mutant RNA, which produced pinpoint plaques (Fig. 2.7B). No increase in plus-strand RNA over input viral RNA was observed after transfection of the three RNAs with lethal mutations, pΔL1, ΔL2, and L1→Cs (Fig. 2.7B). Intracellular viral minus-strand RNA levels were quantified at 2, 12, and 24 hr after transfection of wildtype or mutant RNA using a strand-specific real-time RT-PCR protocol as described in Materials and Methods. Minus-strand RNA levels were calibrated to the amount of signal detected at 2 hr after transfection, the majority of which was due to non-specific detection of plus-strand input RNA. Therefore this normalization stringently removed nonspecific background. An increase in the levels of minus-strand RNA over background was observed at 12 hr after transfection with wildtype RNA and further increased by 24 hr. The minus-strand RNA levels detected for both of the mutant RNAs L1U16→ C and L2ΔU25 were similar to those for the wildtype RNA (Fig. 2.7C). With the L1A18→ C
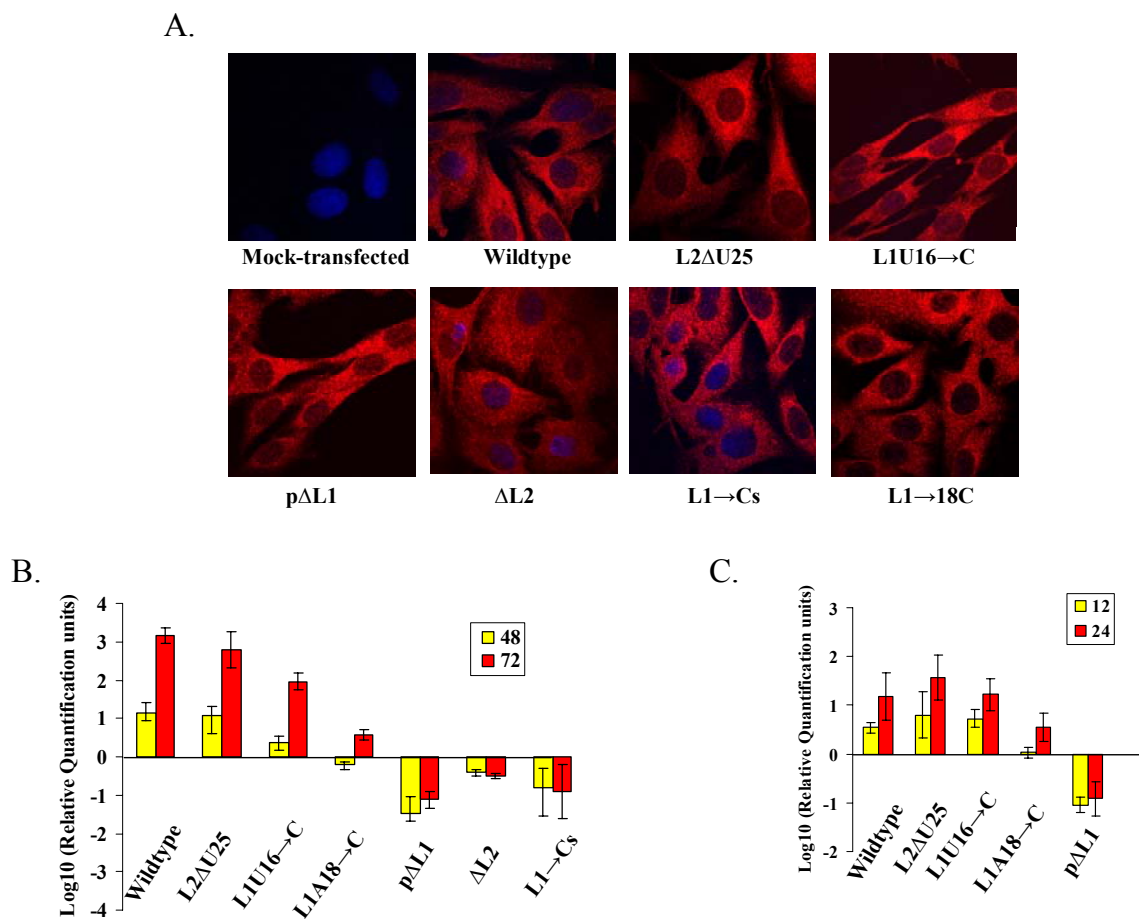
Figure 2.7. Effect of the introduced mutations in L1 or L2 within the WNV3′(-)SL RNA on viral RNA transcription and/or translation. (A) Immunofluorescences imaging of BHK cells that were transfected with wt-, or mutant infectious clone RNA or mock-transfected, and at 3 hr were fixed, permeabilized and incubated with anti-WNV hyperimmune serum (red). Nuclear DNA (blue) was stained with Hoechst 33258 dye. (B) Relative quantification of the levels of the intracellular viral genomic RNA at 6, 48, and 72 hr post transfection of BHK cells with either wildtype or mutant infectious clone RNA by quantitative real-time RT-PCR. (C) Relative quantification of the levels of viral minus-strand RNA at 2, 12, and 24 hr post transfection of either wildtype or mutant infectious clone RNA by strand-specific, real-time RT-PCR.

mutant RNA, which produced pin point plaques, about 4-fold less minus-strand RNA was detected by 12 and 24 hr after transfection (Fig. 2.7C). No increase in the minus-strand RNA levels over background was observed after pΔL1 RNA transfection (Fig. 2.7C). These results showed that the levels of plus-strand RNA synthesis but not of minus-strand RNA correlated well with mutant virus viability as well as with the relative efficiency of TIA-1 and/or TIAR binding in *in vitro* assays.

DISCUSSION

A previous study reported that the cellular proteins, TIA-1 and TIAR, bound specifically to the WNV3′(-) SL RNA (Li et al., 2002). In the present study, the binding sites on the WNV3′(-)SL RNA required for efficient *in vitro* TIA-1 and TIAR binding were fine mapped to two single-stranded UAAUU sequences present in opposite orientation in two adjacent loops, L1 and L2 and a minimum sequence of two A and/or U nt was shown to be required for detectable protein binding to the WNV3′(-)SL RNA probe. This is the first study to fine map binding sites for these proteins.

Although the WNV5′(+)SL RNA contains AU sequences complementary to the TIA-1 and TIAR binding sites in the WNV3′(-)SL RNA, neither protein bound to the 5′(+)SL RNA. Similar results were obtained with the 3′(-)SL mutant RNA, MS2, which has a predicted structure similar to that of the WNV5′(+)SL. In both of these RNAs, the AU sequences were located in double-stranded regions. These observations indicate that TIA-1 and TIAR recognize AU sequences only when they are single-stranded. A previous SELEX study identified 20 RNA sequences that bound to TIA-1 and 20 that

bound to TIAR from random pools of RNA sequences (Dember et al., 1996). About 90% of these RNAs contained at least one U tract of 3 to 11 nts but all of them contained one or more AU sequences. Based on their frequency, the authors proposed that at least one U stretch of at least 3 nts in length was essential for TIA-1 and TIAR protein binding. However, they did not predict the structures of these RNAs. Folds generated using M-fold, version 3.1 (data not shown) for these SELEX selected RNA sequences indicated that there were two or more single-stranded loops in each of these RNA. The majority of these loops contained AU sequences and a few contained U stretches, suggesting that various AU sequences as well as U tracts were the TIA1- or TIAR binding sites in these RNAs.

According to the ARE-mRNA database (ARED) (http://rc.kfshrc.edu.sa/ared/), ARE-mRNAs are classified in one of five clusters depending on the number of canonical AUUUA motifs within their 3′UTRs. mRNAs in clusters I, II, III, and IV contain five, four, three, or two overlapping AUUUA motifs, respectively, whereas cluster V mRNAs contain only one AUUUA. The WNV3′(-)SL RNA does not contain an AUUUA consensus sequence but has two UAAUU sequences that are present in opposite orientation to each other and separated by four base pairs (Fig. 2.1F, 3′(-)S1). The results of the present study indicate that TIA-1 and TIAR can bind efficiently to the WNV3′(-)SL RNA only when two UAAUU sequences are present in L1 and L2. A previous study using Sendai virus RNA showed that TIAR can bind to the viral genome trailer sequence UUUUAAAUUUU. This sequence also does not contain a AUUUA motif (Iseni et al, 2002). Among the cell mRNAs reported to bind TIA-1 and TIAR, the

3′UTRs of both TNF-α and COX-2 mRNAs have been classified as cluster III ARE sequences (http://rc.kfshrc.edu.sa/ared/). TIA-1 also binds to the 3′UTR of cytochrome *c* (Kawai et al., 2006), which has been classified as a cluster V ARE sequence and both TIA-1 and TIAR were reported to bind to the 3′UTR of the β_2-AR mRNA (Kandasamy et al., 2005), which does not contain any conconical AUUUA sequences. Differences in the relative binding activities of TIA-1 and TIAR for different mRNAs could be mediated by different AU sequences.

A significant decrease in the binding of either TIA-1 or TIAR was observed when either AU nt in L1 or L2, but not L3, was deleted. L1 and L2 each contain a UAAUU sequence whereas L3 contains UAA. TIA-1 and TIAR each contain three adjacent N-terminal RRMs. It is not known how many of these RRMs interact with regions of an RNA during an efficient RNA-protein interaction. The spacing as well as the spatial orientation of multiple single-stranded binding sites presented in the context of an RNA structure may be important in determining how many of the RRMs contact an RNA. Evidence from the present study suggests that one TIA-1 or TIAR molecule can simultaneously contact the WNV3′(-) SL RNA at both the L1 and L2 AU sequences. The UAA in L3 is located at the 3′ end of this loop and may not be in an optimal spatial orientation on the RNA helix for protein binding or alternatively, it may be located too far away from L2 for an RRM to bind at this site.

The binding activity of both TIA-1 and TIAR was affected to a greater degree by deletion or mutation of L2 than by the same changes in L1. The larger size of L2 may provide increased flexibility required for an efficient protein interaction. Recent structural

analyses of RNA-protein complexes formed between polypyrimidine tract binding protein, a protein with four RNA binding domains (RBDs), and pre-mRNAs showed that each of the four RBDs bound to a separate pyrimidine tract in the same pre-mRNA forming bridges that looped out regions of sequence thus protecting them from splicing (Oberstrass et al., 2005). RRM2 in both TIA-1 and TIAR has been shown to account for the majority of the binding activity for short U-rich RNAs, but the binding affinity of both proteins increased when either of the other two RRMs was present (Dember et al., 1996).

The 3′(-)SL is thought to function as the promoter for the initiation of plus-strand RNA from the minus strand RNA template. In this study, evidence was obtained indicating that the mapped TIA-1/TIAR binding sites function as *cis*-acting sequences for plus-strand synthesis. In gel mobility shift assays elimination of the L1 and L2 AU nt in the WNV3′(-)SL RNA by deletion or substitution with Cs reduced *in vitro* binding of TIA-1/TIAR to barely detectable levels. The binding activity of TIA-1 and TIAR was resumed with sequential restoration of A or U nt in pΔL1 plus ΔL2 mutant RNA. For example, in mutant RNAs that have L1 deleted with one U, two Us, three AU, four AU, and five AU nt sequentially restored in L2, the binding activity of rTIAR (60 nM) sequentially increased 0.7, 1, 4.5, 8, and 14% than that of pΔL1,ΔL2 mutant RNA, respectively. The results obtained from the *in vitro* gel mobility shift assays of TIA-1/TIAR with various WNV3′(-)SL mutant RNA probes correlated very well to the effect on virus growth when these mutations/deletions were introduced into a WNV infectious clone. Deletion or C substitution of the entire AU-rich sequence in either L1 or

L2 was lethal. Deletion of a single U from either loop or 2 Us in L2 that left the wildtype UUAAU in one loop and 3 or 4 AU nt in the other loop, produced viable virus with wildtype plaque phenotype. When the L1 AU sequences were shortened to 2 AU nt in mutant $L1\Delta U_{19}U_{20}$, no plaques were detected on the transfection plates but after one passage a second site mutation (RG21) occurred at G21 so that after structural rearrangement 3 sequential As were present in L1. Similarly, when L2 contained only one U nt in mutant $L2\Delta UAAUU$, no plaques were detected on the transfection plate, however, a second site mutation (RG24) occurred in G24 leading to a structural rearrangement of 3 AU nt in L1 and 3 sequential Us in L2. Although both RG21 and RG24 were viable, these second site mutations produced virus with different plaque phenotypes. Like other mutant RNAs that left the wildtype UUAAU in one loop and 3 or 4 AU nt in the other loop, RG21 that contained 4 nt (5′UAAA3′) in L1 and the wildtype sequence (5′UUAAU3′) in L2 produced virus with wildtype plaque phenotype. In contrast, RG24 that contained a shorter L1 with 3 nt (5′UAA3′) and a shorter L2 that contained only 3 U nt (5′UUU3′) produced virus with pinpoint plaque phenotype. A single nt substitution to a C in either L1 or L2 leaving the wildtype UUAAU in one loop and only two adjacent UU or two adjacent AU in the other loop also produces a viable virus with a pinpoint plaque phenotype. A low but detectable TIA-1 and TIAR binding activity was observed for these mutant RNAs in *in vitro* gel mobility shift assays. In contrast, a single nt substitution with a C in either loop that left the wildtype UUAAU in one loop and 3 or 4 adjacent AU nt in the other loop, produced viable virus with larger plaque phenotype. These data suggest that as TIA-1 and TIAR binding efficiency to the

WNV3′(-) SL RNA decreases, the size of the plaque produced also decreases. A previous study on the RNA binding protein, U1A, suggested that the flexibility of an RNA loop as well as the placement of positively charged protein residues were important for facilitating the initial interaction of an RNA with a protein by allowing the correct orientation of the RNA backbone within the protein RNA binding site (Katsamba, Myszka, and Laird-Offringa, 2001). It is possible that the lower number of A/U nt in either L1 and L2 in mutant RNAs that produced virus with pinpoint plaques interfere with the flexibility and/or the correct orientation of L1 and/or L2 to be compatible with the RNA binding site and thus reduce the efficiency of TIA-1 and/or TIAR binding.

The minimal binding activity of TIA-1 and TIAR to the WNV3′(-)SL RNA mutants consistently correlated with the undetectable intracellular viral genomic and minus-strand RNA synthesis detected when cells were transfected with a WNV infectious clone RNA with the same mutations. When no intracellular viral genomic or minus-strand RNA was detected, no virus production was also observed. In contrast, mutant L1A18→C, which produced a pin point plaque phenotype and bound to TIA-1 and TIAR with a lower efficiency than did the wildtype RNA (data not shown) produced levels of intracellular viral genomic RNA that were 30 fold lower than those produced by the wildtype infectious clone. This mutant RNA produced levels of minus-strand RNA, which are only 4 fold lower than that of the wildtype RNA. The results suggest that TIA-1 and/or TIAR may function as transcription factors for the initiation of WNV plus-strand RNA synthesis. The WNV3′(-)SL RNA-TIA-1/TIAR protein interactions might aid the viral replication complex in recognizing the 3′ end of the minus strand template and/or assist

in the formation or stabilization of the 3′ terminal minus SL. For poliovirus, another plus-strand RNA virus, interactions between several cellular proteins and the terminal 3′ cloverleaf structure of the minus-strand RNA have also been postulated to be important for the initiation of genomic RNA synthesis. (Brunner et al., 2005; Roehl and Semler, 1995).

A type I cap is added to the 5′ end of the WNV genome. Cap methylation must occur before a cap can function in promoting translation (Muthukrishnan et al., 1975). The C-terminal portion of WNV NS5 is the RNA dependent RNA polymerase (RdRp), while the N-terminal part is a methyltransferase (Koonin, 1993). *A recent mutational analysis of the terminal 74 nt WNV5′(+)SL structure showed that substitution of the sequences complementary to the L1 and L2 sequences ,which were designated Hd and Lb, had no effect on cap N-7 methylation by NS5 (Dong et al., 2007), indicating that these AU sequences were not necessary for capping of the genomic RNA. In contrast, the second and third nt of the viral genome as well as the bottom two helices of the WNV5′(+)SL RNA structure, which were designated Ha and Hb, were found to be required for N-7 methylation. Also, a minimum sequence of 20 nt in the 5′(+)SL that includes the first and the second nt was essential for 2′-OH ribose methylation (Dong et al., 2007). In the present study, the effect of all the mutations/deletions introduced into a WNV infectious clone on the predicted secondary structure of WNV5′(+)SL RNA were analyzed (data not shown). None of these mutations/deletions change any of the critical elements shown to be important for capping by either N-7 methylation or 2′-OH ribose methylation by NS5 (Dong et al., 2007), however, some of them contained a shorter or

single-stranded Hd. These mutations/deletions that showed changes in Hd did not have consistent plaque phenotype but rather different phenotypes that varies from lethal to pinpoint or wildtype plaques. These data suggest that mutations/deletions introduced into the complementary WNV5′(+)SL RNA do not correlate with the viral phenotype observed. The complementary AU L1 and L2 sequences within the WNV5′(+)SL RNA are double-stranded and so do not provide binding sites for TIA-1/TIAR as demonstrated with mutant L1U19→C and MS2 RNAs, which both had the L1 and L2 AU sequences in a double stranded context. Although, none of the deletions or mutations introduced into L1 and L2 in the 3′(-)SL RNA had any effect on the translation of the genomic RNA when the initial input RNA is capped *in vitro*, its not possible to rule out the possibility that if some of these mutations that affect WNV5′(+)SL RNA structure might also affect capping of the nascent RNA genomic RNA synthesized in infected cells.

MATERIALS AND METHODS

Cells.

Baby hamster kidney (BHK) 21, strain W12, cells (Vaheri et al., 1965) were maintained at $37^{\circ}C$ in a CO_2 incubator in Minimal Essential Medium (MEM) supplemented with 5% fetal bovine serum (FBS) (Atlas) and 10 μg/ml of gentamicin (Invitrogen).

Cloning, expression, and purification of recombinant TIA-1 and TIAR from *E. coli*.

The cDNAs of the isoforms TIA-1b and TIARa were amplified from total RNA extracted from C3H/He mouse embryo fibroblasts by RT-PCR, cloned into the TA cloning vector pCR 2.1 (Invitrogen) and then subcloned into pCRT7/CT-TOPO (Invitrogen) to generate the expression vectors pTIA-1b and pTIARa. The expressed proteins contained a C-terminal (His)-tag. All inserts were verified by restriction and sequence analysis. Recombinant TIA-1 and TIAR proteins were expressed in *E. coli* Rosetta (DE3) pLysS cells (Novagen) as follows. Cells were transformed with plasmid DNA (10 ng) and grown in LB media containing carbenicillin (50 μg/μl) and chloramphenicol (34 μg/μl) to an OD_{600} of 0.6 at $37^{o}C$. Protein expression was induced by the addition of 0.05 mM isopropyl-β-D-thiogalactopyranoside (IPTG) for 5 hr with continuous shaking at $37^{o}C$. To purify proteins to near homogeneity, cell pellets from a 0.5 liter culture were resuspended in 1X Extraction/Wash Buffer (50 mM sodium phosphate, 300 mM $NaCl_2$, PH 7.0) containing protease inhibitor cocktail (Complete Mini, EDTA free, Roche) and then lysed with a SLM-Aminco French pressure cell press (Heinemann) at 20,000 psi. Clarified supernatants were loaded onto cobalt columns (Talon metal affinity resin, Clontech), the columns were washed with 1X Extraction/Wash Buffer containing 15 mM imidazole, and the bound proteins were eluted with 1X Extraction/Wash Buffer containing 150 mM imidazole. The eluted protein fractions were combined, dialyzed against Storage buffer (20 mM sodium phosphate, 30 mM KCl, 1 mM $MgCl_2$, 0.5 mM EDTA, and 15% Ficoll 400), aliquoted, and stored at -$80^{o}C$. The protein concentration was measured using a Coomassie Plus Protein Assay

Reagent kit (Pierce) with a bovine serum albumin (BSA) protein standard. Proteins in eluted fractions were analyzed by 10% SDS-PAGE and detected by Coomassie blue staining.

DNA constructs used as templates for RNA synthesis.

The construction of a plasmid containing the first 75 nts of the WNV5′ NCR (p5′NCR) was previously described (Shi, Li, and Brinton, 1996). This plasmid was amplified by PCR to provide the DNA templates used for *in vitro* transcription of the WNV3′(-)SL and WNV5′(+)SL RNAs. Mutant constructs were generated using the Quick-Change Site-Directed Mutagenesis kit (Stratagene) according to the manufacturer's protocol. The sequences of the primers used to introduce mutations are available upon request. DNA extracted from selected positive colonies was sequenced to confirm the presence of the introduced mutations and/or deletions. pWNV-Trun (Elghonemy, Davis, and Brinton, 2005) was used to amplify DNA templates for the *in vitro* synthesis of the 3′ terminal 89 nts of the WNV genome.

***In vitro* transcription of ^{32}P-labelled and unlabeled RNA.**

WNV3′(-) SL RNA, WNV3′(+)SL RNA, WNV5′(+)SL RNA, and a number of WNV3′(-)SL mutant RNAs were i*n vitro* transcribed using a MAXIscript *in vitro* transcription kit (Ambion) in 20 μl reactions that contained T7 RNA polymerase (30 U), a Qiaquick Gel Extraction kit (Qiagen)-purified PCR product (1 μg), 0.8 mM [α-^{32}P] GTP (3000 Ci/mmol, 10 mCi/ml; Amersham Biosciences), 3 μM GTP and 0.5 mM CTP,

UTP, and ATP. The *in vitro* transcription mixture was incubated at 37°C for 2 hrs and transcription was stopped by addition of DNase I (1U) for 15 min at 37°C. After addition of an equal volume of 1X Gel Loading Buffer II (Ambion), the reaction mixture was heated at 95°C for 5 min. RNA transcripts were purified by electrophoresis on a 6 % PAG containing 7 M urea. The wet gel was autoradiographed and the ^{32}P-labelled RNA band was excised. RNA was eluted from the gel slices by rocking overnight at 4°C in Elution Buffer (0.5 M NH$_4$OAC, 1 mM EDTA, and 0.1 % SDS). The eluted RNA was filtered through a 0.45 μm cellulose acetate filter unit (Millipore) to remove gel pieces, precipitated with ethanol, resuspended in water, aliquoted, and stored at -80°C. The amount of radioactivity incorporated into each RNA probe was measured with a scintillation counter (Beckman LS6500) and the specific activity [calculated as described previously, (Blackwell and Brinton, 1997)] was routinely about 1.3 X 10^{7} cpm/μg. Unlabeled viral RNA was *in vitro* transcribed as described above except that 1 mM of each NTP was added to the reaction mixture. After synthesis, these RNAs were purified on NucAway spin columns (Ambion) and RNA concentrations were calculated based on the UV absorbance measured at 260 nm.

Transfection of *in vitro* transcribed full-length WNV genomic RNA.

The infectious clone used in this study is a chimera composed of the lineage I WNV, strain Eg101, and the lineage II WNV, strain 956 D 117 3B, sequences cloned into pBR322 under the control of an SP6 promoter (Yamshchikov et al., 2001). Genomic RNA was synthesized, gel purified, and *XBaI* linearized from WNV infectious clone

DNA (1 μg) using a Message Maker kit (Epicenter) and SP6 RNA polymerase. BHK cells were seeded in six well plates (2 x 10^5 cells per well) and grown to ~ 90% confluency. The cells were washed and then transfected with 100 ng of infectious clone RNA using a mixture of OPTI-MEM (Invitrogen) and DMRIE-C (Invitrogen). After 3 hours of incubation at 37^oC in 5% CO_2, the transfection medium was removed and replaced with either fresh MEM containing 5% FCS or MEM containing 0.5% SeaKem ME agarose (BioWhittaker Molecular Applications) and 2.5% FCS. Three serial passages were done in duplicate by transfer of 100 μl of media harvested at 72 h after transfection/infection to a fresh well in a 6 well plate. Plaque titration was done as previously described (Elghonemy, Davis, and Brinton, 2005).

Site directed mutagenesis of the infectious clone.

The strategy for inserting mutations into the WNV infectious clone, which utilizes a shuttle vector containing the ligated 3′ and 5′ regions of the WNV genome sequence, was described previously (Elghonemy, Davis, and Brinton, 2005). Mutations and deletions in the first 75 nt of the WNV3′(-)SL RNA in the shuttle vector DNA were introduced using a Quick-Change Site Directed Mutagenesis kit (Stratagene), according to the manufacturer's protocol. The sequence of the mutant shuttle vectors as well as of the appropriate regions of the final mutated infectious clone DNAs were checked by DNA sequencing. The primers used for site-directed mutagenesis and RNA synthesis are available upon request.

Gel mobility shift assays.

^{32}P-labelled WNV3′(-)SL RNA probe diluted in Binding Buffer (20 mM sodium phosphate, 30 mM KCl, 1 mM $MgCl_2$, 0.5 mM EDTA, 3% Ficoll 400, and 10 U RNasin) was denatured at 85°C for 10 min and slowly renatured (0.1°C/sec) to 20°C. Reaction mixtures containing the RNA probe (2000 cpm; 0.2 nM) and different concentrations of rTIA-1 (50-900 nM) or rTIAR (5-90 nM) in a final volume of 10 μl of Binding Buffer plus 10 nM of the nonspecific competitor tRNA were incubated at room temperature for 30 min and the RNA-protein complexes formed were electrophoresed on a 5% non-denaturing PAG at 100 V/hr in 0.5X TBE at 4°C. Gels were dried and visualized by autoradiography. For competition gel-shift assays, purified rTIA-1 (600 nM) and purified rTIAR (60 nM) were incubated with increasing concentrations of one of the nonspecific competitors, poly I/C (0.1–1 ng) or tRNA (2.5-20 nM) or with the specific competitor, unlabeled WNV3′(-)SL RNA (0.2-5 nM) for 10 min prior to the addition of 0.2 nM (2000 cpm) of the ^{32}P-labelled RNA probe. The binding activity of each mutant RNA probe was compared to that of the wildtype WNV3′(-)SL RNA probe. The signal intensities of the RNA protein complex and free probe gel bands were quantitated using a Bio-Imaging Analyzer PhosphorImager (Molecular Dynamics). The amount of RNA protein complex was divided by the amount of free probe to determine the percent RNA probe shifted, which was plotted against the rTIA-1 or rTIAR protein concentration used in the reaction. Data points graphed were the average of three replicate binding experiments. Standard deviation of the mean was calculated using the ESTDEV method in Microsoft Excel.

Quantitative Real-time RT-PCR of the intracellular viral RNA.

Confluent BHK monolayers in 6 well plates were transfected with 200 ng of wildtype or mutated WNV infectious clone RNAs as described above. Total cell RNA was extracted at different times post transfection using TRI Reagent (Molecular Research Center, Inc.) according to the manufacture's protocol. The intracellular viral genomic RNA was relatively quantified on an Applied Biosystems 7500 real-time PCR system using the TaqMan one-step RT-PCR kit according to the supplier's instructions. The amplification primer-probe set used targeted the NS1 region and consisted of the forward primer 5′–GGCGGTTCTAGGAGAAGTCA-3′, the reverse primer 5′–CTCCTGTTGTGGTTGCTTCT-3′, and the TaqMan probe 5′–6Fam-TGCACCTGGCCAGAAACCCACACTCTGT-TAMRA-3′. For minus-strand RNA specific detection, T7-tagged primer real-time RT-PCR was done as previously described (Lanford et al., 1994; Samuel and Diamond, 2005). Briefly, a TaqMan one-step RT-PCR reaction mixture containing 800 ng of total cell RNA and 2 pmol of the T7 tagged minus-strand primer (5′**GCGTAATACGACTCACTATA**GAGGGCGGTTCTAGGAGAAGT-3′; the bold sequence is the T7 tag sequence and the rest of the sequence is from the WNV NS1 region) was incubated for 30 min at 50°C for reverse transcription and then at 95°C for 30 min to inactivate the reverse transcriptase enzyme. Following the inactivation step, 20 pmol of the T7 primer (5′–**GCGTAATACGACTCACTATA**-3′), 20 pmol of the specific minus-strand primer (5′–CTCCTGTTGTGGTTGCTTC-3′), and 5 pmol of the TaqMan probe were added and the reaction was subjected to 40 cycles at 95°C for 15 sec and then 60°C for 1 min. Both plus-strand RNA and minus-strand RNA were

normalized using GADPH mRNA detected with the TaqMan Rodent GADPH control kit (Applied Biosystems). The plus- or minus-strand RNA levels were also calibrated to the amount of input viral RNA detected at 6 or 2 hr post transfection, respectively. The relative quantification units of RNA were determined as described previously (Scherbik et al., 2006).

Detection of intracellular viral antigen.

BHK cells (2 x 10^3) were seeded onto 3 mm coverslips and 24 hr later were transfected with 100 ng of WNV infectious clone RNA. Three hours after transfection, cells were fixed in 4% paraformaldehyde and then permeabilized using 100% chilled methanol. The cells were washed several times in PBS and incubated with anti-WNV hyperimmune serum (kindly provided from Robert B. Tesh, University of Texas) at a dilution of 1:100 for 1 hour at 37°C. The cells were then washed three times with cold PBS and incubated with anti-mouse immunoglobulin G antibody conjugated with Rhodamine (1:300) (Santa Cruz Biotechnology). Cell nuclei were stained with 0.5 μg/ml Hoechst 33258 (Molecular probes). After washing, cover slips were mounted in polyvinyl alcohol mounting medium with DABCO (Fluka) and the cells were viewed and photographed with a Zeiss Confocal Microscope LSM 510 (Zeiss, Germany) using 100X oil immersion objective with 1X zoom. The images were merged and analyzed using Zeiss software version 3.5.

RNA secondary structure prediction.

The secondary structure of each RNA probe used in this study was predicted using M-Fold, version 3.1 (Zuker, 2003).

ACKNOWLEDGMENTS

REFERENCES

Anderson, P. (1995). TIA-1: structural and functional studies on a new class of cytolytic effector molecule. *Curr Top Microbiol Immunol* **198,** 131-43.

Anderson, P., Nagler-Anderson, C., O'Brien, C., Levine, H., Watkins, S., Slayter, H. S., Blue, M. L., and Schlossman, S. F. (1990). A monoclonal antibody reactive with a 15-kDa cytoplasmic granule-associated protein defines a subpopulation of CD8+ T lymphocytes. *J Immunol* **144**(2)**,** 574-82.

Beck, A. R., Medley, Q. G., O'Brien, S., Anderson, P., and Streuli, M. (1996). Structure, tissue distribution and genomic organization of the murine RRM-type RNA binding proteins TIA-1 and TIAR. *Nucleic Acids Res* **24**(19)**,** 3829-35.

Beck, A. R., Miller, I. J., Anderson, P., and Streuli, M. (1998). RNA-binding protein TIAR is essential for primordial germ cell development. *Proc Natl Acad Sci U S A* **95**(5)**,** 2331-6.

Blackwell, J. L., and Brinton, M. A. (1997). Translation elongation factor-1 alpha interacts with the 3' stem-loop region of West Nile virus genomic RNA. *J Virol* **71**(9)**,** 6433-44.

Bredenbeek, P. J., Kooi, E. A., Lindenbach, B., Huijkman, N., Rice, C. M., and Spaan, W. J. (2003). A stable full-length yellow fever virus cDNA clone and the role of conserved RNA elements in flavivirus replication. *J Gen Virol* **84**(Pt 5)**,** 1261-8.

Brinton, M. A. (2002). The molecular biology of West Nile Virus: a new invader of the western hemisphere. *Annu Rev Microbiol* **56,** 371-402.

Brinton, M. A., and Dispoto, J. H. (1988). Sequence and secondary structure analysis of the 5'-terminal region of flavivirus genome RNA. *Virology* **162**(2)**,** 290-9.

Brinton, M. A., Fernandez, A. V., and Dispoto, J. H. (1986). The 3'-nucleotides of flavivirus genomic RNA form a conserved secondary structure. *Virology* **153**(1)**,** 113-21.

Brunner, J. E., Nguyen, J. H., Roehl, H. H., Ho, T. V., Swiderek, K. M., and Semler, B. L. (2005). Functional interaction of heterogeneous nuclear ribonucleoprotein C with poliovirus RNA synthesis initiation complexes. *J Virol* **79**(6)**,** 3254-66.

Cahour, A., Pletnev, A., Vazielle-Falcoz, M., Rosen, L., and Lai, C. J. (1995). Growth-restricted dengue virus mutants containing deletions in the 5' noncoding region of the RNA genome. *Virology* **207**(1)**,** 68-76.

Chambers, T. J., Hahn, C. S., Galler, R., and Rice, C. M. (1990). Flavivirus genome organization, expression, and replication. *Annu Rev Microbiol* **44,** 649-88.

Chu, P. W., and Westaway, E. G. (1985). Replication strategy of Kunjin virus: evidence for recycling role of replicative form RNA as template in semiconservative and asymmetric replication. *Virology* **140**(1)**,** 68-79.

Cok, S. J., Acton, S. J., Sexton, A. E., and Morrison, A. R. (2004). Identification of RNA-binding proteins in RAW 264.7 cells that recognize a lipopolysaccharide-responsive element in the 3-untranslated region of the murine cyclooxygenase-2 mRNA. *J Biol Chem* **279**(9)**,** 8196-205.

Dember, L. M., Kim, N. D., Liu, K. Q., and Anderson, P. (1996). Individual RNA recognition motifs of TIA-1 and TIAR have different RNA binding specificities. *J Biol Chem* **271**(5)**,** 2783-8.

Dirksen, W. P., Mohamed, S. A., and Fisher, S. A. (2003). Splicing of a myosin phosphatase targeting subunit 1 alternative exon is regulated by intronic cis-elements and a novel bipartite exonic enhancer/silencer element. *J Biol Chem* **278**(11)**,** 9722-32.

Dixon, D. A., Balch, G. C., Kedersha, N., Anderson, P., Zimmerman, G. A., Beauchamp, R. D., and Prescott, S. M. (2003). Regulation of cyclooxygenase-2 expression by the translational silencer TIA-1. *J Exp Med* **198**(3)**,** 475-81.

Dong, H., Ray, D., Ren, S., Zhang, B., Puig-Basagoiti, F., Takagi, Y., Ho, C. K., Li, H., and Shi, P. Y. (2007). Distinct RNA elements confer specificity to flavivirus RNA cap methylation events. *J Virol* **81**(9)**,** 4412-21.

Elghonemy, S., Davis, W. G., and Brinton, M. A. (2005). The majority of the nucleotides in the top loop of the genomic 3' terminal stem loop structure are cis-acting in a West Nile virus infectious clone. *Virology* **331**(2)**,** 238-46.

Gilks, N., Kedersha, N., Ayodele, M., Shen, L., Stoecklin, G., Dember, L. M., and Anderson, P. (2004). Stress granule assembly is mediated by prion-like aggregation of TIA-1. *Mol Biol Cell* **15**(12)**,** 5383-98.

Gueydan, C., Droogmans, L., Chalon, P., Huez, G., Caput, D., and Kruys, V. (1999). Identification of TIAR as a protein binding to the translational regulatory AU-rich element of tumor necrosis factor alpha mRNA. *J Biol Chem* **274**(4)**,** 2322-6.

Jin, K., Li, W., Nagayama, T., He, X., Sinor, A. D., Chang, J., Mao, X., Graham, S. H., Simon, R. P., and Greenberg, D. A. (2000). Expression of the RNA-binding protein TIAR is increased in neurons after ischemic cerebral injury. *J Neurosci Res* **59**(6)**,** 767-74.

Kandasamy, K., Joseph, K., Subramaniam, K., Raymond, J. R., and Tholanikunnel, B. G. (2005). Translational control of beta2-adrenergic receptor mRNA by T-cell-restricted intracellular antigen-related protein. *J Biol Chem* **280**(3)**,** 1931-43.

Katsamba, P. S., Myszka, D. G., and Laird-Offringa, I. A. (2001). Two functionally distinct steps mediate high affinity binding of U1A protein to U1 hairpin II RNA. *J Biol Chem* **276**(24)**,** 21476-81.

Kawai, T., Lal, A., Yang, X., Galban, S., Mazan-Mamczarz, K., and Gorospe, M. (2006). Translational control of cytochrome c by RNA-binding proteins TIA-1 and HuR. *Mol Cell Biol* **26**(8)**,** 3295-307.

Kawakami, A., Tian, Q., Duan, X., Streuli, M., Schlossman, S. F., and Anderson, P. (1992). Identification and functional characterization of a TIA-1-related nucleolysin. *Proc Natl Acad Sci U S A* **89**(18)**,** 8681-5.

Kedersha, N., Cho, M. R., Li, W., Yacono, P. W., Chen, S., Gilks, N., Golan, D. E., and Anderson, P. (2000). Dynamic shuttling of TIA-1 accompanies the recruitment of mRNA to mammalian stress granules. *J Cell Biol* **151**(6)**,** 1257-68.

Kedersha, N. L., Gupta, M., Li, W., Miller, I., and Anderson, P. (1999). RNA-binding proteins TIA-1 and TIAR link the phosphorylation of eIF-2 alpha to the assembly of mammalian stress granules. *J Cell Biol* **147**(7)**,** 1431-42.

Koonin, E. V. (1993). Computer-assisted identification of a putative methyltransferase domain in NS5 protein of flaviviruses and lambda 2 protein of reovirus. *J Gen Virol* **74 (Pt 4),** 733-40.

Lanford, R. E., Sureau, C., Jacob, J. R., White, R., and Fuerst, T. R. (1994). Demonstration of in vitro infection of chimpanzee hepatocytes with hepatitis C virus using strand-specific RT/PCR. *Virology* **202**(2)**,** 606-14.

Le Guiner, C., Gesnel, M. C., and Breathnach, R. (2003). TIA-1 or TIAR is required for DT40 cell viability. *J Biol Chem* **278**(12)**,** 10465-76.

Lewis, T., Gueydan, C., Huez, G., Toulme, J. J., and Kruys, V. (1998). Mapping of a minimal AU-rich sequence required for lipopolysaccharide-induced binding of a 55-kDa protein on tumor necrosis factor-alpha mRNA. *J Biol Chem* **273**(22)**,** 13781-6.

Li, W., Li, Y., Kedersha, N., Anderson, P., Emara, M., Swiderek, K. M., Moreno, G. T., and Brinton, M. A. (2002). Cell proteins TIA-1 and TIAR interact with the 3' stem-loop of the West Nile virus complementary minus-strand RNA and facilitate virus replication. *J Virol* **76**(23)**,** 11989-2000.

Li, W., Simarro, M., Kedersha, N., and Anderson, P. (2004). FAST is a survival protein that senses mitochondrial stress and modulates TIA-1-regulated changes in protein expression. *Mol Cell Biol* **24**(24)**,** 10718-32.

Lindenbach, B. D., and Rice, C. M. (2007). Flaviviridae: The viruses and their replication. In: Fields, B. N., Knipe, D. N., Howley, P. M., Griffin, D. E., Martin, M. A., Lamb, R. A., Roizman, B., Straus, S. E., (Eds.), Fields Virology, 5th ed., Lippincott William and Wilkins, Philadelphia, Pennsylvania, pp. 1101-52.

Men, R., Bray, M., Clark, D., Chanock, R. M., and Lai, C. J. (1996). Dengue type 4 virus mutants containing deletions in the 3' noncoding region of the RNA genome: analysis of growth restriction in cell culture and altered viremia pattern and immunogenicity in rhesus monkeys. *J Virol* **70**(6)**,** 3930-7.

Muthukrishnan, S., Both, G. W., Furuichi, Y., and Shatkin, A. J. (1975). 5'-Terminal 7-methylguanosine in eukaryotic mRNA is required for translation. *Nature* **255**(5503)**,** 33-7.

Nomaguchi, M., Teramoto, T., Yu, L., Markoff, L., and Padmanabhan, R. (2004). Requirements for West Nile virus (-)- and (+)-strand subgenomic RNA synthesis in vitro by the viral RNA-dependent RNA polymerase expressed in Escherichia coli. *J Biol Chem* **279**(13)**,** 12141-51.

Oberstrass, F. C., Auweter, S. D., Erat, M., Hargous, Y., Henning, A., Wenter, P., Reymond, L., Amir-Ahmady, B., Pitsch, S., Black, D. L., and Allain, F. H. (2005). Structure of PTB bound to RNA: specific binding and implications for splicing regulation. *Science* **309**(5743)**,** 2054-7.

Piecyk, M., Wax, S., Beck, A. R., Kedersha, N., Gupta, M., Maritim, B., Chen, S., Gueydan, C., Kruys, V., Streuli, M., and Anderson, P. (2000). TIA-1 is a translational silencer that selectively regulates the expression of TNF-alpha. *Embo J* **19**(15)**,** 4154-63.

Roehl, H. H., and Semler, B. L. (1995). Poliovirus infection enhances the formation of two ribonucleoprotein complexes at the 3' end of viral negative-strand RNA. *J Virol* **69**(5)**,** 2954-61.

Samuel, M. A., and Diamond, M. S. (2005). Alpha/beta interferon protects against lethal West Nile virus infection by restricting cellular tropism and enhancing neuronal survival. *J Virol* **79**(21)**,** 13350-61.

Scherbik, S. V., Paranjape, J. M., Stockman, B. M., Silverman, R. H., and Brinton, M. A. (2006). RNase L plays a role in the antiviral response to West Nile virus. *J Virol* **80**(6)**,** 2987-99.

Shi, P. Y., Li, W., and Brinton, M. A. (1996). Cell proteins bind specifically to West Nile virus minus-strand 3' stem-loop RNA. *J Virol* **70**(9)**,** 6278-87.

Shukla, S., Del Gatto-Konczak, F., Breathnach, R., and Fisher, S. A. (2005). Competition of PTB with TIA proteins for binding to a U-rich cis-element determines tissue-specific splicing of the myosin phosphatase targeting subunit 1. *Rna* **11**(11)**,** 1725-36.

Shukla, S., Dirksen, W. P., Joyce, K. M., Le Guiner-Blanvillain, C., Breathnach, R., and Fisher, S. A. (2004). TIA proteins are necessary but not sufficient for the tissue-specific splicing of the myosin phosphatase targeting subunit 1. *J Biol Chem* **279**(14)**,** 13668-76.

Taupin, J. L., Tian, Q., Kedersha, N., Robertson, M., and Anderson, P. (1995). The RNA-binding protein TIAR is translocated from the nucleus to the cytoplasm during Fas-mediated apoptotic cell death. *Proc Natl Acad Sci U S A* **92**(5)**,** 1629-33.

Tian, Q., Streuli, M., Saito, H., Schlossman, S. F., and Anderson, P. (1991). A polyadenylate binding protein localized to the granules of cytolytic lymphocytes induces DNA fragmentation in target cells. *Cell* **67**(3)**,** 629-39.

Tian, Q., Taupin, J., Elledge, S., Robertson, M., and Anderson, P. (1995). Fas-activated serine/threonine kinase (FAST) phosphorylates TIA-1 during Fas-mediated apoptosis. *J Exp Med* **182**(3)**,** 865-74.

Vaheri, A., Sedwick, W. D., Plotkin, S. A., and Maes, R. (1965). Cytopathic effect of rubella virus in RHK21 cells and growth to high titers in suspension culture. *Virology* **27**(2)**,** 239-41.

Yamshchikov, V. F., Wengler, G., Perelygin, A. A., Brinton, M. A., and Compans, R. W. (2001). An infectious clone of the West Nile flavivirus. *Virology* **281**(2)**,** 294-304.

Yu, Q., Cok, S. J., Zeng, C., and Morrison, A. R. (2003). Translational repression of human matrix metalloproteinases-13 by an alternatively spliced form of T-cell-restricted intracellular antigen-related protein (TIAR). *J Biol Chem* **278**(3)**,** 1579-84.

Zhang, T., Delestienne, N., Huez, G., Kruys, V., and Gueydan, C. (2005). Identification of the sequence determinants mediating the nucleo-cytoplasmic shuttling of TIAR and TIA-1 RNA-binding proteins. *J Cell Sci* **118**(Pt 23)**,** 5453-63.

Zhu, H., Hasman, R. A., Young, K. M., Kedersha, N. L., and Lou, H. (2003). U1 snRNP-dependent function of TIAR in the regulation of alternative RNA processing of the human calcitonin/CGRP pre-mRNA. *Mol Cell Biol* **23**(17)**,** 5959-71.

Zuker, M. (2003). M fold web server for nucleic acid folding and hybridization prediction *Nucleic Acids Res* **31,** 3406-3415.

CHAPTER III

ADDITIONAL DATA

Effect of substitution of L1, L2, or L3 with As or Us.

Both TIA-1 and TIAR were previously reported to bind to poly(A) (Taupin et al., 1995; Tian et al., 1991) and poly(U) (Kawakami et al., 1992; Taupin et al., 1995). Although both proteins have a higher binding affinity for poly(U) than for poly(A), TIA-1 binds to poly(A) more efficiently than does TIAR (Kawakami et al., 1992; Taupin et al., 1995). To determine whether increasing the number of As in L1 and/or L2 preferentially increased the binding activity of rTIA-1 for the WNV3′(-)SL RNA, the Us and Cs in L1, L2, and L3 were replaced with As separately or in combination and the mutant RNAs were tested in *in vitro* binding assays with each of the proteins. Specifically, L1 (5′UAAUU3′) was replaced by 5′AAAAC3′ to form the L1→As mutant RNA. In this mutant, U_{20} was substituted with C to preserve the predicted RNA secondary structure. L2 and L3 were replaced separately with As to make RNA mutants L2→As and L3→As, respectively. The L1+L2→As mutant RNA had As in both L1 and L2. None of these mutations altered the predicted RNA secondary structure (Fig. 3.1A). With rTIAR, similar levels of binding were observed with the wild type, L1→As, L2→As, and L3→As RNAs (Fig. 3.1B lower panel, lanes 2-5, 7-10, 12-15, and 22-25 and Fig. 3.1D), but increased binding activity was observed with the L1+L2→As RNA (Fig. 3.1B lower panel, lanes 17-20 and Fig. 3.1D). In contrast, all of these mutant RNAs bound more efficiently to rTIA-1 than did the wild type RNA. The L1+L2→As RNA

showed the most efficient binding, L2→As bound more efficiently than L1→As RNA and L3→As RNA bound more efficiently than either the L2→As or L1→As RNAs (Fig. 3.1B upper panel and Fig. 3.1C).

The nts in L1, L2, and L3 were next replaced with Us and the mutant RNAs were designated L1→Us, L2→Us, and L3→Us, respectively. The predicted RNA secondary structure was preserved in all of these mutant RNAs. Both proteins bound more efficiently to all of the U substitution RNAs than to the wild type RNA. L3→Us RNA gave the highest level of binding (Fig. 3.2B). Increases of 4, 11, and 19% in the binding activity of rTIAR (60 nM) were observed with the L1→Us, L2→Us, and L3→Us mutant RNAs, respectively, as compared to the wild type RNA (data not shown). The binding activity of rTIA-1 (600 nM) for the L1→Us, L2→Us, and L3→Us mutant RNAs was 10, 23, and 35%, respectively, higher than that for the wild type RNA (data not shown). An additional RPC band that migrated slower than the RPC usually observed with the wild type RNA was observed in assays with either protein and the L3→Us RNA (Fig. 3.2B).

These results indicate that substituting L1 or L2 with As did not alter TIAR binding activity but enhanced TIA-1 binding activity. However, the binding activity of both proteins increased when As were present in both L1 and L2 or when L1 or L2 consisted of single-stranded U tracts, but the binding of TIA-1 to U tracts was enhanced to a greater degree than that of TIAR. The increase in the binding efficiencies of both rTIA-1 and rTIAR observed for the L3→Us mutant RNA and the observation of an additional RPC band strongly suggested that the substitution of 9 Us in the terminal loop of the structure had created an additional binding site.

To further analyze this new binding site, deletions in L1 or L2 were made separately or in combination in the L3→Us mutant RNA (Fig. 3.2A). The binding activities of both recombinant proteins for the mutant RNAs L3→Us, pΔL1, L3→Us, ΔL2, and L3→Us, pΔL1,ΔL2 progressively declined (Fig. 3.2B, Lanes 7-10, 12-15, and 17-21; Fig. 3.2C and D) as compared to those for the L3→Us RNA (Fig. 3.2B, Lanes 2-5; Fig. 3.2C and D). With both proteins, the percent decrease in binding when either L1 or L2 or both L1 and L2 were deleted in the L3→Us RNA was similar to that observed when these loops were deleted in the wild type RNA (compare Fig. 3.2B, C, and D with Fig. 2.3B, C, and D). The additional RPC band that was observed with the L3→Us RNA was also observed when the L3→Us,ΔL2, and L3→Us,pΔL1,ΔL2 RNAs were used but was not observed with L3→Us,pΔL1 RNA.

Effect of increasing the distance between L1 and L2 on TIA-1 and TIAR binding activity.

The mapping experiments described above indicated that both L1 and L2 are required for efficient TIA-1 or TIAR binding to the WNV3′(-)SL RNA. In the predicted secondary structure of the WNV3′(-)SL RNA, these two loops are separated by a 4 base pair stem (Fig.3.3A). To determine if the distance between L1 and L2 is important for efficient protein binding, four additional base pairs were inserted to increase the distance between the two loops (LS RNA). This mutation did not alter the overall predicted secondary structure of the WNV3′(-)SL RNA (Fig. 3.3A). The LS RNA probe bound significantly less efficiently to both proteins (Fig. 3.3B, lanes 7-10; Fig. 3.3C and D) than
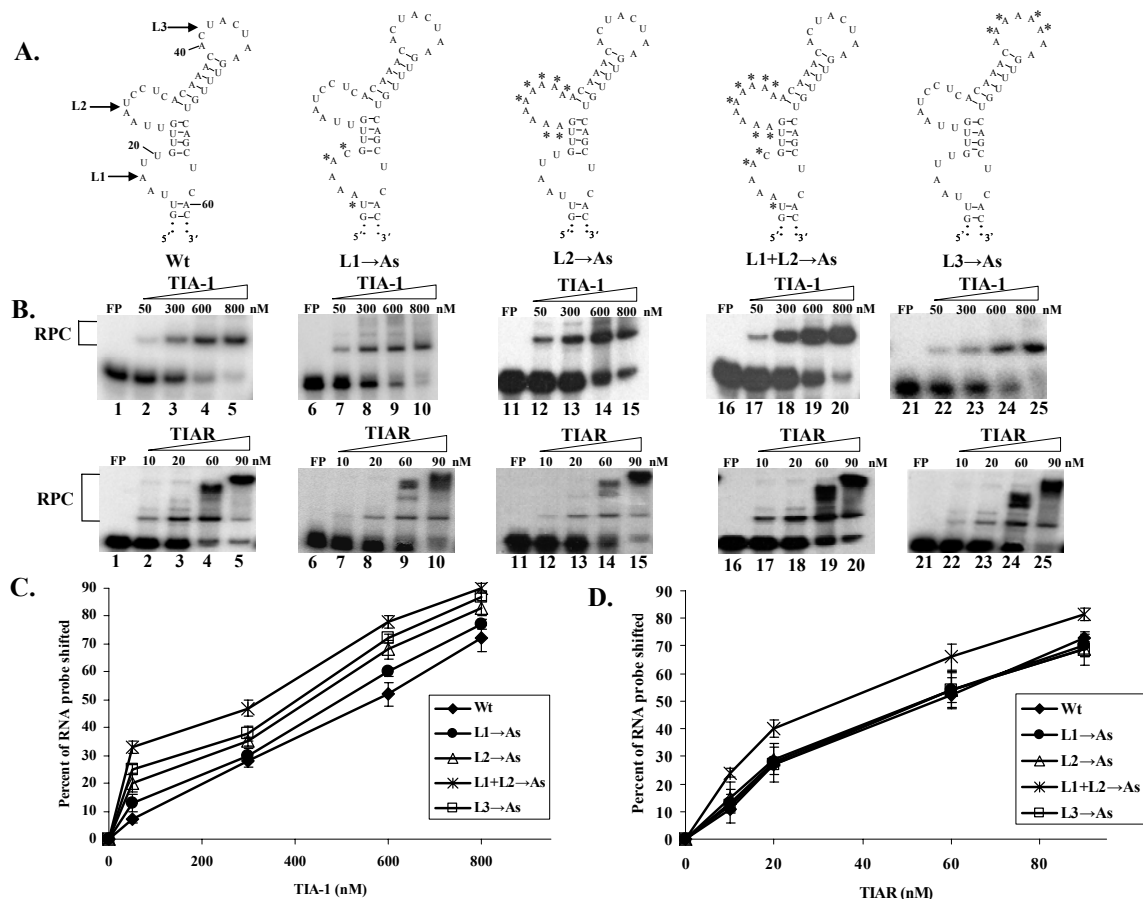
Figure 3.1: Effect of A substitutions in L1, L2, and L3 within the WNV3′(-)SL RNA on rTIA-1 and rTIAR binding activity. (A) Predicted secondary structures of mutant RNAs. Mutations are indicated by asterisks. (B) Representative gel mobility shift assays with rTIA-1(upper panel) or rTIAR (lower panel) and each mutant RNA probe. (Lanes 1-5) wild type RNA; (Lanes 6-10) L1→As RNA; (Lanes 11-15) L2→As RNA; (Lanes 16-20) L1+L2→As RNA; and (Lanes 21-25) L3→As RNA. (C) and (D) Percent RNA probe shifted.
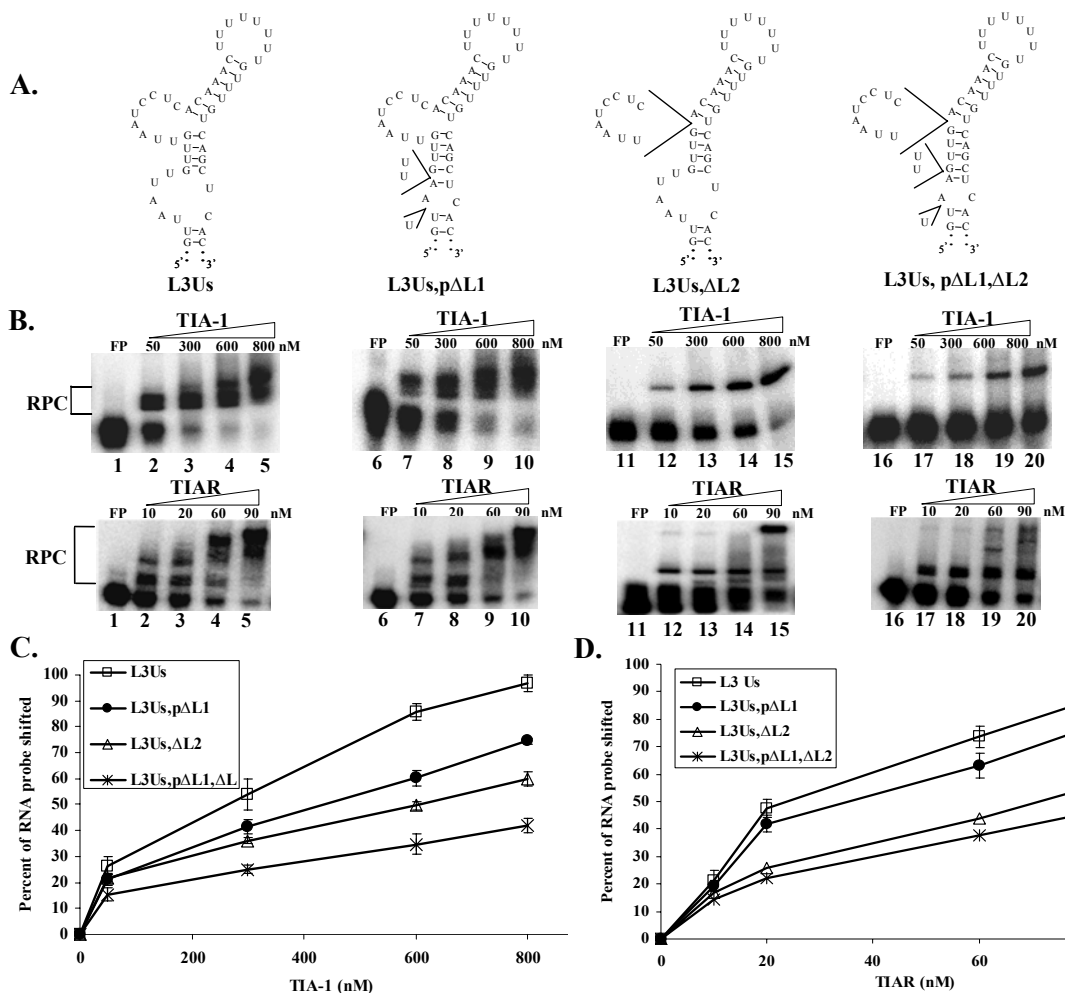
Figure 3.2: Effect of deletions in L1 and/or L2 of the L3→Us mutant RNA on rTIA-1 and rTIAR binding activity. (A) Predicted secondary structures of the mutant RNAs. Deletions are indicated by wedges. (B) Representative gel mobility shift assays with rTIA-1(upper panel) or rTIAR (lower panel) and the WNV3′(-)SL or mutant RNA probes. (Lanes 1-5) L3→Us RNA; (Lanes 6-10) L3→Us,pΔL1; (Lanes 11-15) L3→Us,ΔL2 RNA; (Lanes 16-20) L3→Us, pΔL1,ΔL2 RNA. (C) and (D) Percent RNA probe shifted.
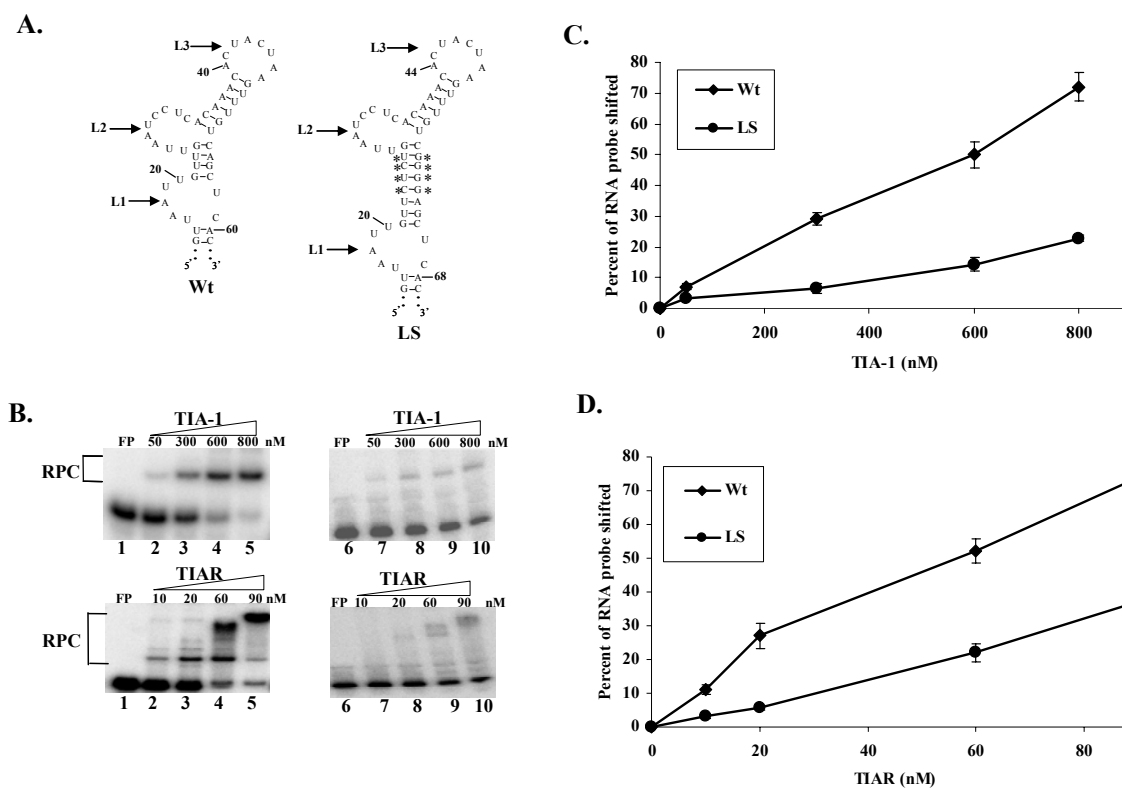
Figure 3.3: Effect of increasing the distance between L1 and L2 within the WNV3′(-)SL RNA on rTIA-1 and rTIAR binding activity. (A) Predicted secondary structures of the LS mutant RNA. Mutations are indicated by asterisks. (B) Representative gel mobility shift assays with rTIA-1(upper panel) or rTIAR (lower panel) and the WNV3′(-)SL or LS RNA probes. (Lanes 1-5) wild type RNA; (Lanes 6-10) LS RNA. (C) and (D) Percent RNA probe shifted.

did the wild type RNA. The protein binding efficiency for the LS RNA was similar to that observed with RNAs that had either L1 or L2 deleted or mutated to Cs (compare Fig. 3.3 with Fig. 2.2 and 2.3). These results indicated that the efficiency of protein binding was dependent on an optimal distance between L1 and L2.

DISCUSSION

A significant decrease in the binding of either TIA-1 or TIAR was observed when either L1 or L2, but not L3, was deleted. Although all these loops contains an AU stretch, L1 and L2 each contain a UAAUU sequence whereas L3 contains UAA. TIA-1 and TIAR each contain three adjacent RRMs. It is not known how many of the RRMs in a single protein molecule interact with an RNA molecule during efficient binding. The spatial orientation of multiple single-stranded binding sites presented on an RNA structure may determine how many of the RRMs contact the RNA. Evidence from the present study suggests that a protein molecule can simultaneously contact the L1 and L2 AU sequences but not those in L3 in the WNV3′(-)SL RNA. The minimal binding site located at the 3′ end of L3 in the WNV3′(-)SL RNA may not be in an optimal orientation for protein binding or it may be located too far away from L2. L1 and L2 are separated by a 4 base pair stem, while L3 is separated from L2 by a 6 base pair stem. Increasing the distance between L1 and L2 by four additional base pairs, decreased the binding of either protein to levels similar to those obtained when L1 or L2 was deleted or mutated to Cs. The distance between L1 and L2 in this mutant was similar to that between L3 and L2 in the WNV3′(-)SL RNA. Also, the binding activity of either protein

was affected to a greater degree by deletion or mutation of L2 than by the same changes in L1. The larger size of L2 (9 nt) as compared to L1 (5 nt) may provide an increased flexibility that enhances the efficiency of protein interaction with the binding site. The significant increase in binding observed when the 9 nts of L3 were substituted with Us suggests that these 9 Us created one or possibly two, additional protein contact sites. This hypothesis is further supported by the observation of an additional RNA-protein complex band in the gel mobility shift assays done with either protein and the L3→Us probe and also by the ability of both proteins to bind efficiently to the L3→Us RNA in the absence of both L1 and L2 (Fig. 3.2). Recent structural analysis of RNA-protein complexes formed by polypyrimidine tract binding protein, a protein with four RNA binding domains (RBDs), showed that each of these four domains bound to separate pyrimidine tracts in the same pre-mRNA (Oberstrass et al., 2005). RRM2 of both TIA-1 and TIAR has been shown to account for the majority of the binding activity for short U-rich RNAs, but the binding affinity of both proteins increased when either of the other two RRMs were present (Dember et al., 1996). An alternative possibility is that two TIA-1 or TIAR molecules bind to one WNV3′(-)SL RNA. In the present study, this appeared to occur only when L3 was mutated to Us.

In the initial study, TIA-1 was not detected among the bound proteins eluted from an WNV3′(-)SL RNA affinity column (Li et al., 2002) and subsequent gel mobility shift assays showed that TIA-1 binds to this RNA 10 times less efficiently than does TIAR. The 10 fold higher binding efficiency of TIAR for the WNV3′(-)SL RNA suggests that TIAR would out-compete TIA-1 for binding to the WNV3′(-)SL RNA except when

TIAR concentrations are low. It is possible that other AU-rich sequence binding proteins may also be able to interact with the WNV3′(-)SL RNA. Translational regulation of some cell mRNAs has been previously reported to be combinatorially regulated by multimeric protein complexes that contain TIA-1 and/or TIAR and different combinations of other ARE-binding proteins including FUSE-binding proteins (FBPs) (Rothe et al., 2006), HuR proteins (Kawai et al., 2006), HuR and AU-binding factor 1 (AUF1) (Cok et al., 2004), or tristetraprolin (TTP) (Zhang et al., 2002). The AU sequences in the mRNA 3′UTRs binding to these complexes contain multiple, redundant, and/or long AU tracts and it is currently not known how protein binding specificity is determined or whether multiple proteins compete for the same binding sites. It is expected that not only the presence and location of specific binding sites in the RNA but also the conformation of the RNA would play important roles in determining the binding affinities of the various ARE-binding proteins that form a complex with a particular 3′UTRs. Protein-protein interactions also appear to play a role in the formation of these complexes (Katsanou et al., 2005).

REFERENCES

Cok, S. J., Acton, S. J., Sexton, A. E., and Morrison, A. R. (2004). Identification of RNA-binding proteins in RAW 264.7 cells that recognize a lipopolysaccharide-responsive element in the 3-untranslated region of the murine cyclooxygenase-2 mRNA. *J Biol Chem* **279**(9)**,** 8196-205.

Dember, L. M., Kim, N. D., Liu, K. Q., and Anderson, P. (1996). Individual RNA recognition motifs of TIA-1 and TIAR have different RNA binding specificities. *J Biol Chem* **271**(5)**,** 2783-8.

Katsanou, V., Papadaki, O., Milatos, S., Blackshear, P. J., Anderson, P., Kollias, G., and Kontoyiannis, D. L. (2005). HuR as a negative posttranscriptional modulator in inflammation. *Mol Cell* **19**(6)**,** 777-89.

Kawai, T., Lal, A., Yang, X., Galban, S., Mazan-Mamczarz, K., and Gorospe, M. (2006). Translational control of cytochrome c by RNA-binding proteins TIA-1 and HuR. *Mol Cell Biol* **26**(8)**,** 3295-307.

Kawakami, A., Tian, Q., Duan, X., Streuli, M., Schlossman, S. F., and Anderson, P. (1992). Identification and functional characterization of a TIA-1-related nucleolysin. *Proc Natl Acad Sci U S A* **89**(18)**,** 8681-5.

Li, W., Li, Y., Kedersha, N., Anderson, P., Emara, M., Swiderek, K. M., Moreno, G. T., and Brinton, M. A. (2002). Cell proteins TIA-1 and TIAR interact with the 3' stem-loop of the West Nile virus complementary minus-strand RNA and facilitate virus replication. *J Virol* **76**(23)**,** 11989-2000.

Oberstrass, F. C., Auweter, S. D., Erat, M., Hargous, Y., Henning, A., Wenter, P., Reymond, L., Amir-Ahmady, B., Pitsch, S., Black, D. L., and Allain, F. H. (2005). Structure of PTB bound to RNA: specific binding and implications for splicing regulation. *Science* **309**(5743)**,** 2054-7.

Rothe, F., Gueydan, C., Bellefroid, E., Huez, G., and Kruys, V. (2006). Identification of FUSE-binding proteins as interacting partners of TIA proteins. *Biochem Biophys Res Commun* **343**(1)**,** 57-68.

Taupin, J. L., Tian, Q., Kedersha, N., Robertson, M., and Anderson, P. (1995). The RNA-binding protein TIAR is translocated from the nucleus to the cytoplasm during Fas-mediated apoptotic cell death. *Proc Natl Acad Sci U S A* **92**(5)**,** 1629-33.

Tian, Q., Streuli, M., Saito, H., Schlossman, S. F., and Anderson, P. (1991). A polyadenylate binding protein localized to the granules of cytolytic lymphocytes induces DNA fragmentation in target cells. *Cell* **67**(3)**,** 629-39.

Zhang, T., Kruys, V., Huez, G., and Gueydan, C. (2002). AU-rich element-mediated translational control: complexity and multiple activities of trans-activating factors. *Biochem Soc Trans* **30**(Pt 6)**,** 952-8.

CHAPTER IV

Interaction of TIA-1/TIAR with West Nile and dengue virus products in infected cells interferes with SG formation and PB assembly.

ABSTRACT

The West Nile virus minus-strand 3′ terminal stem loop (SL) RNA was previously shown to bind specifically to cellular stress granule (SG) components, T-cell intracellular antigen-1 (TIA-1) and the related protein TIAR. *In vitro* TIAR binding was 10 times more efficient than TIA-1. The 3′(−)SL functions as the promoter for genomic RNA synthesis. Colocalization of TIAR and TIA-1 with the viral replication complex components, dsRNA and NS3, was observed in the perinuclear regions of WNV and dengue virus infected cells. The kinetics of accumulation of TIAR in the perinuclear region was similar to those of genomic RNA synthesis. In contrast, relocation of TIA-1 to the perinuclear region began only after maximal levels of RNA synthesis had been achieved except when TIAR was absent. Virus infection did not induce stress granules and progressive resistance to SG induction by arsenite developed coincident with TIAR relocation. A progressive decrease in the number of Processing Bodies (PB) was also observed in infected cells. These data suggest that the interaction of TIAR with viral components facilitates flavivirus genome RNA synthesis and inhibits SG formation which prevents the shutoff of host translation.

INTRODUCTION

Eukaryotic cells respond to environmental stresses, such as oxidative stress, heat shock, UV irradiation, and endoplasmic reticulum (ER) stress, and some viral infections, by altering the protein expression machinery (Kedersha and Anderson, 2002). The expression of proteins responsible for damage repair is increased, whereas translation of constitutively expressed proteins is aborted via redirection of these mRNAs from polysomes to discrete cytoplasmic foci known as stress granules (SG) for transient storage (Kedersha et al., 1999). Several cell proteins, including T cell intracellular antigen-1 (TIA-1), TIA-1 related protein (TIAR) (Kedersha et al., 1999), and Ras-Gap-SH3 domain-binding protein (G3BP) are involved in SG assembly (Tourriere et al., 2003). Phosphorylation of eukaryotic translation initiation factor 2α (eIF2α) by protein kinase R (PKR) and other kinases prevents the assembly of the active ternary preinitiation complex eIF2-GTP-tRNA^{Met} and inhibits translation initiation and polysome assembly (Anderson and Kedersha, 2006). TIA-1 and TIAR bind to these inactive translation initiation complexes as well as to poly(A)$^{+}$ of cell mRNAs and self-aggregate promoting the assembly of SG (Kedersha et al., 1999). Processing Bodies (PB), another type of foci identified in the cytoplasm of eukaryotic cells (Eulalio, Behm-Ansmant, and Izaurralde, 2007), contain components of the 5′-3′ mRNA degradation pathway as well as the miRNA-dependent silencing protein GW182 (Eystathioy et al., 2002). PB do not require eIF2α phosphorylation for their assembly (Kedersha et al., 2005). Although SG and PB differ in their size and shape as well as in their mechanism of assembly, the two types of foci are found side by side in mammalian cells and a physical association

between them was previously demonstrated by real-time fluorescence imaging (Kedersha et al., 2005). This study also showed that PB are highly motile whereas the positions of SG are relatively fixed and that SG deliver mRNAs to associated PB for degradation.

TIA-1 and TIAR are essential, multifunctional, nucleocytoplasmic shuttling proteins that are expressed in most types of cells and tissues (Beck et al., 1996; Jin et al., 2000). TIA-1 and TIAR contain three N-terminal RNA recognition motifs (RRM) (Anderson, 1995) and a glutamine-rich C-terminal domain, called prion related domain (PRD), that shares structural and functional characteristics with the aggregation domains of mammalian and yeast prion proteins (Gilks et al., 2004). A recombinant TIA-1 protein lacking the three RNA binding domains was unable to bind poly(A)$^+$ RNA and recruit it to SG (Kedersha et al., 1999). Deletion of the TIA-1 PRD inhibited protein aggregation and SG assembly (Gilks et al., 2004). PRD aggregation is regulated by the molecular chaperone heat shock protein 70 (HSP70) and over expression of HSP70 prevented cytosolic aggregation of PRD (Gilks et al., 2004). TIA-1 and TIAR also regulate translational silencing of a subset of cellular mRNAs via binding to AU-rich sequences in the 3′ noncoding regions (NCRs) of these mRNAs (Anderson and Kedersha, 2002b). In addition, TIA-1 and TIAR proteins interact specifically with the 3′-terminal stem loop structure of the West Nile virus minus-strand RNA [WNV3′(-)SL] (Li et al., 2002).

WNV is classified in the family Flaviviridae, genus Flavivirus, along with a number of other human pathogens including dengue virus (DV), Japanese encephalitis virus, yellow fever virus, and tick-borne encephalitis virus. The *flavivirus* genome is a single-stranded, positive sense RNA of ~11 Kb containing a single open reading frame and *is*

the only viral mRNA produced during the virus replication cycle. Flavivirus replication takes place in the perinuclear region of the cytoplasm of infected cells. Three structural (capsid, membrane, and envelope) and seven non-structural (NS1, NS2a, NS2b, NS3, NS4a, NS4b, and NS5) viral proteins are produced via proteolytic processing of the single polyprotein by viral and cellular proteases (Brinton, 2002; Lindenbach and Rice, 2007). The C-terminal portion of NS5 is the RNA dependent RNA polymerase (RdRp), while the N-terminal part is a methyltransferase involved in RNA capping (Koonin, 1993). The N-terminus of NS3 has serine protease activity, while the C-terminus contains helicase, NTPase, and triphosphatase activities (Brinton, 2002; Lindenbach and Rice, 2007). The NS3, NS5, and NS1 proteins as well as the hydrophobic NS2a, NS2b, NS4a, and NS4b proteins were previously shown to be components of membrane bound viral RNA replication complexes located in the perinuclear region of infected cells (Kapoor et al., 1995; Uchil and Satchidanandam, 2003; Vasudevan et al., 2001).

In this study, both TIA-1 and TIAR were shown to colocalize with the WNV and DV NS3 protein as well as with viral dsRNA, a marker for viral replication complexes, in infected mammalian cells. The data obtained suggest that these interactions facilitate viral genomic RNA synthesis and downregulate SG formation in infected cells.

RESULTS

TIA-1 and TIAR colocalize with WNV and DV2 proteins in infected BHK cells.

A previous study showed that in C57/BL/6 TIAR-/- mouse embryo fibroblasts (MEFs), the replication of WNV was reduced by 6- to 8-fold compared to control MEFs,

whereas WNV grew to the same levels in TIA-1-/- MEFs and control MEFs (Li et al., 2002). This was consistent with the 10 fold higher binding efficiency of TIAR for the WNV3′(-)SL as compared to TIA-1 (Li et al., 2002). To determine whether a flavivirus infection altered the distribution of these cell proteins, BHK cells were infected with WNV at MOI of 5 and at 3, 6, 12, and 24 hpi, the cells were fixed, permeabilized, incubated with anti-TIA-1 or anti-TIAR and then anti-WNV antibody, and visualized by confocal microscopy as described in Materials and Methods. As expected, TIAR (Fig. 4.1A, green) and TIA-1 (Fig. 4.1E, green) were evenly distributed throughout mock infected cells (Anderson and Kedersha, 2002a). Under these infection conditions, WNV proteins were detected in about 90% of the cells. WNV proteins were faintly detected by 6 hpi (Fig. 4.1B, red). Although at 6 hpi, TIAR was still found in both the cytoplasm and nucleus, this protein was also concentrated in a few bright foci in the cytoplasm (Fig. 4.1B, green). Merged images obtained at 6 hpi showed colocalization of TIAR foci with foci of viral protein (Fig. 4.1B, merge). Foci of TIA-1 were not observed at this time (data not shown). By 12 hpi, the majority of TIAR was in the cytoplasm (Fig. 4.1C, green) and the amount of WNV protein had increased and was concentrated in the perinuclear region (Fig. 4.1C, red). Again, colocalization of TIAR but not TIA-1 (data not shown) with the viral proteins was observed mainly in perinuclear foci (Fig. 4.1C, merge). By 24 hpi, the intensity of WNV protein staining had increased significantly (Fig. 4.1D and F, red) and TIAR strongly colocalized in the perinuclear region with the WNV proteins (Fig. 4.1D, merge). In contrast, only a few bright cytoplasmic foci of TIA-1 colocalized with the WNV proteins by 24 hpi (Fig. 4.1F, merge; a pattern similar to that

seen at 6 hpi with TIAR). Strong colocalization of TIA-1 with the WNV proteins was observed by 36 hpi (Fig. 4.1G, merge). Quantification of the amount of TIAR or TIA-1 in the nucleus confirmed that the distribution of both TIA-1 and TIAR was altered with time after WNV infection but the redistribution of TIAR occurred more rapidly (Fig. 4.1H).

It was previously reported that the expression of TIA-1 was three times higher in TIAR-/- than in wildtype MEFs (Li et al., 2002). To determine if the time course of TIA-1 redistribution was altered when TIAR was not present, TIAR-/- MEFs were infected with WNV (MOI of 5) and the locations of TIA-1 and WNV proteins were analyzed at 12 and 24 hpi. TIA-1 was equally distributed in both the cytoplasm and nucleus of mock infected TIAR-/- MEFs (Fig. 4.2A, green], but these cells were significantly larger than BHK cells. The time course of appearance, staining intensity, and distribution of the WNV proteins in these cells (Fig. 4.2B and C, red) were similar to those observed with infected BHK cells. At 12 hpi, a few bright foci of TIA-1 that colocalized with WNV proteins were observed (Fig. 4.2B, merge), similar to what was observed by 12 hpi for TIAR in BHK cells. By 24 hpi, a significant increase in TIA-1 in the perinuclear region and strong colocalization with viral proteins was observed (Fig. 4.2C). At all times, a significant portion of TIA-1 remained in the nucleus. These results indicate that in the absence of TIAR, colocalization of TIA-1 with the viral proteins occurred more quickly with a time course similar to that of TIAR colocalization in cells expressing both proteins.

To determine whether TIA-1/TIAR colocalization with viral proteins was also characteristic of other flavivirus infections, BHK cells were infected with DV2, (MOI of
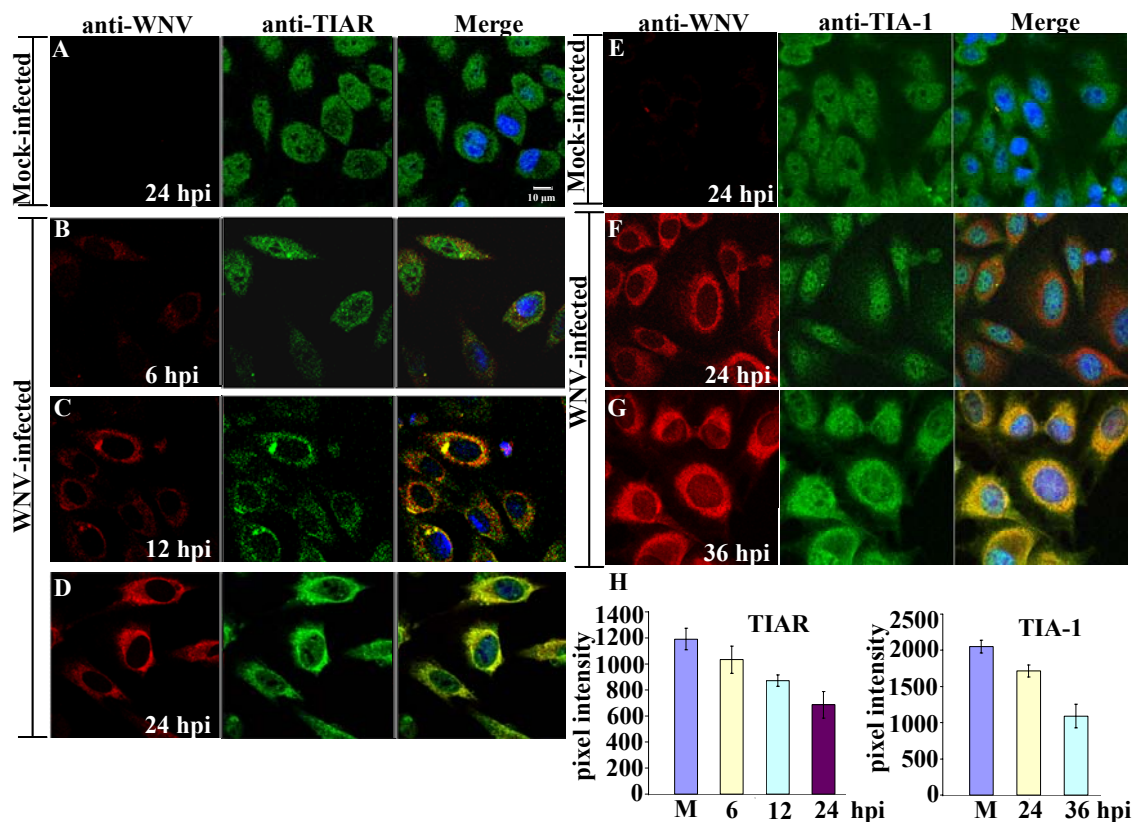
Figure 4.1. Colocalization of TIA-1 and TIAR with WNV proteins in infected BHK cells. Laser scanning confocal microscopy of (A) mock infected or (B-D) WNV infected (MOI of 5) BHK cells stained with anti-WNV (red) and anti-TIAR antibody (green) at the indicated times post infection. (E, F, and G) BHK stained with anti-WNV (red) and anti-TIA-1 antibody (green) at the indicated times after WNV (F and G) or mock (E) infection. Nuclear DNA (blue) was stained with Hoechst 33258 dye. (H) Quantification of the amount of TIAR (left panel) or TIA-1 (right panel) in the nucleus of mock-infected cells (M) and WNV-infected cells at the indicated times after infection. The relative pixel intensity in the nuclei of 20 cells at each time after infection was measured and the mean values were plotted. Error bars indicate the standard deviation of the mean. Bar = 10μm.
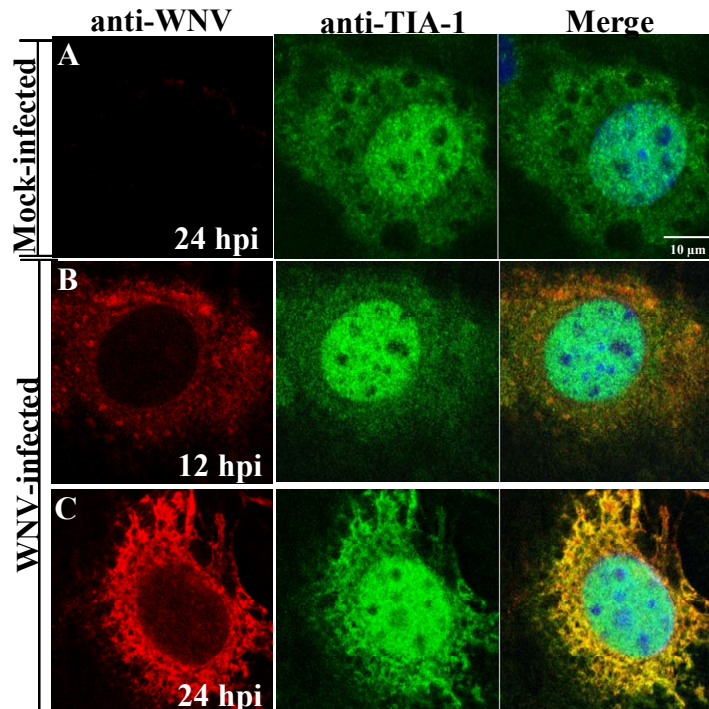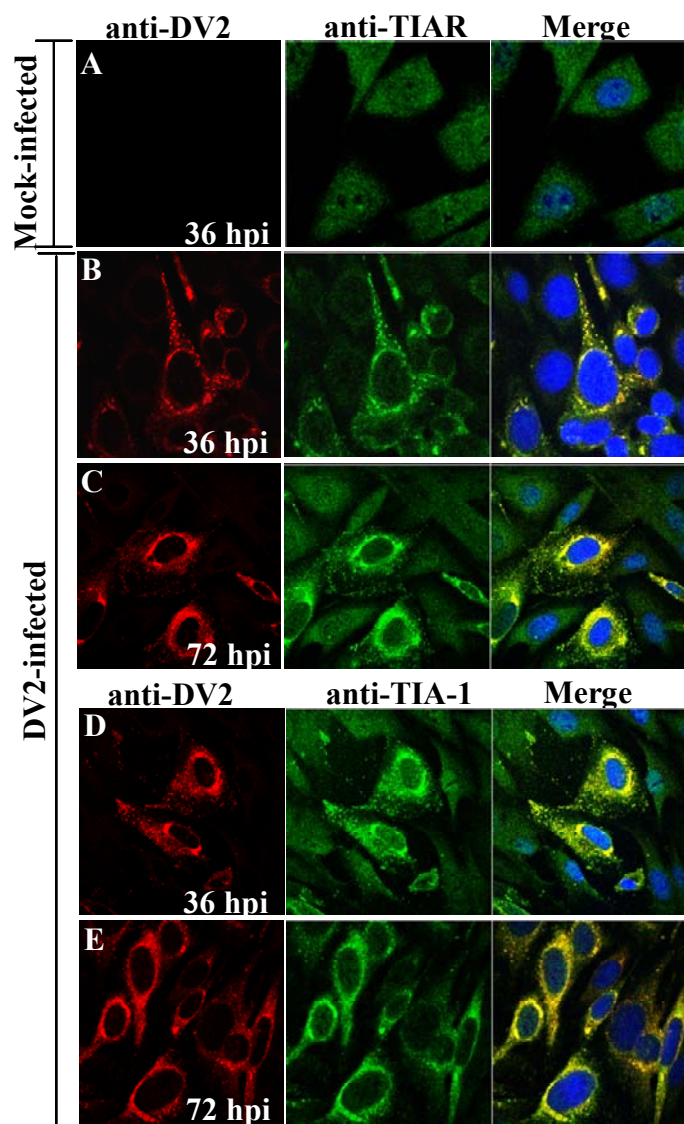
Figure 4.2. Colocalization of TIA-1 with WNV proteins in infected TIAR-/- MEFs. Laser scanning confocal microscopy of (A) mock infected or (B-C) WNV infected (MOI of 5) TIAR-/- MEFs stained with anti-WNV (red) and anti-TIA-1 antibody (green) at the indicated times post infection. Bar = 10µm.

0.1), a divergent flavivirus from a different serocomplex than WNV, and analyzed at 12, 24, 36, and 72 hpi as described in Materials and Methods. Due to the lower MOI, at 12 and 24 hpi, DV2 proteins were detected in only about 5% of the cells (data not shown). By 36 hpi, clusters of infected cells with bright virus-specific cytoplasmic foci were observed (~40% of the cells) (Fig. 4.3B and D, red). At 72 hpi, in about 60% of the cells, DV2 proteins were detected with a distribution and staining intensity (Fig. 4.3C and E, red) similar to that observed in WNV infected cells at 24 hpi (Fig. 4.1D and F, red). Strong colocalization of both TIAR (Fig. 4.3B and C, merge) and TIA-1 (Fig. 4.3D and E, merge) with DV2 proteins was detected at 36 and 72 hpi. This colocalization was primarily in the perinuclear region but was also observed in foci extending into the cytoplasm of the infected cells (Fig. 4.3B-E, merge). In the uninfected cells visible in the middle panels of Fig. 4.3B-E, TIA-1 and TIAR were equally distributed in the cytoplasm and nucleus. These results suggest that the colocalization of TIA-1/TIAR with viral proteins is a general feature of flavivirus infections.

TIA-1 and TIAR interact with sites of WNV and DV2 RNA replication.

In previous *in vitro* RNA-protein interaction assays, the TIA-1/TIAR proteins were shown to bind specifically to the WNV3′(-)SL RNA (Li et al., 2002). The minus-strand RNA of flaviviruses is present in infected cells only in RNA replication complexes (Brinton, 2002; Lindenbach and Rice, 2007). An antibody to dsRNA that does not detect either cellular ribosomal RNA or tRNA was previously utilized to detect flavivirus
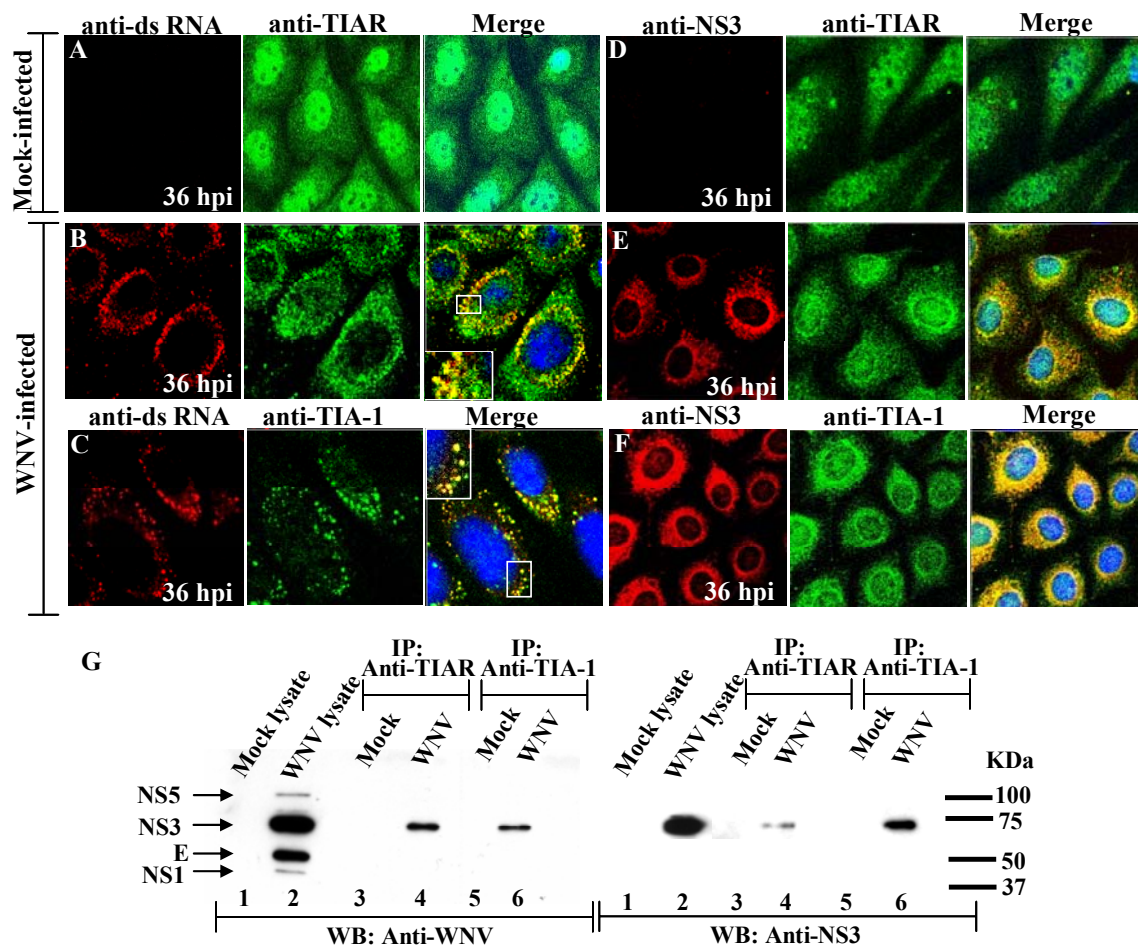
Figure 4.3. Colocalization of TIA-1 and TIAR with DV2 proteins in infected BHK cells. (A) Mock infected or (B-E) DV2 infected (MOI of 0.1) BHK cells stained with anti-DV2 (red) and anti-TIAR (B and C, green) or anti-TIA-1 (D and E, green) antibodies at 36 and 72 hpi.

replication complexes in infected cells (Miller, Sparacio, and Bartenschlager, 2006). To test whether TIA-1/TIAR colocalized with viral dsRNA in infected cells, BHK cells infected with WNV (MOI of 0.1) or DV2 (MOI of 0.1) were fixed and incubated with anti-dsRNA and anti-TIA-1 or anti-TIAR antibody. A lower MOI for WNV and later time points were used to better visualize the replication complexes. Perinuclear foci stained with anti-dsRNA antibody were observed in WNV infected cells at 36 hpi (Fig. 4.4B and C, red) but not in mock infected cells (Fig. 4.4A). In WNV infected cells, strong colocalization of TIA-1/TIAR with the dsRNA was observed in bright perinuclear foci (Fig. 4.4B and C, merge). Similar dsRNA perinuclear foci and similar TIA-1/TIAR colocalization with these foci were observed in DV2 infected cells at 72 hpi (Fig. 4.5B and C), indicating that TIA-1/TIAR strongly colocalized with flavivirus RNA complexes in infected cells.

Previous immunofluorescence studies using antibodies specific to dsRNA as well as to individual flavivirus NS proteins suggested that NS3 and NS5 as well as NS1, NS2a, and NS4a associate with ds viral RNA in flavivirus replication complexes located in the perinuclear region of infected cells (Westaway et al., 1997; Westaway, Mackenzie, and Khromykh, 2003). Broader areas of colocalization were observed with the anti-WNV (Fig. 4.1) than with the anti-dsRNA antibody, suggesting that TIA-1/TIAR might also interact with a viral nonstructural protein. Coimmunoprecipitation experiments were done using lysates prepared from mock infected or WNV infected BHK cells at 24 hpi and anti-TIAR or anti-TIA-1 antibody as described in Materials and Methods. Cell lysates as well as immunoprecipitates were then analyzed by SDS-PAGE and transferred to

nitrocellulose membranes for Western blot analysis using anti-WNV (Fig. 4.4G, left panel). Four WNV proteins, presumed to be NS5, NS3, E, and NS1, were detected in lysates from WNV infected cells (Fig. 4.4G, left panel, lane 2), but not in lysates or immunoprecipitates from mock infected cells (Fig. 4.4G, left panel, lanes 1, 3, and 5). In immunoprecipitates from WNV infected cells, both anti-TIAR (Fig. 4.4G, left panel, lane 4) and anti-TIA-1 (Fig. 4.4G, left panel, lane 6) antibody coimmunoprecipitated a viral protein with the expected size of NS3. To verify that this was NS3, samples precipitated with anti-TIA-1 or anti-TIAR antibodies was analyzed by Western blot analysis using an anti-WNV NS3 monoclonal antibody. NS3 was detected in lysates from WNV infected cells after immunoprecipitation with both anti-TIAR (Fig. 4.4G, right panel, lane 4) or anti-TIA-1 (Fig. 4.4G, right panel, lane 6) antibody.

Anti-WNV NS3 monoclonal antibody was next used to study the colocalization of TIA-1/TIAR with NS3 in BHK cells infected with WNV or DV2 at 36 or 72 hpi, respectively. NS3 was previously shown to be broadly distributed around the nucleus and to colocalize with dsRNA foci in flavivirus-infected cells (Miller, Sparacio, and Bartenschlager, 2006). In the merged images, both TIA-1 and TIAR strongly colocalized with NS3 in WNV infected cells (Fig. 4.4E and F, merge). Bright focal areas as well as more diffuse areas of colocalization were observed. Similar results were observed in DV2 infected cells at 72 hpi (Fig. 4.5E and F).

Figure 4.4. Interaction of TIA-1 and TIAR with WNV replication complex components. BHK cells were infected with WNV at a MOI of 0.1. Laser scanning confocal microscopy of (A and D) mock infected and WNV (B, C, E, and F) infected cells stained with anti-dsRNA (A-C, red) or anti-NS3 (D-F, red) and then with either anti-TIAR (A, B, D, and E, green) or anti-TIA-1 (C and F, green) antibodies at 36 hpi. Enlarged views are included in the B and C merged panels. (G) Coimmunoprecipitation of WNV proteins by anti-TIA-1 and anti-TIAR antibodies. BHK cells were infected with WNV at a MOI of 5. Immunoprecipitates were visualized by Western blot using anti-WNV (left panel) or anti-NS3 antibody (right panel). Lane 1, Mock infected lysate; Lane 2, WNV infected lysate; Lanes 3 and 5, Mock infected immunoprecipitates; Lanes 4 and 6, WNV infected immunoprecipitates. Arrows indicate the positions of the WNV proteins detected. Positions of molecular weight standards are indicated on the left.
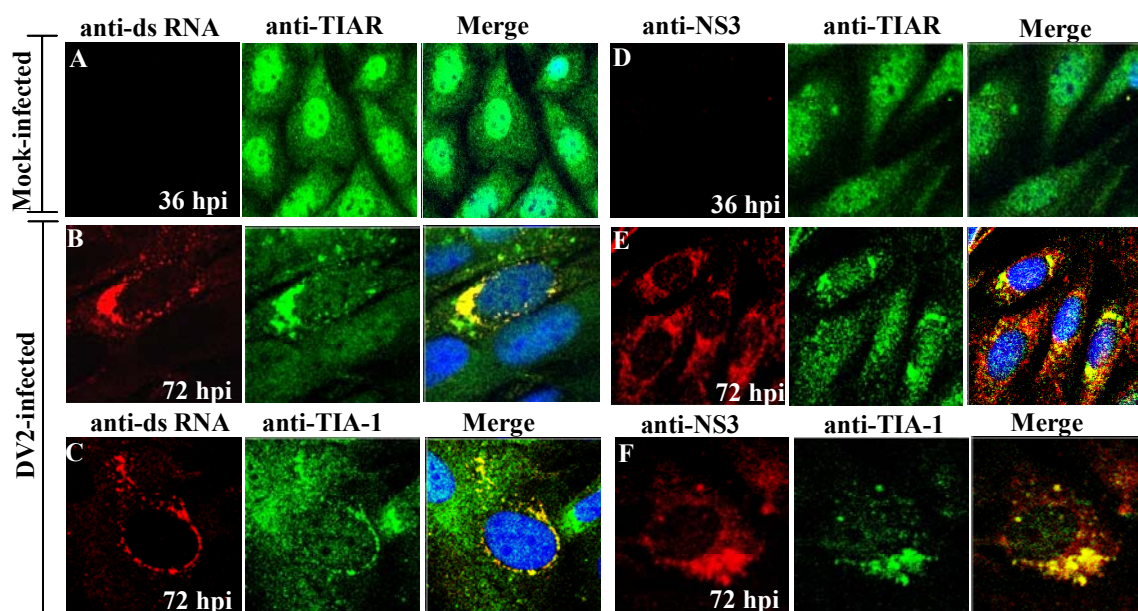
Figure 4.5. Interaction of TIA-1 and TIAR with DV2 replication complex components. BHK cells were infected with DV2 (MOI of 0.1). Laser scanning confocal microscopy of (A and D) mock infected and DV2 infected (B, C, E, and F) cells stained with anti-dsRNA (A-C, red) or anti-NS3 (D-F, red) and then with anti-TIAR (A, B, D, and E, green) or anti-TIA-1 (C and F, green) antibodies at 72 hpi.

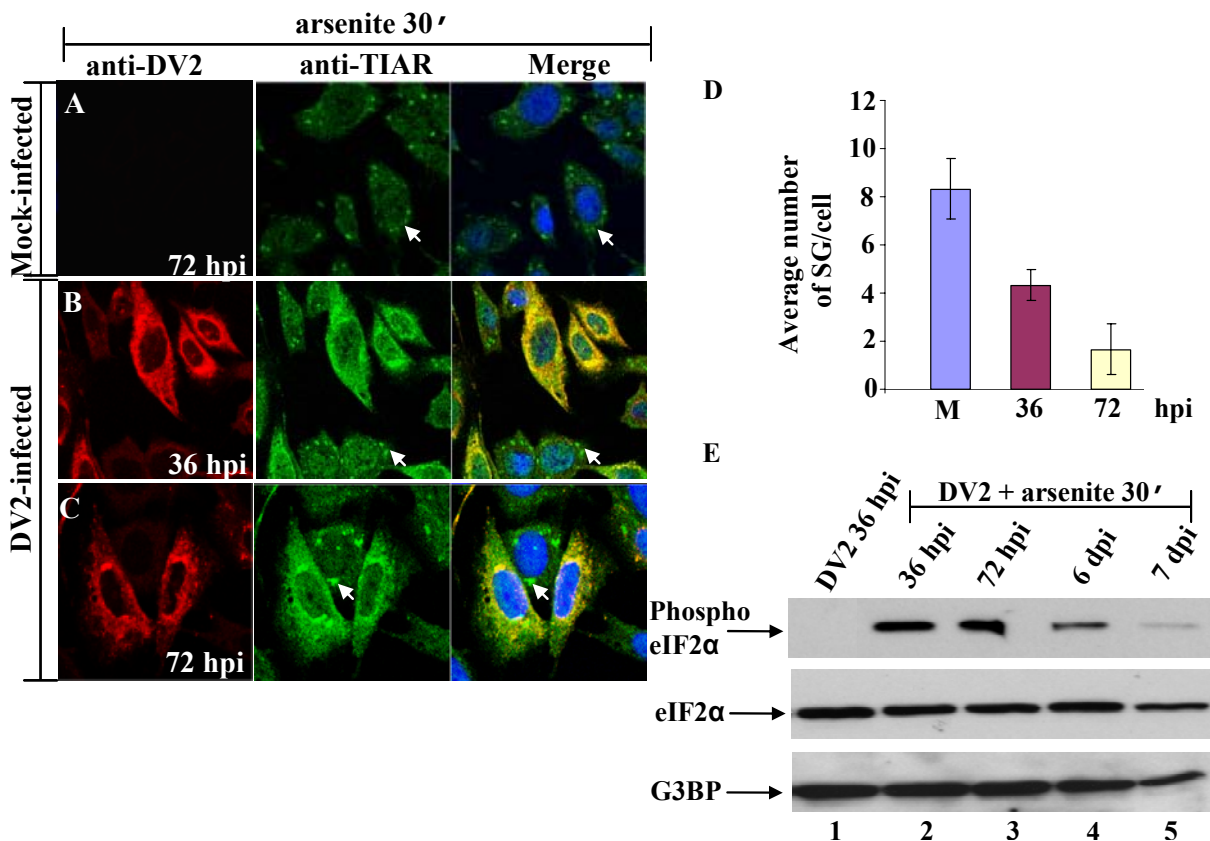**WNV and DV2 interfere with SG formation in infected BHK cells.**

TIA-1/TIAR were previously reported to be required for the formation of SG in cells after treatment with arsenite (Kedersha et al., 1999) and both proteins were shown to colocalize with viral nonstructural proteins and replication complexes in flavivirus infected cells. To determine whether a flavivirus infection would interfere with cellular SG formation, BHK cells were mock infected or infected with WNV and exposed to oxidative stress by treatment with 0.5 mM arsenite for 30 min. Infected cells were treated at 6, 12, or 24 hpi. The cells were then fixed and stained with anti-WNV (Fig. 4.6A-D, red) and anti-TIAR antibody (Fig. 4.6A-D, green). As described previously, at 6 hpi, only a small amount of colocalization of TIAR with WNV proteins was observed (Fig. 4.6B, merge). The number of SG induced by the arsenite was slightly reduced (Fig. 4.6B, green; Fig. 4.6E) as compared to mock infected cells (Fig. 4.6A, green; Fig. 4.6E). At 12 hpi, SG formation further decreased (Fig. 4.6C, green; Fig 4.6E) as colocalization of TIAR and WNV proteins increased (Fig. 4.6C, merge). Few if any SG were detected at 24 hpi (Fig. 4.6D, green; Fig 4.6E) in cells showing strong colocalization between TIAR and WNV proteins (Fig. 4.6D, merge). WNV infection alone did not induce SG formation at any time after infection (Fig. 4.1B-D, green). The effect of DV2 infection on SG formation was also investigated. BHK cells infected with DV2 for 36 or 72 hr were treated with 0.5 mM arsenite for 30 min and immunostained with anti-DV2 and anti-TIAR (Fig. 4.7). At both times, strong colocalization of TIAR and DV2 proteins was observed. Few SGs was observed in infected cells (Fig. 4.7B and C, green; Fig. 4.7D), whereas many SG were observed in uninfected cells (Fig. 4.7A, green).

Since phosphorylation of eIF2α at S51 also regulates SG formation, the effect of WNV and DV2 infections on eIF2α phosphorylation was assayed. BHK cells were infected with either virus and at various times after infection, cells were treated for 30 min with 0.5 mM arsenite. Control infected cells were not treated with arsenite. Proteins in cell lysates were analyzed by Western blot using a polyclonal antibody specific for eIF2α phosphorylated at S51 (Fig. 4.6F). Under these experimental conditions, phosphorylation of eIF2α was not detected in mock infected cells or by 24 hr after WNV (Fig. 4.6F, lane 3) or 36 hr after DV2 (Fig. 4.7E, lane 1) infection. High levels of eIF2α phosphorylation were observed in extracts of mock infected cells treated with arsenite (Fig. 4.6F, lane 2). Reduced levels of phospho-eIF2α were detected in WNV infected extracts by 12 hpi and were further decreased by 24 hpi (Fig. 4.6F, lanes 4-6). In the DV2 extracts, decreased phosphorylation of eIF2α was observed at later times post infection (Fig. 4.7E, lanes 2-5). The large number of uninfected cells present in the DV2 infected cultures are the source of the higher levels of phospho-eIF2α observed until 6 dpi. The levels of total eIF2α and of another protein involved in SG formation, G3BP, remained constant under all conditions tested and after infection with both viruses (Fig. 4.6F and 4.7E). Although neither WNV nor DV2 infection induced SG formation in BHK cells, cells infected with both flaviviruses became progressively more resistant to SG induction by arsenite with time after infection.
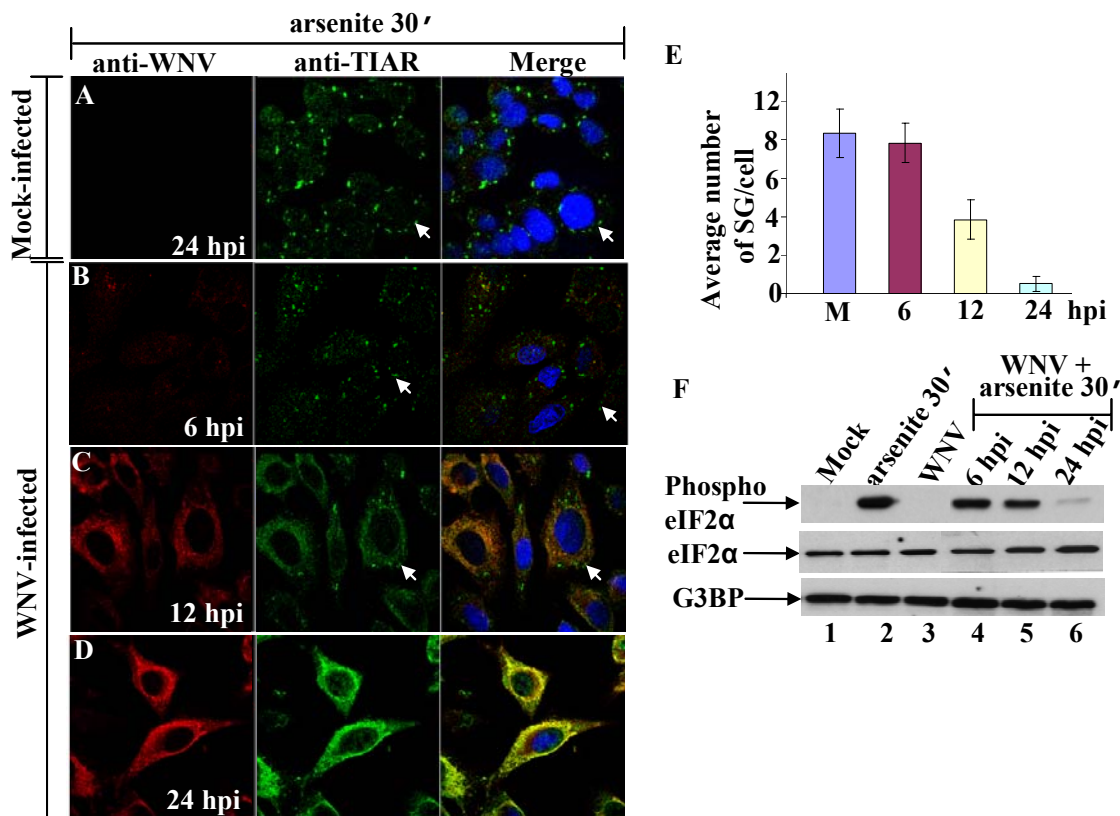
Figure 4.6. WNV infection interferes with SG formation. Laser scanning confocal microscopy of mock infected (A) and WNV infected (MOI of 5) (B, C, and D) BHK cells treated with 0.5 mM arsenite for 30 min at the indicated times after infection. The cells were fixed, permeabilized, and stained with anti-WNV (A-D, red) and with the SG marker, anti-TIAR (A-D, green). Arrows indicate representative SG. (E) Quantification of the number of SG in mock-infected (M) cells and WNV-infected cells at the indicated times after infection. SG in 70 cells were counted for each experimental condition and the average number of SG/cell was plotted. Error bars indicate the standard deviation of the mean. (F) Western blot analysis of phospho-eIF2α in BHK cells mock infected or infected with WNV (MOI of 5) and then treated or not treated with 0.5 mM of arsenite for 30 min at the indicated times after infection. Lane 1, Mock infected BHK cells; Lane 2, cells treated with 0.5 mM arsenite for 30 min; Lane 3, cells infected with WNV; Lanes 4-6, cells infected with WNV and then treated with arsenite for 30 min at the indicated times. Phospho-eIF2α (S51) (upper panel), total eIF2α (middle panel), and G3BP (lower panel) were detected with specific antibodies.
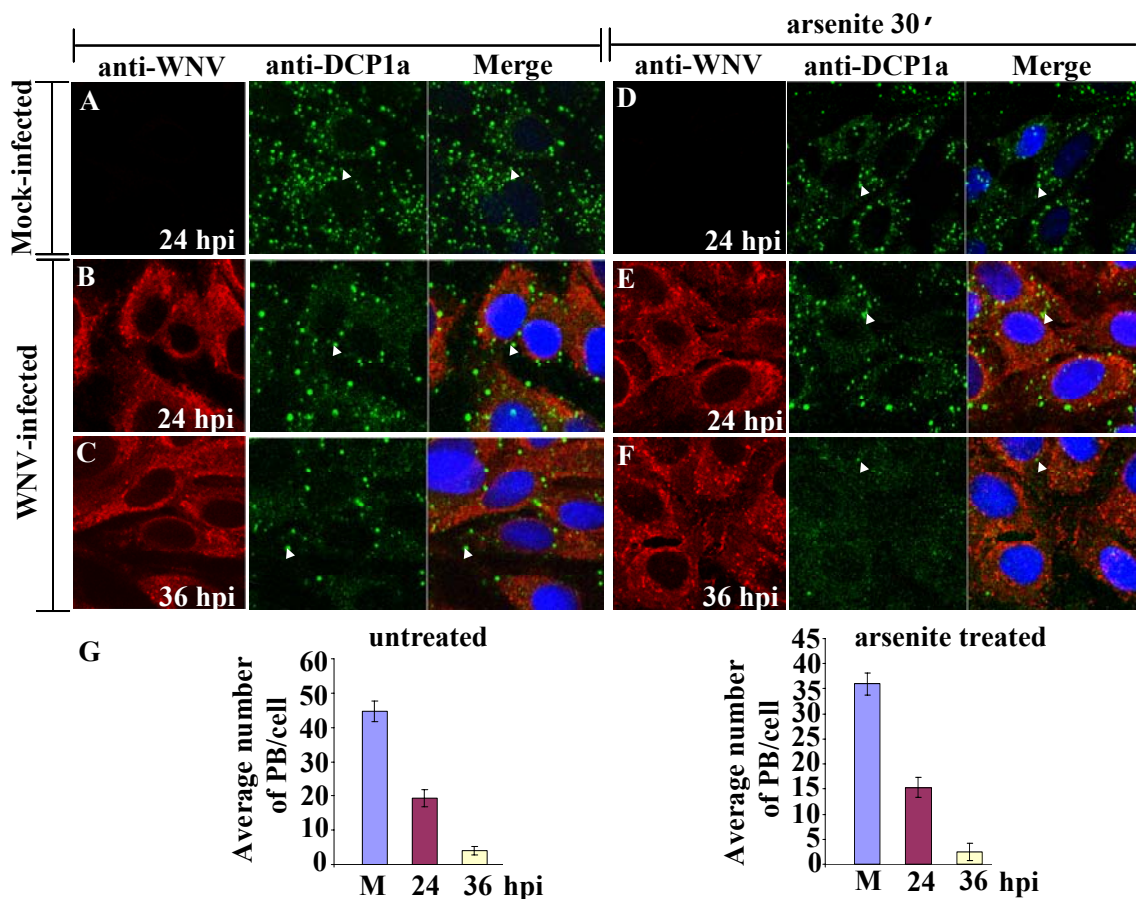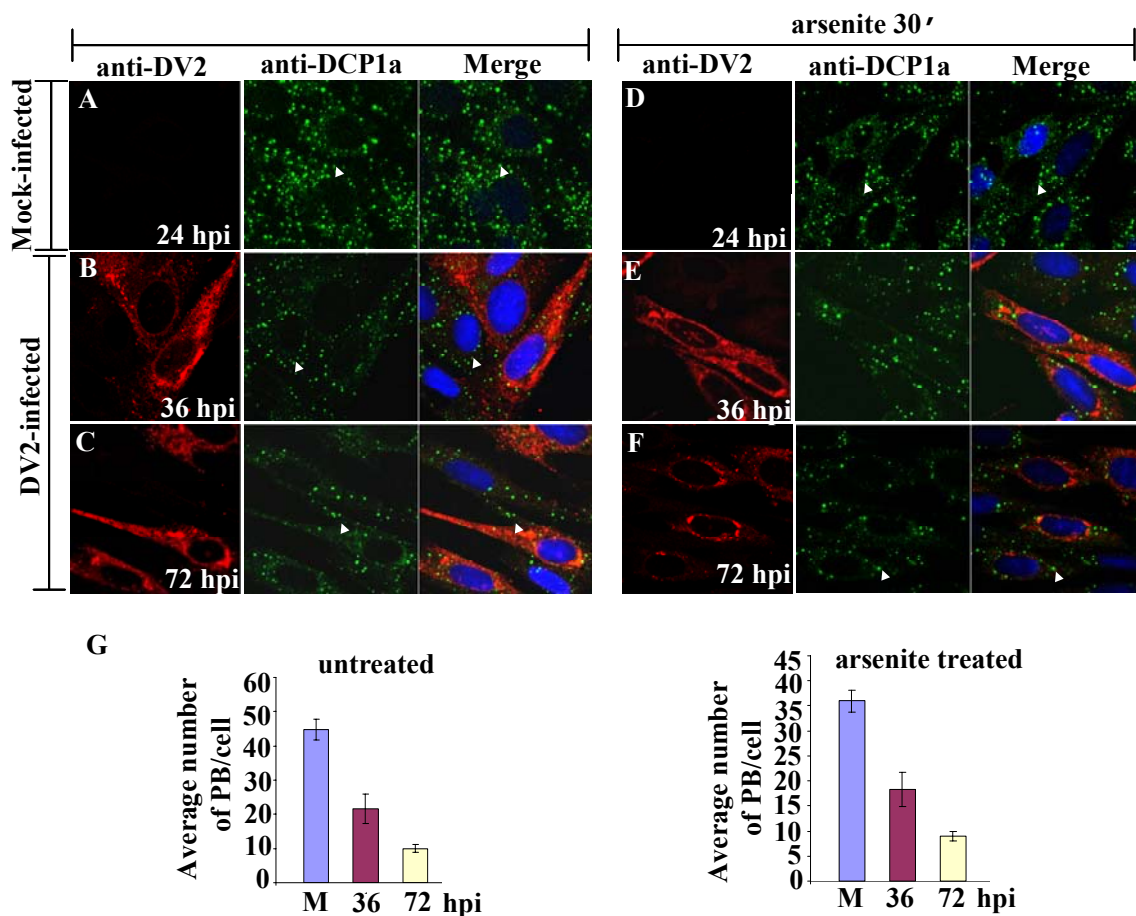
Figure 4.7. DV2 infection interferes with SG formation. Laser scanning confocal microscopy of mock infected (A) and DV2 infected (MOI of 0.1) (B and C) BHK cells treated with 0.5 mM arsenite for 30 min at the indicated times. The cells were fixed, permeabilized, and stained with anti-DV2 (A-C, red) and with the SG marker, anti-TIAR (A-C, green). Arrows indicate representative SG. (D) Quantification of SG in mock-infected cells (M) and DV2-infected cells at different times after infection (36 and 72 hpi). The number of SG in 70 cells for each experimental condition was counted and the average number of SG/cell was plotted. Error bars indicate the standard deviation of the mean. (E) Western blot analysis of phospho-eIF2α in BHK cells mock infected or infected with DV2 and then treated or not treated with of arsenite for 30 min at various times after infection. Lane 1, cells infected with DV2 (MOI of 0.1); Lanes 2-5, cells infected with DV2 and then treated with arsenite at the indicated times post infection. Phospho-eIF2α (S51) (upper panel), total eIF2α (middle panel), and G3BP (lower panel) were detected with specific antibodies.

WNV and DV2 infections interfere with PB assembly.

SG and PB share some components and are dynamically linked via their role in regulating cytoplasmic mRNA storage and/or degradation (Kedersha et al., 2005; Wilczynska et al., 2005). To test whether WNV and DV2 infections also interfere with PB assembly, BHK cells mock infected or infected with either WNV or DV2 were treated or not treated for 30 min with 0.5 mM arsenite at various times after infection. The cells were then fixed and incubated with antibody to the PB marker DCP1a and anti-WNV (Fig. 4.8) or anti-DV2 (Fig. 4.9). PB were detected in untreated cells (Fig. 4.8A-C, green; Fig. 4.9A-C, green) as well as in arsenite treated cells (Fig. 4.8D-F, green; Fig. 4.9D-F, green). In uninfected, WNV infected, and DV2 infected cells, PB were evenly distributed throughout the cytoplasm (Fig. 4.8 and Fig. 4.9). In both uninfected and infected cells treated with arsenite, the number of PB was decreased (Fig. 4.8 G; Fig. 4.9G) and the remaining PB were mainly located around the nucleus (Fig. 4.8D-F, green; Fig. 4.9D-F, green). In WNV infected cells, a noticeable reduction in PB formation was observed by 24 hpi in untreated (Fig. 4.8B, green; Fig 4.8G, left panel) and arsenite-treated (Fig. 4.8E, green; Fig 4.8G, right panel) cells as compared to mock infected cells (Fig. 4.8A and Fig. 4.8D, green; Fig 4.8G). A further reduction in PB formation was observed in both arsenite-untreated (Fig. 4.8C, green; Fig 4.8G, left panel) and treated (Fig. 4.8F, green; Fig 4.8G, right panel) WNV-infected cells at 36 hpi. In DV2 infected cells, a reduction in PB formation was observed at later times post infection (Fig. 4.9B, C, E, and F, green; Fig 4.9G) consistent with the slower replication kinetics of DV2.

Figure 4.8. WNV infection interferes with PB assembly. Laser scanning confocal microscopy of mock infected (A and D) and WNV infected (MOI of 5) (B, C, E, and F) cells that were treated (right) or not treated (left) with arsenite for 30 min at the indicated times. The cells were stained with anti-WNV (A-F, red) and then with anti-DCP1a (a PB marker) (A-F, green) antibody. Arrowheads indicate representative PB. (G) Quantification of the number of PB in mock-infected cells (M) and WNV-infected cells treated (right) or not treated (left) with arsenite. PB in 50 cells were counted for each experimental condition at the indicated times after infection and the average number of PB/cell was plotted. Error bars indicate the standard deviation of the mean.

Figure 4.9. DV2 infection interferes with PB assembly. Laser scanning confocal microscopy of mock infected (A and D) and DV2 infected (MOI of 0.1) (B, C, E, and F) cells that were not treated (A-C) or treated (D-F) with arsenite for 30 min at the indicated times after infection. The cells were then stained with anti-DV2 (A-F, red) and anti-DCP1a (a PB marker) (A-F, green) antibody. Arrowheads indicate representative PB. (G) Quantification of PB in mock-infected cells (M) and DV2-infected cells treated (right) or not treated (left) with arsenite. PB were counted in 50 cells under each experimental condition at the indicated times and the average number of PB/cell was plotted. Error bars indicate the standard deviation of the mean.

These results indicate that both WNV and DV2 infections interfere with PB assembly in BHK cells.

DISCUSSION

In normal cells that are not undergoing stress, TIA-1 and TIAR are distributed fairly evenly between the cytoplasm and nucleus. In response to stress, TIA-1 and TIAR aggregate with cell mRNAs in SG (Kedersha et al., 1999). In the present study, a unique distribution pattern for these proteins was observed in cells infected with two different flaviviruses, WNV and DV2. First TIAR and then TIA-1 relocated to the perinuclear region in flavivirus infected cells. In WNV infected cells, perinuclear foci of TIAR were detected by 6 hpi and a significant amount of TIAR were observed in this region by 12 hpi. With TIA-1, perinuclear foci were not detected until 24 hpi and significant concentrations of TIA-1 in this region were not seen until 36 hpi. Interestingly, the initiation of TIA-1 relocation to the perinuclear region in infected cells did not begin until the majority of TIAR had already relocated to this region.

By 6 hpi, newly translated viral proteins were detectable in the cytoplasm by immunoflourescence and by 12 hpi, the amount of viral protein had increased and was concentrated in the perinuclear region. Colocalization of bright foci of TIAR and of viral proteins was detected by 6 hpi and the amount of colocalization progressively increased thereafter. These bright perinuclear foci also contained dsRNA identifying them as viral replication complexes. Previous *in vitro* RNA-protein binding assays showed that TIAR bound 10 times more efficiently than TIA-1 to the WNV 3′(-)SL RNA (Li et al., 2002).

The different kinetics of TIA-1 and TIAR redistribution in flavivirus infected cells could be due to the more efficient interaction between cytoplasmic TIAR and the 3′ ends of viral minus strand RNAs. The 3′(-)SL is thought to contain promoter elements for genomic RNA initiation and it was previously proposed that TIAR functions as a transcription factor for genomic RNA initiation (Li et al., 2002). This hypothesis was recently supported by data showing that mutagenesis of the mapped protein binding sites on the WNV 3′(-)SL RNA in a WNV infectious clone negatively affected genomic RNA synthesis (Emara and Brinton, unpublished data). Previous analyses of the kinetics of flavivirus RNA synthesis showed an initial low peak of genomic RNA synthesis between 6 and 10-12 hpi followed by a switch to exponentially increasing genomic RNA synthesis (Brinton, 2002; Trent, Swensen, and Qureshi, 1969). The level of genomic RNA synthesis infected cells correlates temporally with the extent of TIAR relocation to the perinuclear region.

It was previously shown that the yield of WNV produced by TIAR-/- MEFs, which express three times more TIA-1 than wildtype MEFs, was reduced by only 6-to-8 fold as compared to TIA-1-/- or control MEFs (Li et al., 2002). These data suggested that TIA-1 could also function as a viral transcription factor when TIAR was not present. Consistent with this hypothesis, colocalization of TIA-1 and WNV proteins in infected TIAR-/- MEFs occurred in a time course similar to that observed with TIAR in cells expressing both proteins. This data also suggests that the ability of TIA-1 to relocate to the perinuclear region is not being actively prevented in infected cells. However, the

possibility that TIA-1 is interacting with a cell protein partner and so is not available for interaction with viral components until later times after infection can not be ruled out.

The data suggest the possibility that TIA-1/TIAR may also interact with a viral nonstructural protein as well as with the 3′(-)SL RNA. WNV NS3, but not NS5, NS1, or E, was co-immunoprecipatated by both anti-TIA-1 and anti-TIAR antibodies. The four hydrophobic nonstructural proteins (NS2a, NS2b, NS4a, and NS4b) have been reported to be tightly complexed with NS3 in dense membrane fractions (Chu and Westaway, 1992) while the RdRp NS5 is more loosely associated (Grun and Brinton, 1987). Since antibodies to the four hydrophobic proteins were not available, it was not possible to rule out an additional interaction between one of these hydrophobic proteins and TIA-1 and/or TIAR. Flaviviruses initiate RNA synthesis de novo. The interaction of TIA-1 or TIAR with a protein in a flavivirus RdRp complex might enhance the preferential recognition of minus strand templates by these complexes. TIA-1/TIAR do not bind to the 3′ terminal SL RNA of the genomic (+) RNA template (Emara and Brinton, unpublished data). As the number of such complexes progressively accumulates in infected cells, the synthesis of genomic RNA would be significantly and preferentially amplified over minus strand RNA. The binding of TIA-1/TIAR to the 3′(-)SL RNA might stabilize it allowing other necessary factors to assemble and initiation of genomic RNA synthesis to begin. It is currently not known whether the self-aggregating domains of TIA-1/TIAR play a role in these protein-protein and RNA-protein interactions.

Flaviviruses are unique among animal positive strand RNA viruses in preventing rather than facilitating the shutoff of host cell translation. Flaviviruses replicate at

significantly slower rates than most other positive strand RNA viruses in mammalian and avian cells, and rapid shutoff of cell protein synthesis with the resulting negative effect on cell viability would have a deleterious effect on flavivirus yields. This is the first report showing that flavivirus infections do not induce SG formation and that infected cells become increasingly resistant to the induction of SG by arsenite treatment with time after infection. These data suggest that flavivirus infections actively inhibit SG formation. The time course of the resistance to SG formation coincided with that of the relocation of TIAR to the perinuclear region rather than with the relocation of TIA-1 or with decreased phosphorylation of eIF2α. These observations suggest that the sequestration of TIAR via its interaction with the viral 3′(-)SL RNA and possibly also a viral nonstructural protein is the initial reason for the observed decrease in SG formation in flavivirus infected cells. A previous study showed that although eIF2α was phosphorylated in both TIA-/- and TIAR-/- MEFs, SG formation was impaired in TIA-/- MEFs but not in TIAR-/- MEFs, suggesting that TIAR alone could not form SG (Gilks et al., 2004). The observation that SG formation was inhibited to some extent when TIAR but not TIA-1 was sequestered in the perinuclear suggests the possibility that additional components necessary for SG formation may also be sequestered in the perinuclear region of flavivirus infected cells. If self-aggregation of TIAR in the perinuclear region occurs, this might be what attracts the additional SG components. In the previous study that identified TIAR as a WNV 3′(-) SL RNA binding protein, three additional cell proteins (p50, p60, and p108) were also shown to bind to this viral RNA (Li et al., 2002). Some of these viral RNA binding proteins could also be components of SG. The assembly of pseudo-SG complexes around

the viral minus strand RNA replication complexes might be part of the remodeling of the perinuclear membranes by virus infection to create an environment for efficient genomic RNA synthesis and encapsidation.

Complete resistance to SG induction and a significant decrease in eIF2α phosphorylation at S51 were not observed in WNV infected cells until 24 hpi, a time by which maximum levels of virus replication had been achieved. Unlike flaviviruses, both Semliki Forest virus (SFV), a positive-strand RNA alpha togavirus (McInerney et al., 2005) and some strains of reovirus, a double-stranded RNA virus (Smith et al., 2006), rapidly shut off host cell protein synthesis and induce SG formation via the induction of eIF2α (S51) phosphorylation. For both viruses, the phosphorylation of eIF2α as well as the aggregation of TIA-1/TIAR into SG were shown to be important for shut off of host cell protein translation (McInerney et al., 2005; Smith et al., 2006). In cells subjected to environmental stresses, the activation of PKR and/or other cellular kinases leads to the phosphorylation of eIF2α (Anderson and Kedersha, 2002a). Activation of PKR followed by phosphorylation of eIF2α by PKR and the formation of SG was postulated to result in the shut off host cell translation in cells infected with SFV (McInerney et al., 2005; Ventoso et al., 2006) or Sindbis virus (Ventoso et al., 2006). The expression of P58[IPK], a PKR/PERK inhibitor, was shown to be decreased in L929 cells infected with host shutoff-inducing strains of reovirus and high levels of phospho-eIF2α were detected (Smith et al., 2006). In contrast, in cells infected with two flaviviruses, DV2 or Japanese encephalitis virus (MOI of 3), the expression of P58[IPK] was significantly upregulated at 24 hpi (Yu et al., 2006). The timing of this upregulation was exactly coincident with the

decrease in eIF2a phosphorylation observed in arsenite treated WNV infected (MOI of 5) cells in the present study. Yu et al.(Yu et al., 2006) also showed that the upregulation of P58[IPK] was the result of activation of the cellular unfolded protein response by the accumulation of several different flavivirus proteins in infected cells. The initial shut off of SG formation in flavivirus infected cells appears to be due to the sequestration of TIAR, and possibly also of other SG components, in the perinuclear region of infected cells via interaction with viral components. A direct benefit of this interaction for the virus is that it likely facilitates significant amplification of genomic RNA synthesis. An indirect benefit is that this interaction inhibits the shut off of host protein synthesis. However, flaviviruses appear to utilize multiple mechanisms to inhibit SG formation as evidenced by the upregulation of P58[IPK] at later times after infection mediated by the accumulation of viral proteins.

PB are involved in mRNA degradation and in translational repression (Eulalio, Behm-Ansmant, and Izaurralde, 2007). In the present study, a similar decrease in PB assembly was observed in both untreated and arsenite treated flavivirus infected cells. This decrease was temporally correlated with the initiation of TIA-1 relocation and the decrease in eIF2α phsophorylation in arsenite treated cells. The mechanism by which flaviviruses interfere with PB assembly in infected cells is not yet known. The interference with PB assembly may be related to activation of the unfolded protein response and would provide an additional mechanism to prevent translational repression and protect viral RNA as well as cell mRNA from degradation.

MATERIALS AND METHODS

Cells.

Baby hamster kidney (BHK-21, strain W12) cells (Vaheri et al., 1965) (referred to as BHK cells) were maintained as described previously (Scherbik et al., 2006). C57/BL/6 and C57/BL/6 TIAR-/- MEF cell lines were provided by Paul Anderson (Brigham and Woman's Hospital, Boston, MA) and grown in MEM supplemented with 10% FCS, 1X MEM non-essential amino acids (Invitrogen), 1mM sodium pyruvate (Invitrogen), 2 mM glutamine (Invitrogen), and 10 μg/ml of gentamycin.

Viruses.

A stock of WNV strain Eg101 was prepared in BHK cells (2 x 10^8 PFU/ml) as previously described (Scherbik et al., 2006). DV2, strain Bangkok D80-100 was provided by Walter Brandt (Walter Reed Army Institute of Research, Washington, DC). The titer of a 10% W/V suckling mouse brain homogenate was 2 x 10^6 PFU/ml. Cells were infected with WNV at a MOI of 5 or 0.1 and with DV2 at a MOI of 0.1. Virus was adsorbed to cells for 1 hr at room temperature, the inoculum was removed and the cells were washed three times with serum free medium. MEM containing 5% FCS was added and the infected cells were incubated at 37^oC in a CO_2 incubator. To induce stress, cells were treated at various times after infection with 0.5 mM sodium m-arsenite (Sigma-Aldrich St. Louis, Mo.) in MEM for 30 min. Virus growth experiments were done as described previously (Li et al., 2002).

Antibodies.

Goat polyclonal antibodies to the C-terminus of TIAR, the C-terminus of TIA-1, eIF2α Texas red-conjugated bovine anti-mouse, FITC-conjugated donkey anti-goat, FITC-conjugated chicken anti-rabbit, and HRP-conjugated anti-goat, anti-mouse and anti-chicken antibodies were purchased from Santa Cruz Biotechnology, Inc (Santa Cruz, CA). Rabbit polyclonal anti-phospho-eIF2α (serine 51) and anti-rabbit immunoglobulin G antibody conjugated with horseradish peroxidase (HRP) were from Cell signaling (Beverly, MA), chicken polyclonal anti-G3BP was from Abcam (Cambridge, MA), mouse monoclonal anti-dsRNA antibody was from English & Scientific Consulting (Szirak, Hungary), and mouse anti-WNV NS3 monoclonal antibody was from R&D Systems (Minneapolis, MN). Rabbit anti-human DCP1a serum was a gift from J. Lykke-Anderson (University of Colorado, Boulder, CO). Mouse anti-WNV hyperimmune serum was from Robert Tesh (University of Texas Medical Branch, Galveston, TX). Mouse anti-DV2 hyperimmune serum was provided by Walter Brandt (Walter Reed Army Institute of Research, Washington, DC).

Western blotting.

Western blot analysis was carried out as previously described (Scherbik et al., 2006). Primary antibodies were diluted in 1X Tris-buffered saline (TBS) containing 5% bovine serum albumin (1:1000 for anti-phospho-eIF2α, 1:500 for anti-eIF2α, 1:3000 for anti-G3BP, and 1:500 for anti-WNV and anti-WNV NS3 antibodies) and the secondary antibody was diluted 1:2000 in 1X TBS containing 5% non-fat dry milk (NFDM).

Coimmunoprecipitation assays.

BHK cells (2 x 10^6) were mock infected or infected with WNV at a MOI of 5. At 24 hpi, cell lysates were prepared using lysis buffer containing 50 mM sodium phosphate (pH 7.2), 150 mM Nacl, 1% NP40, and Complete, Mini, EDTA-free protease inhibitor cocktail (Roche). Cell lysates were incubated on ice for 30 min, sonicated, and then centrifuged at 2000 xg for 5 min at 4°C. The supernatant (250 µl/ ~100 µg total protein) was precleared with protein A/G-magnetic beads (New England Biolabs, Beverly, MA) for 1 hr at 4°C with rotation. The clarified supernatants were incubated with 1 µg of anti-TIA-1 or anti-TIAR antibody at 4°C for 1 hr with rotation, then beads were added and incubated for 1 hr. Beads were collected magnetically, washed seven times with 1 ml of lysis buffer, and proteins eluted by boiling for 5 min. Proteins were separated by 12% SDS-PAGE, transferred to nitrocellulose membranes, and analyzed by Western blotting using either mouse anti-WNV or anti-NS3 antibody.

Detection of intracellular and cellular viral proteins by immunofluorescence.

BHK, C57BL/6, and TIAR-/- cells (2 x 10^4) were seeded onto 3 mm cover slips (Fisher Scientific, Pittsburgh, PA) and grown to about 50% confluency. At various times after infection, cells were fixed in 4% paraformaldehyde (Sigma-Aldrich) in PBS for 10 min at room temperature, permeabilized with 100% chilled methanol for 10 min at -20°C, washed three times in PBS and incubated with blocking buffer [PBS containing 5% heat inactivated horse serum (Invitrogen)] overnight at 4°C. Primary antibodies were diluted in blocking buffer (1:1000 for anti-TIAR, anti-TIA-1 and anti-Dcap1, 1:200 for anti-

dsRNA, and 1:100 for anti-WNV, anti-DV2 and anti-WNV NS3 antibody) and incubated with cells at 37°C for 1 hr. Cells were then washed 3X 10 min with PBS, and incubated for 1 hr at 37°C with Texas red-labeled and FITC-labeled secondary antibodies diluted 1:300 in blocking buffer containing 0.5 μg/ml Hoechst 33258 dye (Molecular Probes, Bedford, MA) to stain the nuclear DNA. Cover slips were mounted in Prolong Gold antifade reagent (Invitrogen) and the cells were viewed and photographed with a Zeiss Confocal Microscope LSM 510 (Zeiss, Germany) using a 100X oil immersion objective. The images compared for each experimental series were collected using the same instrimuent settings and the images were analyzed using Zeiss software version 3.5.

Laser confocal imaging settings.

FITC was excited with the 488 nm line of an Argon ion laser, and emitted light was collected through a 505-530 nm band-pass filter. Texas red was excited with the 543 nm line of a He-Ne laser, and the emitted light was collected through a 560 nm long-pass filter. Hoechst 33258 dye was excited with the 364 nm line of an Enterprise laser, and the emitted light was collected through a 385-470 nm band-pass filter.

REFERENCES

Anderson, P. (1995). TIA-1: structural and functional studies on a new class of cytolytic effector molecule. *Curr Top Microbiol Immunol* **198,** 131-43.

Anderson, P., and Kedersha, N. (2002a). Stressful initiations. *J Cell Sci* **115**(Pt 16)**,** 3227-34.

Anderson, P., and Kedersha, N. (2002b). Visibly stressed: the role of eIF2, TIA-1, and stress granules in protein translation. *Cell Stress Chaperones* **7**(2)**,** 213-21.

Anderson, P., and Kedersha, N. (2006). RNA granules. *J Cell Biol* **172**(6)**,** 803-8.

Beck, A. R., Medley, Q. G., O'Brien, S., Anderson, P., and Streuli, M. (1996). Structure, tissue distribution and genomic organization of the murine RRM-type RNA binding proteins TIA-1 and TIAR. *Nucleic Acids Res* **24**(19)**,** 3829-35.

Brinton, M. A. (2002). The molecular biology of West Nile Virus: a new invader of the western hemisphere. *Annu Rev Microbiol* **56,** 371-402.

Chu, P. W., and Westaway, E. G. (1992). Molecular and ultrastructural analysis of heavy membrane fractions associated with the replication of Kunjin virus RNA. *Arch Virol* **125**(1-4)**,** 177-91.

Eulalio, A., Behm-Ansmant, I., and Izaurralde, E. (2007). P bodies: at the crossroads of post-transcriptional pathways. *Nat Rev Mol Cell Biol* **8**(1)**,** 9-22.

Eystathioy, T., Chan, E. K., Tenenbaum, S. A., Keene, J. D., Griffith, K., and Fritzler, M. J. (2002). A phosphorylated cytoplasmic autoantigen, GW182, associates with a unique population of human mRNAs within novel cytoplasmic speckles. *Mol Biol Cell* **13**(4)**,** 1338-51.

Gilks, N., Kedersha, N., Ayodele, M., Shen, L., Stoecklin, G., Dember, L. M., and Anderson, P. (2004). Stress granule assembly is mediated by prion-like aggregation of TIA-1. *Mol Biol Cell* **15**(12)**,** 5383-98.

Grun, J. B., and Brinton, M. A. (1987). Dissociation of NS5 from cell fractions containing West Nile virus-specific polymerase activity. *J Virol* **61**(11)**,** 3641-4.

Jin, K., Li, W., Nagayama, T., He, X., Sinor, A. D., Chang, J., Mao, X., Graham, S. H., Simon, R. P., and Greenberg, D. A. (2000). Expression of the RNA-binding protein TIAR is increased in neurons after ischemic cerebral injury. *J Neurosci Res* **59**(6)**,** 767-74.

Kapoor, M., Zhang, L., Ramachandra, M., Kusukawa, J., Ebner, K. E., and Padmanabhan, R. (1995). Association between NS3 and NS5 proteins of dengue virus type 2 in the putative RNA replicase is linked to differential phosphorylation of NS5. *J Biol Chem* **270**(32)**,** 19100-6.

Kedersha, N., and Anderson, P. (2002). Stress granules: sites of mRNA triage that regulate mRNA stability and translatability. *Biochem Soc Trans* **30**(Pt 6)**,** 963-9.

Kedersha, N., Stoecklin, G., Ayodele, M., Yacono, P., Lykke-Andersen, J., Fritzler, M. J., Scheuner, D., Kaufman, R. J., Golan, D. E., and Anderson, P. (2005). Stress granules and processing bodies are dynamically linked sites of mRNP remodeling. *J Cell Biol* **169**(6)**,** 871-84.

Kedersha, N. L., Gupta, M., Li, W., Miller, I., and Anderson, P. (1999). RNA-binding proteins TIA-1 and TIAR link the phosphorylation of eIF-2 alpha to the assembly of mammalian stress granules. *J Cell Biol* **147**(7)**,** 1431-42.

Koonin, E. V. (1993). Computer-assisted identification of a putative methyltransferase domain in NS5 protein of flaviviruses and lambda 2 protein of reovirus. *J Gen Virol* **74 (Pt 4),** 733-40.

Li, W., Li, Y., Kedersha, N., Anderson, P., Emara, M., Swiderek, K. M., Moreno, G. T., and Brinton, M. A. (2002). Cell proteins TIA-1 and TIAR interact with the 3'

stem-loop of the West Nile virus complementary minus-strand RNA and facilitate virus replication. *J Virol* **76**(23)**,** 11989-2000.

Lindenbach, B. D., and Rice, C. M. (2007). Flaviviridae: The viruses and their replication. In: Fields, B. N., Knipe, D. N., Howley, P. M., Griffin, D. E., Martin, M. A., Lamb, R. A., Roizman, B., Straus, S. E., (Eds.), Fields Virology, 5th ed., Lippincott William and Wilkins, Philadelphia, Pennsylvania, pp. 1101-52.

McInerney, G. M., Kedersha, N. L., Kaufman, R. J., Anderson, P., and Liljestrom, P. (2005). Importance of eIF2alpha phosphorylation and stress granule assembly in alphavirus translation regulation. *Mol Biol Cell* **16**(8)**,** 3753-63.

Miller, S., Sparacio, S., and Bartenschlager, R. (2006). Subcellular localization and membrane topology of the Dengue virus type 2 Non-structural protein 4B. *J Biol Chem* **281**(13)**,** 8854-63.

Scherbik, S. V., Paranjape, J. M., Stockman, B. M., Silverman, R. H., and Brinton, M. A. (2006). RNase L plays a role in the antiviral response to West Nile virus. *J Virol* **80**(6)**,** 2987-99.

Smith, J. A., Schmechel, S. C., Raghavan, A., Abelson, M., Reilly, C., Katze, M. G., Kaufman, R. J., Bohjanen, P. R., and Schiff, L. A. (2006). Reovirus induces and benefits from an integrated cellular stress response. *J Virol* **80**(4)**,** 2019-33.

Tourriere, H., Chebli, K., Zekri, L., Courselaud, B., Blanchard, J. M., Bertrand, E., and Tazi, J. (2003). The RasGAP-associated endoribonuclease G3BP assembles stress granules. *J Cell Biol* **160**(6)**,** 823-31.

Trent, D. W., Swensen, C. C., and Qureshi, A. A. (1969). Synthesis of Saint Louis encephalitis virus ribonucleic acid in BHK-21-13 cells. *J Virol* **3**(4)**,** 385-94.

Uchil, P. D., and Satchidanandam, V. (2003). Architecture of the flaviviral replication complex. Protease, nuclease, and detergents reveal encasement within double-layered membrane compartments. *J Biol Chem* **278**(27)**,** 24388-98.

Vaheri, A., Sedwick, W. D., Plotkin, S. A., and Maes, R. (1965). Cytopathic effect of rubella virus in RHK21 cells and growth to high titers in suspension culture. *Virology* **27**(2)**,** 239-41.

Vasudevan, S. G., Johansson, M., Brooks, A. J., Llewellyn, L. E., and Jans, D. A. (2001). Characterisation of inter- and intra-molecular interactions of the dengue virus RNA dependent RNA polymerase as potential drug targets. *Farmaco* **56**(1-2)**,** 33-6.

Ventoso, I., Sanz, M. A., Molina, S., Berlanga, J. J., Carrasco, L., and Esteban, M. (2006). Translational resistance of late alphavirus mRNA to eIF2alpha phosphorylation: a strategy to overcome the antiviral effect of protein kinase PKR. *Genes Dev* **20**(1)**,** 87-100.

Westaway, E. G., Mackenzie, J. M., Kenney, M. T., Jones, M. K., and Khromykh, A. A. (1997). Ultrastructure of Kunjin virus-infected cells: colocalization of NS1 and NS3 with double-stranded RNA, and of NS2B with NS3, in virus-induced membrane structures. *J Virol* **71**(9)**,** 6650-61.

Westaway, E. G., Mackenzie, J. M., and Khromykh, A. A. (2003). Kunjin RNA replication and applications of Kunjin replicons. *Adv Virus Res* **59,** 99-140.

Wilczynska, A., Aigueperse, C., Kress, M., Dautry, F., and Weil, D. (2005). The translational regulator CPEB1 provides a link between dcp1 bodies and stress granules. *J Cell Sci* **118**(Pt 5)**,** 981-92.

Yu, C. Y., Hsu, Y. W., Liao, C. L., and Lin, Y. L. (2006). Flavivirus infection activates the XBP1 pathway of the unfolded protein response to cope with endoplasmic reticulum stress. *J Virol* **80**(23)**,** 11868-80.